



FACULTY OF TECHNOLOGY

EFFECT OF ROTOR TIP SPEED ON FLOTATION CELL PERFORMANCE

Katariina Kauppila

Degree Programme in Process Engineering

Master's Thesis

May 2019



FACULTY OF TECHNOLOGY

EFFECT OF ROTOR TIP SPEED ON FLOTATION CELL PERFORMANCE

Katariina Kauppila

Supervisors:

Teemu Alatalo

Saija Luukkanen

Degree Programme in Process Engineering

Master's Thesis

May 2019

ABSTRACT FOR THESIS

University of Oulu Faculty of Technology

Degree Programme (Bachelor's Thesis, Master's Thesis) Degree Programme in Process Engineering		Major Subject (Licentiate Thesis)	
Author Kauppila, Katariina		Thesis Supervisor Luukkanen S, Professor	
Title of Thesis Effect of rotor tip speed on flotation cell performance			
Major Subject Industrial Engineering and Management	Type of Thesis Master's Thesis	Submission Date May 2019	Number of Pages 91p., 5 App.
Abstract			
<p>Energy consumption of a mechanical flotation cell comprises of the level of rotor tip speed and air supply. According to previous studies, there is evidence that reduction of rotation speed may not lead into significant losses in flotation rate in regard to grade and recovery. Similarly, reduction of rotor tip speed would create savings as the electricity consumption decreases. Purpose of this master's thesis was to investigate whether the profitability of froth flotation could be increased by rotor tip speed reduction.</p> <p>The effect of rotor tip speed on flotation cell performance was investigated as an assignment of Pöyry Finland Oy by laboratory flotation tests executed in Oulu Mining School R&D Centre. Flotation tests were performed with Ni-Cu-PGE ore with nickel flotation as a primary interest of the study. The flotation tests were executed as a sequential flotation where the tailings of copper flotation were the feed of nickel flotation. Outotec GTK LabCell[®] flotation machine was used in the tests. The objective of the laboratory tests was to simulate the industrial scale flotation plant performance and to gain useful information for the optimization of flotation plant. The examination was executed on nickel flotation with four different rotation speeds and one reference series of tests was performed. Other process variables were kept stable. Grades of concentrates and tailings were analyzed with X-ray fluorescence spectrometer. Recoveries were calculated according to the analyzed grades and masses of concentrates.</p> <p>The results showed that decreased rotor tip speed improved the grade of nickel concentrate while recovery was decreasing. There was some variation between the reference tests executed in similar conditions which primary source was thought to be heterogeneous copper content of the feed. According to the results the importance of evenly performed copper flotation was emphasized. However, the trend in performance between different flotation conditions was assumed to be reliable. Cumulative nickel recovery was the greatest with the highest tested rotor tip speed (6.28 m/s) and the smallest with lowest tested rotor tip speed (3.46 m/s). The cumulative nickel grade was performing reversed. Furthermore, the rotor tip speed was found to have a non-linear relationship with nickel recovery. A reduction of rotor tip speed on higher speed was shown to have a smaller effect on flotation cell performance compared to a similar extent of reduction with lower rotor tip speed.</p> <p>Lastly, the results were scaled into industrial scale and the profitability of the speed reduction was evaluated financially. The improvements in grade and losses in recovery were compared to earnings in energy savings. With current nickel \$12,810/t and energy price \$0.1/kWh the most optimal rotor tip speed is 5.34 m/s (1700 rpm). Based on the research it would be recommended to impugn the rotor tips speeds used in industrial conditions and further investigate whether savings could be created by the speed reduction. The results cannot be assumed to be applicable to all the conditions as the behaviour may change according to ore type and grades of minerals.</p>			
Additional Information			

TIIVISTELMÄ

OPINNÄYTETYÖSTÄ Oulun yliopisto Teknillinen tiedekunta

Koulutusohjelma (kandidaatintyö, diplomityö) Prosessitekniikan koulutusohjelma		Pääaineopintojen ala (lisensiaatintyö)	
Tekijä Kauppila, Katariina		Työn ohjaaja yliopistolla Luukkanen S, professori	
Työn nimi Effect of rotor tip speed on flotation cell performance			
Opintosuunta Tuotantotalous	Työn laji Diplomityö	Aika Toukokuu 2019	Sivumäärä 91s., 5 liitettä
Tiivistelmä			
<p>Mekaanisen vaahdotuskennon energiankulutus määräytyy roottorin pyörimisnopeuden ja ilman syöttövirtauksen suuruuden mukaan. Aiempien tutkimusten perusteella voidaan odottaa, ettei rikasteen saanti kärsi merkittävästi roottorin pyörimisnopeutta laskettaessa. Sen sijaan tehdasmittakaavassa saavutettaisiin merkittäviä säästöjä energiankulutuksessa, kun pyörimisnopeutta lasketaan. Työn tarkoituksena oli tutkia, voitaisiinko roottorin pyörimisnopeutta laskemalla parantaa vaahdotuksen taloudellista kannattavuutta.</p> <p>Roottorin pyörimisnopeuden vaikutusta vaahdotuskennon suorituskykyyn tutkittiin Pöyry Finland Oy:n toimeksiantona. Kokeellinen osuus suoritettiin laboratorioskokein Oulun yliopiston kaivannaisalan tiedekunnan tutkimuskeskuksessa. Vaahdotuskokeet tehtiin Ni-Cu-PGE malmilla nikkeli-vaahdotuksen ollessa pääasiallinen tutkimuskohde. Vaahdotus suoritettiin vaiheittaisena vaahdotuksena, jossa kuparivaahdotuksen jäte oli nikkeli-vaahdotuksen syöte. Kokeet suoritettiin Outotec GTK LabCell® vaahdotuskoneella. Laboratorioskokeiden tarkoituksena oli simuloida tehdasmittakaavan olosuhteita ja saavuttaa hyödyllistä tietoa rikastamon optimointiin. Vaahdotuskokeet suoritettiin muuttamalla roottorin pyörimisnopeutta nikkelin esivaahdotuksessa ja pitämällä samanaikaisesti muut prosessiarvot vakioina. Kokeet tehtiin neljällä eri pyörimisnopeudella ja lisäksi tehtiin yksi vertailusarja. Mineraalien pitoisuudet rikasteissa ja vaahdotuksen jätteissä määritettiin röntgenfluoresenssin avulla. Rikasteiden saannit määritettiin mitattujen pitoisuuksien ja massojen avulla.</p> <p>Tulosten perusteella nikkelin pitoisuus rikasteissa parani pyörimisnopeutta laskettaessa, mutta samanaikaisesti saanti heikkeni. Samoissa olosuhteissa suoritettujen vertailusarjojen välillä havaittiin vaihtelua, jonka pääasiallinen lähde arvioitiin olevan epätasainen kuparipitoisuus. Tulosten perusteella tasaisesti suoritettujen kuparivaahdotuksen tärkeys korostui. Kuitenkin eri olosuhteiden välillä havaitun trendin arvioitiin olevan luotettava. Kumulatiivinen nikkelin saanti oli suurin korkeimmalla testatulla roottorin pyörimisnopeudella (6.28 m/s) ja pienin matalimmalla nopeudella (3.46 m/s). Kumulatiivinen nikkelin pitoisuus käyttäytyi päinvastaisesti. Lisäksi roottorin pyörimisnopeudella havaittiin olevan epälineaarinen suhde nikkelin saantiin. Samansuuruisen pyörimisnopeuden laskun vaikutuksen havaittiin olevan pienempi suurella pyörimisnopeudella.</p> <p>Lopuksi tulokset skaalattiin tehdasmittakaavaan roottorin pyörimisnopeuden laskun taloudellisen kannattavuuden arvioimiseksi. Energiankulutuksen pienemisestä saavutettuja hyötyjä verrattiin muuttuneisiin saantien ja pitoisuuksien arvoihin. Analyysin perusteella nykyisellä nikkelin \$12,810/t ja energian hinnalla \$0.1/kWh optimaalinen roottorin pyörimisnopeus on 5.34 m/s (1700 rpm). Tutkimuksen perusteella voidaan todeta, että tehdasolosuhteissa käytettäviä vaahdotuskonon pyörimisnopeuksia olisi syytä kyseenalaistaa ja kokeilla, saavutettaisiinko roottorin pyörimisnopeutta laskemalla taloudellista hyötyä. Tuloksia ei voida yleistää kaikkiin olosuhteisiin, sillä havainnot eivät välttämättä päde kaikille malmityypeille ja mineraalien pitoisuuksille.</p>			
Muita tietoja			

PREFACE

Effect of rotor tip speed on flotation cell performance was studied as an assignment of Pöyry Finland Oy during academic year 2018-2019.

I want to thank my manager Janne Tikka and Pöyry Finland Oy for making this study possible.

I want to express the most sincere world of thanks to my supervisors Teemu Alatalo and Saija Luukkanen. Thank you for your guidance and answers to all of my questions. Teemu, thank you for providing a great topic for my thesis. Saija, thank you for the thorough comments on the written thesis and all the arrangements in the Oulu Mining School.

I want to thank the personnel of Oulu Mining School for all of your help and the possibility to execute the laboratory experiments in your premises. I want to thank especially Miika Peltoniemi and Riitta Kontio for all of your advice and help in the laboratory. Thank you all the co-researchers for your advice. Thank you the personnel of The Center of Microscopy and Nanotechnology in the University of Oulu for the professional sample analysis.

I want to thank all my Pöyry colleagues and especially the Mining and Metals team in Oulu. Thank you Kati Maunuksela, Kristian Colpaert, Matti Sakaranaho, Riku Sarkkinen, Saku Leskelä and Sauli Pisilä for all of your spurring. Thank you project managers Martti Korpi, Jukka Viheriälehto and Toni Talja for your flexibility with the project work. Thank you Pauliina Hellstén for being a hardworking substitute. Thank you Pöyry Trainees in the Oulu office for your peer support.

I want to thank my friends and family for your support. I want to thank especially Sanna Torniainen for sharing the ups and downs of student life. It has been an unforgettable journey of seven years!

Oulu, 8.5.2019

Katariina Kauppila

TABLE OF CONTENTS

ABSTRACT	
TIIVISTELMÄ	
PREFACE	
TABLE OF CONTENTS	
SYMBOLS	
ABBREVIATIONS	
1 INTRODUCTION	11
2 FROTH FLOTATION	13
2.1 Liberation	13
2.2 Flotation mechanism	14
2.3 Flotation chemicals	15
2.4 Flotation response	16
2.4.1 Particle size	18
2.4.2 Bubble size	19
2.4.3 Air flow rate and air dispersion	20
2.4.4 Slurry properties	23
2.4.5 Froth depth	23
2.4.6 Chemicals dosage	24
2.4.7 Power input – rotation speed	25
2.5 Energy consumption of mechanical flotation cells	30
3 DESIGN OF EXPERIMENTS	33
4 EXPERIMENTAL	36
4.1 Ore properties	36
4.2 Preparations	36
4.2.1 Grinding tests	36
4.2.2 Accuracy of equipment	37
4.2.3 Preparation of chemicals	38
4.3 Machinery	39
4.4 Flotation test procedure	42
5 SAMPLE ANALYSIS	50
5.1 Methods, sample preparation and analysis procedure	50
6 RESULTS AND DISCUSSION	51
6.1 Properties of nickel flotation feed	53

6.2 Performance of nickel flotation.....	60
6.3 Profitability of flotation in regard to rotor tip speed	66
6.4 Discussion on particle size	74
6.5 Laboratory flotation cell performance and reliability of results	77
7 CONCLUSIONS.....	83
7.1 Recommendations	84
8 SUMMARY	86
9 REFERENCES.....	88

APPENDICES:

Appendix 1. Flotation test procedure

Appendix 2. Original XRF data

Appendix 3. XRF data examination

Appendix 4. Profitability examination

Appendix 5. Original particle size analysis reports

SYMBOLS

A	area, cross-sectional area of slurry
A_b	bubble surface area
a	bubble surface area per unit cell volume
C_{flow}	mass of concentrate
c	assay of valuable metal in concentrate
D	rotor diameter
d_{32}	Sauter mean bubble diameter
F_{flow}	mass of feed
f	assay of valuable metal in feed
I	current
J_g	superficial gas velocity
k	flotation rate constant
m	mass
N	rotor tip speed
N_p	power number
N_q	flow rate
P	power
P_{80}	size that 80% of particles passes
Q	volumetric gas flow rate
R	recovery
r	radial distance
S_b	bubble surface area flux
U	voltage
V_b	volume of bubbles collected in burette
v	tangential speed
ε	energy dissipation rate
ε_g	gas holdup
κ	total kinetic energy
ρ	slurry density
τ	residence time
τ_{fg}	froth residence time

τ_{fs}	specific froth residence time
φ	power ratio
ω	rotational speed

ABBREVIATIONS

CMC	carboxy methyl cellulose
CuCC1	copper cleaner concentrate 1
CuCT	copper cleaner tailings
CuRT	copper rougher tailings
NiRC1	nickel rougher concentrate 1
NiRC2	nickel rougher concentrate 2
NiRC3	nickel rougher concentrate 3
NiRC4	nickel rougher concentrate 4
NiRT	nickel rougher tailings
PGE	platinum group element
SIPX	sodium isopropyl xanthate
XRF	X-ray fluorescence

1 INTRODUCTION

The purpose of this master's thesis is to examine the effect of rotor tip speed on flotation cell performance. The topic is examined because of its energy saving and process optimization potential. The experiments are conducted with Ni–Cu–PGE ore in the laboratory of Oulu Mining School R&D Centre in University of Oulu. The flotation cell performance is investigated in regard to grade and recovery by changing the rotor tip speed while keeping other conditions stable. Grade is the content of marketable end product in the material and recovery is the percentage of the total metal content in the ore that is recovered in the concentrate (Wills and Napier-Munn 2006, p. 17). Based on the results financial analysis are conducted in order to evaluate the financial profitability of the reduction of rotor tip speed as the energy consumption decreases. The thesis is executed as an assignment of Pöyry Finland Oy.

Traditionally, research of energy efficiency in mineral processing has been concentrated on comminution as it represents the greatest energy consumer in the operation. However, awareness towards both environmental effects and profitability of the operation has been increasing which have led to development of more and more energy efficient equipment together with more efficient operation methods of flotation cells. There is some previous study made on the topic. A study conducted by Rinne and Peltola (2008) suggests that a minor reduction of rotor tip speed may not have a significant effect on the flotation cell performance but will lead to savings in the form of decreased energy consumption. Development of efficient flotation cells have made the processing of some earlier uneconomic low grade ores now economic (Wills and Napier-Munn 2006 p. 267). The processing of low grade ores is becoming more and more common as many high grade mineral deposits have already been exploited. However, the metal products and mineral processing is needed even increasingly in the future because of technological development. As modern lifestyle is highly dependent on minerals more efficient processing methods have been developed in order to be able to exploit even the smallest traces of minerals. Similarly, as the head grades of minerals are decreasing the amount of treated material is assumed to increase. Larger throughputs increase the energy consumption of flotation plant. This study investigates whether energy can be saved by reducing the rotor tip speed without a significant effect on the metallurgical performance of flotation cell. Savings in energy are directly proportional

to savings in money which will be relevant especially in the future as energy price is presumed to increase.

The experiments are executed with Ni-Cu-PGE ore. Main sulphide minerals of the ore are pyrrhotite, chalcopyrite and pentlandite. Copper and nickel concentrates are produced by froth flotation. Main copper mineral is chalcopyrite and nickel mineral pentlandite. Talc, serpentine and amphibole are the main gangue minerals in the ore and pyrrhotite is the main sulphide gangue mineral in the ore. Minerals appear in the ore in low concentrates which makes the operation challenging. Efficient technology is needed in order to produce high grade concentrates with good recovery to cover the production costs (Wills and Napier-Munn 2006, p.327). The head grades of the ore are ~0.3% Cu and ~0.25% NiS and the approximate produced concentrate grades in industrial scale are ~25% and ~11% for copper and nickel, respectively. Total copper recovery in industrial scale with the ore is around 71% and nickel recovery around 60%. At the moment the price of nickel is about twice the price of copper (London Metal Exchange 2019). That is why improvements especially in nickel flotation are financially beneficial and thus it is under examination of this study.

Nickel is utilized especially as alloyed with other metals to increase metals' strength, toughness and corrosion resistance over a wide temperature range. Due to these properties nickel is essential to the iron and steel industry. Nickel does not occur as native metal but economically important ores can be divided into sulfide and oxide minerals. About 80% of nickel in the identified world resource deposits exists in laterite ore bodies with only 20% in sulfide deposits. However, greater part of the nickel produced is recovered from sulfide ores because sulfide ore deposits lie largely in politically stable countries and in the vicinity of major markets. (Kerfoot 2012, p. 37-38, 40, 42)

At first, theoretical background about the principles of froth flotation and factors affecting flotation response are examined in chapter 2 and in its sub-chapters. Details of the experimental part and sample analysis procedures are to be found in chapters 3, 4 and 5. Results and discussion are presented in chapter 6. Finally, conclusions of the study are presented in chapter 7.

2 FROTH FLOTATION

Froth flotation is a separation method based on the surface property differences of particles. In minerals processing flotation is used to separate valuable minerals and gangue minerals from each other. Flotation is utilized also in other fields of technology, such as in water treatment process and deinking process of recycled office paper. In minerals processing flotation is applied after size reduction, classification and conditioning of the feed material (Yarar and Richter 2003, p. 1). (Wills and Napier-Munn 2006, p.267; Yianatos 2007; Goel and Jameson 2012)

In concentrating process the valuable minerals are separated from unwanted gangue minerals. In addition to flotation there are many other concentrating methods available. According to Wills and Napier-Munn (2006) the most important physical separation methods are: sorting based on optical properties, gravity concentration based on density differences, magnetic separation based on differences in magnetic properties and electrical concentration based on conductivity differences. Often concentration is performed in combination of two or more methods in order to create high quality of concentrate. Furthermore, there are chemical and biological concentrating methods available. (Wills and Napier-Munn 2006, p. 8-12)

2.1 Liberation

Before the actual concentrating process may take place valuable minerals must be released from gangue minerals. This is called a liberation process. Liberation is achieved by crushing and grinding the feed material leading to an end product that consists of relatively clean individual particles of valuable minerals and gangue. Well performed size reduction process plays an important role in following processing stages, including flotation where it is an important factor in determining the overall recovery of a mineral. If the particle size of minerals is not small enough to liberate valuables from gangue the recovery of bare valuable minerals is not possible either in latter flotation process. Moreover, collection of too large particles is not possible by flotation as the particles must be small enough to create adhesion forces between the air bubbles and the air bubble must be able to float the particle up to the froth. On the other hand over grinding leads to formation of ultrafine slime particles which may easily end up into tailings. Besides leading to recovery losses excess comminution consumes lots of

energy. Traditionally grinding has been the greatest energy consumer in the concentrating plant and it can consume up to 50% of the whole plant's share. Accordingly, grinding process is a balance between clean concentrates, operating costs and mineral losses. (Wills and Napier-Munn 2006, p. 7, 268)

2.2 Flotation mechanism

The recovery of particles in flotation is based on three mechanisms. Selective attachment to the air bubbles is the true flotation mechanism. In addition, recovery may take place by entrainment with the water passing through the froth and by physical entrapment between particles which are attached to air bubbles in the froth. Majority of the particles are recovered by attachment to air bubbles and it is the most important flotation mechanism. As entrainment and entrapment are physical mechanisms and not based on chemical selectivity also the unwanted gangue particles have the same probability of being recovered by the two mentioned mechanisms. The entrained particles have either a positive or negative effect on recovery depending on whether the particles are gangue or valuable mineral (Schubert 2008). A single flotation stage is uncommon in an industrial scale and flotation is usually taken place in several stages in order to enhance the concentrate's quality. Single flotation cells arranged in series can be called as a bank, row or line of flotation cells (Maldonado et al. 2011). Furthermore, banks are connected parallel to form circuits. The different stages of flotation operation can be separated into rougher, scavenger and cleaning circuits. (Wills and Napier-Munn 2006, p. 267, 292)

In the first flotation cell of a bank relatively high amount of valuable minerals are collected to the froth as the concentration of slurry is the greatest in regard to the valuable mineral content. Minerals remaining in the slurry phase pass to the second cell, where more minerals are collected to the froth. Thus, fewer valuable minerals are floated as the flotation operation proceeds leading to a barren tailings flow in the last cell of the row. As the valuable mineral content in the slurry is progressively reducing also the thickness of froth bed is reducing down the bank. The last few cells in a bank containing low grade froths are called scavenger cells. The fast floating material is to be recovered in rougher cells and the more reluctant in scavenger cells. Therefore, rougher concentrate consists of the most optimal particle composition which is the intermediate

particle size fraction while scavenger concentrate consists of coarse and fine particles. (Wills and Napier-Munn 2006, p. 292, 296)

2.3 Flotation chemicals

Since flotation is a physico-chemical separation method certain chemicals are used to intensify the separation process. The use of chemicals allows modifying the mineral properties in such a way that even minerals which natural surface properties are close to each other can be separated. The most important chemical property of minerals in flotation is hydrophobicity. As slurry is a water solution the minerals must be water repellent in order to be separated from the solution. Hydrophobicity can be described by a contact angle that is an angle between bubble-particle aggregate and it describes the strength of adhesion force between them (Dai et al. 1999 cited by Grano 2006; Wills and Napier-Munn 2006, p. 268-269). The more hydrophobic a particle is the greater the contact angle is and stability of the system increases (Grano 2006; Wills and Napier-Munn 2006, p. 268-269). Surfactants called collectors are used to make the minerals hydrophobic. Collectors are organic compounds which are added to the slurry usually prior the actual flotation in a conditioning tank. By adsorption of molecules or ions to the mineral surface collectors reduce the stability of hydrated layer between particle and air bubble to such a level that the mineral particle is able to attach an air bubble. Collector chemicals are classified to ionising and non-ionising compounds and ionising compounds furthermore into anionic and cationic compounds. Anionic compounds are divided into oxyhydril and sulphydril compounds based on their chemical properties. Xanthates and dithiophosphates are commonly used collectors. They both belong to the sulphydril group. (Wills and Napier-Munn 2006, p. 267-272)

Frothers are used to create a stable froth bed, to reduce the slurry's surface tension and to increase flotation kinetics. Stable froth helps collecting particles that are transported by the air bubbles, the reduced surface tension maximizes the slurry-air interface area and the increased flotation kinetics allows faster collision of particles and air bubbles. Frothers are generally organic compounds that are chemically very similar to ionic collectors. They commonly comprise of a polar and non-polar group. The polar group interacts with water molecules while non-polar group orients towards the air bubbles. For example pine oil and long-chain alcohols are used as frothers. (Wills and Napier-Munn 2006, p. 276; Yazar and Richter 2016, p. 7)

Regulators are used to modify the collectors' behavior either by intensifying or reducing their water repellent effect. Thus, regulators make collectors more selective towards certain minerals. Regulators can be classified into activators, depressants and pH modifiers. Activators modify the surface of minerals in such a way that they can react and be recovered by action of the collector. Depressants are used to increase the selectivity in flotation. Their function is to modify the surfaces of unwanted minerals hydrophilic preventing them to float. According to Wills and Napier-Munn (2006) depressants are in a key role in performing the flotation of nickel sulphides economically. Depressants' actions are complex and varied and they are not yet fully understood. Thus, depressants' action is much more difficult to control than the other reagents types (Bradshaw et al. 2005 cited by Wills and Napier-Munn 2006, p. 279). Third regulator group, pH regulators are used in creating favorable circumstances to the action of other chemicals and the performance of flotation. When possible, flotation is performed in alkaline conditions as most of the collectors are stable under these conditions and moreover, corrosion of equipment is avoided. Lime and soda ash are widely used in controlling of alkalinity. Although pH regulators are cheaper than other flotation chemicals they form higher overall cost in flotation operations as they are used in much higher amounts compared to other chemicals. (Wills and Napier-Munn 2006, p. 277-279, 282; Yazar and Richter 2016, p. 7)

2.4 Flotation response

Flotation response is a sum of several factors and all the reactions are not yet completely understood (Wills and Napier-Munn 2006, p. 267). In order to a particle to be collected by flotation the following steps are required: collision with an air bubble, attachment to the bubble with adhesion forces and formation of a stable aggregate which floats into the froth layer for the final recovery (Wills and Napier-Munn 2006, p. 267-268; Yazar and Richter 2016, p. 19). In the following chapters 2.4.1 - 2.4.7 different factors affecting flotation response are examined among others bubble and particle size, air flow rate, froth residence time, use of chemicals as well as power input. At first, commonly used definitions to describe flotation performance are examined. In the following chapters the role of individual factors affecting flotation are emphasized. It will become evident that flotation is a very complex phenomenon and the interaction of individual factors is that matters and creates the overall performance. That is why conclusions cannot necessarily be made out of the individual factors but the overall

circumstances should be always kept in mind. Furthermore, the cited studies were executed with different ore types and thus the performance in different conditions may be dependent on the mineral type.

Metallurgical flotation response can be measured by recovery, concentrate grade and flotation rate constant. In the case of metallic ore recovery describes the percentage of total metal contained in the ore that is recovered to the concentrate (Wills and Napier-Munn 2006, p. 17). Recovery can be calculated with the following equation 1 after the grade of concentrate has been analyzed.

$$R = \frac{c \cdot C_{flow}}{f \cdot F_{flow}} \cdot 100 \quad (1)$$

where

- R is recovery (%)
- c is assay of valuable metal in concentrate
- C_{flow} is the mass of concentrate (g)
- f is the assay of valuable metal in feed
- F_{flow} is mass of feed (g)

(Amini et al. 2016)

Grade is the content of marketable end product in the material. Concentrating process is about optimizing between concentrate grade and recovery as grade and recovery have an inverse relationship (Figure 1). When producing a high-grade concentrate it is not possible to attain high recovery as the low-grade particles end up to tailings and for high recovery also the low grade particles must be recovered to the concentrate which leads to low concentrate grade. (Wills and Napier-Munn 2006, p. 17)

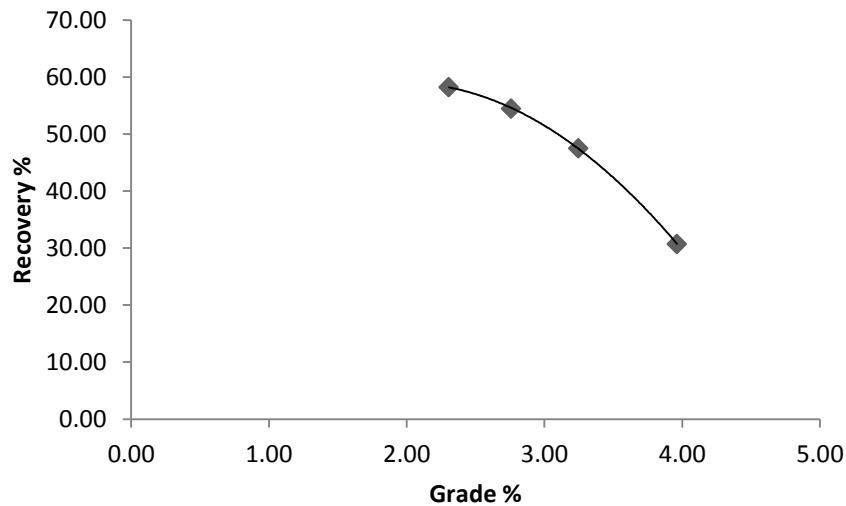


Figure 1. Relationship between concentrate grade and recovery (retelling Wills and Napier-Munn 2006, p. 17).

Furthermore, flotation response can be described by flotation rate constant (k) which takes account the mean residence time in the cell (Levenspiel (1972) cited by Gorain et al. 1997):

$$k = \frac{R}{\tau(1-R)} \quad (2)$$

where k is flotation rate constant (1/min)
 R is recovery (%)
 τ is mean residence time in the cell (min)

2.4.1 Particle size

The significance of particle size in mineral processing is based on the degree of liberation. The composition of minerals in ore influence on the grinding requirements as the occurrence and grain size of the valuable mineral define the necessary particle size for effective flotation. The degree of liberation of valuable minerals is directly affecting to the grade and recovery of the concentrate. Moreover, too large particle size will decrease recovery because the adhesion force is not strong enough to float the particle (Wills and Napier-Munn 2006, p. 268). Low recovery can be reached equally by overgrinding as smaller particles have lower probability to attach an air bubble and they can easily end up to tailings (Grano 2006; Safari et al. 2016; Tabosa et al. 2016). (Wills and Napier-Munn 2006, p. 7-8)

Each mineral has different degree of hydrophobicity and therefore different response on flotation chemicals and likelihood to attach an air bubble. Moreover, both the particle size of the mineral and the size and amount of air bubbles are determining the flotation performance. Therefore, to analyze the flotation cell performance in detail measurements and analyses including the definition of mineral type and particle and bubble size distributions must be executed. (Wills and Napier-Munn 2006, p. 267-269)

There is evidence that particle size has a strong effect on the flotation response depending on the energy input i.e. rotation speed. The topic is examined more in chapter 2.4.7.

2.4.2 Bubble size

Bubble size is generally measured by Sauter mean bubble diameter (d_{32}). It is a ratio between volume of bubbles and their measured surface area

$$d_{32} = \frac{6 \cdot V_b}{A_b} \quad (3)$$

where d_{32} is Sauter mean bubble diameter (mm)

V_b is total volume of bubbles collected in burette (ml)

A_b is total bubble surface area measured by the bubble sizer (mm²)

(Gorain et al. 1997).

Bubble size describes the surface area available for flotation (Gorain et al. 1995a). With the same volume of air smaller bubbles have greater relative surface area and increased probability to attach particles compared to larger ones (Safari et al. 2016). However, the bubble size must be aligned with particle size as the adhesion force between bubble and particle must be stronger than particle weight in order to a particle to float (Wills and Napier-Munn 2006, p. 268). The adhesion can be described by contact angle which is an angle between particle and bubble (Wills and Napier-Munn 2006, p. 268). Contact angle is the greater the stable the bubble-particle contact is (Wills and Napier-Munn 2006, p. 268-269).

Typical industrial range of bubble diameter is 2-10 mm (Evans et al. 2008). Typically, the influence of impeller speed on bubble size diminishes with the increase of flotation cell size (Amini et al. 2013). Amini et al. (2013) suggest that the impeller tip speed may

not itself have an influence on the generated bubble size but the size of flotation cell determines whether the rotor speed has an influence or not. However, there are several studies available about the control of bubble size with agitation speed and air flow rate. Gorain et al. (1995a, 1995b, 1996, 1997, 1998a, 1998b) have thoroughly studied the various effects of impeller type, rotation speed and air flow rate on the flotation cell performance in the series of studies that are conducted during years 1995-1998.

In the first part of the Gorain et al. (1995a) study it was found that the mean bubble size increased with an increase of air flow rate for all the impeller types. At low air flow rate all the four impellers dispersed air into small bubbles. As the air flow rate increased also the mean bubble size increased. The similar observation was made by Nasset et al. (2006) who suggested that a reason for the increased mean bubble size with the increased gas rate might be the coalescence processes. It should be remembered that the bubble size is also affected by secondary processes in the flotation cell which is for example the coalescence of air bubbles to form larger bubbles (Nasset et al. 2006). (Gorain et al. 1995a)

Moreover, it was found that with an increase of impeller speed the mean bubble size was decreased until certain rotation speed. Furthermore, both the mean bubble size and the shape of bubble size distribution varied at different locations in the cell. Thus, locations of measurements should be carefully justified. According to Gorain et al. (1997) the bubble size on its own does not correlate with the flotation rate constant k . That is most probably because instead of the size only the amount of air bubbles in the cell has a significant role in flotation performance. (Gorain et al. 1995a; Gorain et al. 1997)

2.4.3 Air flow rate and air dispersion

The flotation cell performance is not merely based on the bubble size but mainly the air dispersion characteristics which can be described by gas holdup, superficial gas velocity and bubble surface area flux (Nasset et al. 2006).

Gas holdup (ε_g)

$$\varepsilon_g = \frac{a \cdot J_g}{S_b} \quad (4)$$

where ε_g is gas holdup (%)
 a is total bubble surface area per unit cell volume (m^2/m^3)
 J_g is superficial gas velocity (m/s)
 S_b is bubble surface area flux (1/s)
 (Gorain et al. 1997)

is volumetric fraction of air per unit volume of slurry (Gorain et al. 1997; Nasset et al. 2006). It describes the ability of impeller to disperse air into small bubbles and the residence time of air bubbles in the slurry (Gorain et al. 1995b). Small bubbles have slower rise velocity compared to larger bubbles and thus they have longer residence time in the flotation cell and thus greater holdup (Gorain et al. 1995b). Gorain et al. (1997) did not find statistically meaningful relationship between flotation rate and gas holdup. Nevertheless, Gorain et al. (1995b) found that the gas holdup (ε_g) increased with an increase of air flow rate. That can be also concluded by the equation of gas holdup and superficial gas velocity. In the study gas holdup also generally increased with an increase of impeller speed as the bubble size decreased (Gorain et al. 1995b). As mentioned before the residence time of small bubbles is longer and thus the value of gas holdup is greater (Gorain et al. 1995b).

Superficial gas velocity (J_g) is a measure of the air volume passing through the cell cross-sectional area of slurry (Gorain et al. 1997; Amini et al. 2016).

$$J_g = \frac{Q}{A} \quad (5)$$

where J_g is superficial gas velocity, typically (m/s)
 Q is volume of air (m^3/s)
 A is cross-sectional area of slurry in the cell (m^2)
 (Dobby and Finch (1990) cited by Amini et al. (2016); Nasset al. (2006))

Improved air dispersion was found with an increase in impeller speed which was detected as uniformity of superficial gas velocity values (J_g) at different locations nevertheless, the dispersion characteristics were depended on the impeller type (Gorain et al. 1996). According to Gorain et al. (1997) at low air flow rates there is a trend of increasing flotation rate with an increase in superficial gas velocity but the effect disappears when air flow rate is considerably increased. Hadler et al. (2012) proposes that with high air flow rates air bubbles are less loaded which leads to reasonable

recovery but low concentrate grade. With low air flow rate the mobility of froth decreases as the attached particles stabilize bubbles and make the froth stable (Hadler et al. 2012). The decreased mobility causes increased bursting of bubbles which leads to low recovery but high concentrate grade (Hadler et al. 2012).

However, the pure superficial gas velocity does not take into account the bubble size: the value would stay the same as only the volumetric air flow rate stays constant. It can be conducted from the Gorain et al. (1997) investigations that with bubble size and superficial gas velocity together the investigation of flotation cell performance by flotation rate is possible. The values of superficial gas velocity and Sauter mean bubble diameter are taken into account when calculating bubble surface area flux. (Gorain et al. 1997)

Bubble surface area flux (S_b) is a rate of bubble surface area moving through the flotation cell per unit of cell cross-sectional area

$$S_b = \frac{6J_g}{d_{32}} \quad (6)$$

where S_b is bubble surface area flux (1/s)
 J_g is superficial gas velocity (m/s)
 d_{32} is Sauter mean bubble diameter (m)
 (Finch and Dobby 1990 cited by Gorain et al. 1997)

and it describes the gas dispersion characteristics (Gorain et al. 1997; Wills and Napier-Munn 2006, p. 285; Amini et al. 2016) as well as capacity of the flotation equipment to carry solids into the froth phase (Grau and Heiskanen 2003). There is dependence between bubble surface area flux and superficial gas velocity so that increasing superficial gas velocity improves bubble surface area flux (Amini et al. 2016). Gorain et al. (1997) found linear relationship between flotation rate constant (k) and bubble surface area flux (S_b). The relationship can be justified with the fact that the value of bubble surface area flux takes into account both the bubble size and the amount of air bubbles (Gorain et al. 1997). Furthermore, it was found in the study of Gorain et al. (1997) that the relationship was independent of the impeller type in use.

2.4.4 Slurry properties

Nesset et al. (2006) suggests that slurry properties such as solids concentration of slurry and viscosity affect more on air dispersion than on bubble generation. Bubble rise velocity depends on the solids concentration of slurry which can be detected in the value of gas holdup (Basini et al. 1995 cited by Nesset et al. 2006). In general, selectivity of separation is the effective the more dilute the slurry is (Wills and Napier-Munn 2006, p. 290). That is why the optimum slurry density is a balance between operating and capital costs and selectivity since the dilute slurry requires larger cell volume and larger quantities of chemicals (Wills and Napier-Munn 2006, p. 290). Typical solids content is around 30 w% (Evans et al. 2008).

Viscosity has been proved to have a direct effect on the bubble-particle coalescence in flotation cell as in low viscosity fluid bubbles and particles are more probable to collide and thus viscosity has an influence on flotation rate constant (Schubert 2008; Abrahamson 1975, Nguyen-Van 1994, Schubert 1999, Pyke 2004 cited by Amini et al. 2016). Viscosity can be controlled by dispersant chemicals. Schubert (2008) reminds that finding a dispersant that does not cause any harmful effect for the flotation operation is difficult. As an alternative for using dispersants Schubert (2008) suggests desliming of the flotation feed by multi-stage hydrocyclone arrangement. Moreover, desliming is efficient in reduction of entrainment. (Schubert 2008)

2.4.5 Froth depth

Froth depth indicates flotation performance with both too deep and shallow froth depths being unfavourable for the performance of flotation. The feed grade has an effect on the froth bed stability and recovery (Wills and Napier-Munn 2006, p. 316). When the feed is high grade a stable mineralized froth bed will be formed whereas in the case of a low grade feed it can be difficult to create a stable froth (Wills and Napier-Munn 2006, p. 316).

Gorain et al. (1998a) conducted an experiment on different froth depths by adjusting impeller speed and air flow rate one at a time. They found that flotation rate constant was decreasing with an increasing froth depth. According to the Gorain et al. (1998a) research the most favorable flotation conditions have a low froth bed thickness when maximizing the flotation rate constant. Gorain et al. (1998b) suggests that relationship

between flotation rate constant (k) and bubble surface area flux (S_b) is strongly dependent on froth residence time (τ_{fg} , τ_{fs}). Froth residence time (τ_{fg}) is a ratio of froth height to superficial gas rate. Specific froth residence time (τ_{fs}) takes into account the cell size by the froth transportation distance. A shallow froth depth represents short residence time (τ_{fg}) and deep froth bed long residence time (τ_{fg}). The short froth residence time leads to an improved flotation rate constant. Moreover, the flotation rate constant was the greater the greater bubble surface area flux was. (Gorain et al. 1998b)

Deeper froth provides longer residence time and thus there is more time for coalescence of bubbles and drainage of unattached, entrained material (Wills and Napier-Munn 2006, p. 268; Schubert 2008; Hadler et al. 2012; Amini et al. 2016). That is why deep froth depth usually increases concentrate grade (Hadler et al. 2012). Nevertheless, Hadler et al. (2012) reminds that at some point when increasing the froth depth the froth mobility decreases and bubble loading increases which will lead to collapsing of bubbles before overflowing the cell lip. The enhanced drainage of entrained material may have positive or negative effect on grade and recovery depending on the value of particle in question (Schubert 2008).

2.4.6 Chemicals dosage

Frothers as well as other flotation chemicals change the solution chemistry. According to Nasset et al. (2006) frothers restrain coalescence and also fatty acid and amine collectors may affect coalescence. Nasset et al. (2006) concluded that the decreased coalescence might lead to smaller bubble size distribution as the coalescence to form large bubbles does not occur. In the study by Nasset et al. (2006) Sauter mean bubble diameter decreased to a constant value with increasing collector dosage. Also Liu et al. (2014) found that the addition of frother decreased Sauter mean bubble diameter.

Safari et al. (2016) have proofed the increase of flotation rate constant with increasing collector dosage. Collector chemicals increase the affinity of bubbles and particles to attach (Wills and Napier-Munn 2006, p.270-272; Pushkarova and Horn 2008 cited by Safari et al. 2016). However, an excessive dosage of collector may have an adverse effect on recovery because of development of collector multi-layers on the particles (Wills and Napier-Munn 2006, p. 271).

Correct slurry pH allows necessary chemical reactions to take place and is thus an important factor in successful flotation. Alkaline conditions are favored as most collectors are stable in alkaline pH and moreover corrosion of the equipment is minimized. Generally, alkalinity is controlled by addition of lime or soda ash. (Wills and Napier-Munn 2006, p.282)

2.4.7 Power input – rotation speed

In mechanical flotation cells agitation is in an important role as it disperses air, keeps the slurry in suspension and enables bubble-particle collision (Deglon 2005; Tabosa et al. 2016). Rotation speed is generally described by rotor tip speed which is the velocity at the far end of the rotor blades (Amini et al. 2016). Alternative terms for rotor tip speed that are generally used in literature include impeller (tip) speed and agitation speed. Also the terms power input, power intensity, power draw and energy input are used in the meaning as the rotor is the main energy conveyor into the flotation cell. Typical industrial energy input is 1-2 kW/m³ (Deglon 2005; Schubert 2008).

Impeller tip speed is calculated with the following equation 7 by the rotor diameter and rotation speed:

$$\omega = \pi DN \quad (7)$$

where ω is impeller tip speed (m/s)
 D is rotor diameter (m)
 N is rotation speed (1/s)
 (Deglon et al. 2000).

Energy dissipation rate (ϵ) describes the effective energy input to the mass of slurry (Amini et al. 2016) while specific power is the power used per unit volume of a flotation cell (kW/m³) (Tabosa et al. 2016). Energy dissipation rate (ϵ) is a function of the power input of rotor (P) and the total mass of the fluid (m):

$$\epsilon = \frac{P}{m} \quad (8)$$

where ϵ is energy dissipation rate (W/kg)
 P is power input (W)
 m is mass (kg)

(Schubert 2008; Tabosa et al. 2016).

The energy dissipation rate varies throughout the cell and is the highest close to the impeller although in many studies the dissipation rate is assumed to be constant (Kresta and Wood 1991, Lee and Yianneskis 1998 cited by Goel and Jameson 2012). At typical rotation speeds in flotation the slurry flow is fully turbulent (Goel and Jameson 2012). In a small region close to the impeller the turbulent flow is isotropic (Goel and Jameson 2012). Increase of rotor tip speed increases energy dissipation through the flotation cell and thus increases the probability of bubbles and particles to collide (Deglon 2005; Grano 2006; Safari et al. 2016; Tabosa et al. 2016). Increased collision rates are especially beneficial to the fine particles as being smaller they are more improbable to collide with air bubbles (Deglon 2005; Schubert 2008; Safari et al. 2016). However, too vigorous agitation causes instability in the flotation cell that is discussed later in the chapter.

Power input is in an important role in flotation kinetics as it influences to all of the sub-processes of flotation directly or indirectly (Safari and Deglon 2018). Hydrodynamic conditions in the flotation cell determine the recovered particles and thus the recovery rate of flotation (Grano 2006; Schubert 2008; Safari et al. 2016; Tabosa 2016). Different particle sizes and also different minerals need different hydrodynamic flotation conditions (Grano 2006; Schubert 2008; Safari et al. 2016; Jameson 2013 cited by Tabosa 2016). That is why Schubert (2008) recommends feed classification before froth flotation and flotation of coarse and fine particle feeds separately. Grano (2006) was studying the effect of rotation speed in flotation on different particle sizes and found no apparent effects on flotation rate with change in rotor tip speed when the concentrate was not sized. However, on sized basis the effect was obvious. The flotation rate of small particles increased and large particles decreased with increase in rotation speed. Thus, it can be concluded that the increased flotation rate of small particles was equal to the decreased flotation rate of the coarse particles with increase in rotation speed. (Grano 2006)

Also Safari et al. (2016) found significant changes in flotation rates in terms of power input which proves the important role of energy input in flotation. They found increasing flotation rate of fine particles with increase in energy input, an optimum flotation rate for middle size particles and decrease in flotation rate for coarse particles

(Safari et al. 2016). Power input plays an important role especially in the flotation of fine particles which flotation efficiency is usually poor (Safari and Deglon 2018). Moreover, the behaviour of sulphide minerals over oxide minerals was studied and it was found that less energy is needed in reaching the optimal flotation rate for sulphide minerals compared to oxide minerals (Safari et al. 2016).

Tabosa et al. (2016) was studying the hydrodynamic conditions within a flotation cell in order to investigate the effect of different energy dissipation conditions on the flotation cell performance. There are three areas in a flotation cell based on different flow conditions: turbulent, quiescent and froth zone. Turbulent zone provides conditions necessary for true flotation. Quiescent zone is less energy intensive and enables detachment of entrained or entrapped particles and is thus important for improvement of concentrate grade. Quiescent zone is essential to stabilize the froth zone. Drainage of entrained and entrapped material is further continued in the froth zone (Wills and Napier-Munn 2006, p. 267). Froth zone recovery determines the overall recovery (Wills and Napier-Munn 2006, p. 268). By optimizing the conditions in all of these phases a maximum recovery can be reached. Froth zone recovery is decreased with increase of energy input because of instability of froth zone (Deglon 2005; Schubert 2008; Tabosa et al. 2016). Moreover, the increased energy input increases the instability of the bubble-particle aggregates resulting to detachment of particles and losses in recovery (Deglon 2005; Safari et al. 2016; Safari and Deglon 2018). However, the recovery in collection zone was improved with increase in power number N_p . Thus, there is a limit up to which the specific power input can be increased to improve the flotation kinetics and recovery of fine particles (Schubert 2008). (Tabosa et al. 2016)

Efficient use of energy in the form of high power number N_p might affect more on recovery than the pure increase in energy input (Tabosa et al. 2016). Power number (N_p) describes the ratio between dissipated energy as shear and energy used for bulk flow generation (Tabosa et al. 2016):

$$N_p = \frac{P}{\rho N^3 D^5} = (\kappa N^2 D^2) \cdot (N_q \rho N D^3) \quad (9)$$

where N_p is power number
 P is power draw (W)
 ρ is slurry density (kg/m^3)

N is rotor tip speed (1/s)

D is rotor diameter (m)

κ is total kinetic energy (J)

N_q is flow rate (m^3/s)

(Hemrajani and Tatterson (2004) cited by Tabosa et al. 2016).

Power number can be increased for example by low cell aspect ratio, low rotor tip speed and oversized rotor-stator system which will increase the volume of highly turbulent zone (Tabosa et al. 2016). Tabosa et al. (2016) suggests operating flotation cell with a large power number (N_p) to achieve high local energy dissipation in the impeller stream which will provide more efficient use of energy and may promote higher collision rates and recovery. For fine particle feed the local energy dissipation rate should be as large as possible and kinematic viscosity of the slurry as small as possible (Schubert 2008). To achieve the conditions a large power number is needed at sufficiently high rotation speed (Schubert 2008).

In the study conducted by Deglon (2005) bubble size and bubble surface area flux remained fairly constant despite a wide range of tested rotor tip speeds and air flow rates. That is why Deglon (2005) concluded that the flotation rate was increased due to better bubble-particle contact by the increased turbulence. The better gas dispersion was not assumed to have an effect as the bubble size and bubble surface area flux remained constant. Increase in flotation rate constant was found with increasing power input but similarly the grade of concentrate was found to decrease remarkably. According to Deglon (2005) the effect is expected because of the nature of grade-recovery relationship which is also mentioned by Wills and Napier-Munn (2006, p. 17). Deglon (2005) suggests that the reduction of grade is either due to entrainment or increased flotation of poorly liberated particles or flotation of gangue. (Deglon 2005)

Nevertheless, Amini et al. (2016) found out that the increase in impeller tip speed reduces bubble size and therefore the bubble surface area flux is increased for small 5 l laboratory cell until certain tip speed. The increased bubble surface area flux provides greater probability of bubbles and particles to collide which increases flotation rate (Gorain 2006 cited by Amini et al. 2016). Nevertheless, for larger 60 l cell the influence was not reported as the bubble size remained constant though the impeller tip speed variation. However, the flotation rate constant was found to increase. It was obvious that

bubble surface area flux is not the only factor affecting flotation rate constant. Bubble-particle attachment might also be enhanced by increased turbulent kinetic energy dissipation rate in flotation cell without increase of bubble surface area (Abrahamson 1975, Schubert 1999, Dai et al. 1999, Pyke 2004, Newell and Grano 2007 cited by Amini et al. 2016). (Amini et al. 2016)

Floatability of small and medium size particles was found to increase with increase in impeller tip speed. Floatability of large particles ($> 90 \mu\text{m}$) first increased but then started to decrease or remain constant when the rotor tip speed was further increased. Moreover, the effect of impeller tip speed on entrainment was found. Highest degree of entrainment was attained with highest impeller speed in all particle size fractions. Flotation rate was increased with an increase in impeller speed when taking the entrainment into account. (Amini et al. 2016)

Amini et al. (2016) confirms that reduction of energy input by reduction of impeller speed decreases the energy dissipation rate in the cell. However, they found out that introducing air to the cell reduced the variation of energy dissipation rate by damping the mean energy dissipation rate. Also Schubert (1999) cited by Tabosa (2016) found the damping effect with presence of air and solids. Amini et al. (2016) proposes it might be due to increased slurry mobility but reminds that more research is needed. Moreover, it was found that energy dissipation rate is directly proportional to the impeller tip speed but it varies with changes of air rate. At fixed impeller tip speed the mean energy dissipation rate decreases with increase in superficial gas rate. Also Deglon et al. (2000) found the significant effect of air flow rate to the power draw and power number. Power number was found to decrease by 1.0 unit by increase of air flow rate by $3.9 \text{ m}^3/\text{min}$ (Deglon et al. 2000). (Amini et al. 2016)

In the study by Lelinski et al. (2011) it was proposed that the recovery at the head of the row was limited most probably by froth carrying capacity than kinetics. That is why the effect of rotor tip speed was assumed to be the most powerful at the tail end of the flotation bank where the interaction with froth recovery is removed (Lelinski et al. 2011). Also Deglon (2005) found that the recovery of first rougher cell is limited by the froth carrying capacity. Deglon (2005) found substantial increase in flotation rate constant with increasing energy input especially in the last flotation cells of the bank. In the study by Lelinski et al. (2011) the rotor tip speed was adjusted in the final cell of

rougher-scavenger flotation bank comprising of five flotation cells and the recovery was increased with the increase of adsorbed power on the cell.

2.5 Energy consumption of mechanical flotation cells

In minerals processing the research of energy consumption has been conventionally concentrated on size reduction processes as they consume the largest proportion of energy. According to US Department of Energy (2010) cited by Lelinski et al. (2011) in mining and mineral processing the sub-process of flotation and centrifugal separation consume only 4% of the total energy spent. However, interest in improving the energy efficiency of flotation process has been increasing and studies of the topic have been carried out among others by Rinne and Peltola (2008), Coleman and Rinne (2011), Lelinski et al. (2011), Safari et al. (2016) and Tabosa et al. (2016). The size of flotation cells has been progressively increasing in recent years with more than 600 m³ cells being the largest available at the moment (Outotec 2016; Tabosa et al. 2016; FLSmidth 2019). The reason for development of larger cells is their ability to process larger amounts of feed material. As the trend in minerals processing is towards low grade ores consequently larger throughputs must be processed. Moreover, larger cells have economic advantages: fewer units require less maintenance and instrumentation but also building costs are lower as the footprint is smaller (Rinne and Peltola 2008). Furthermore, it was shown in the study of Rinne and Peltola (2008) that the relative energy consumption is smaller in large cells compared to smaller ones when comparing the same total flotation volume. Rinne and Peltola (2008) were examining the energy efficiency of different flotation cell arrangements with all having a total flotation volume of 1800 m³. The energy efficiency was a lot better in the case of six 300 m³ compared to 18 individual 100 m³ flotation cells.

Specific power is the power used per unit volume of a flotation cell (kW/m³). Power draw is the installed power per cell (kW). The increase of power draw (kW) is nearly linear with the increase in cell volume for the all cell sizes. However, the specific power decreases in small flotation cells with an increase in cell size. In flotation cells larger than 100 m³ the specific power stays constant around 1 kW/m³. Thus, large flotation cells are more efficient and have low installed specific power. (Tabosa et al. 2016)

Energy consumption in mechanical flotation cells is due to agitation and air supply (Rinne and Peltola 2008; Wills and Napier-Munn 2006, p. 307). Usually mechanical impeller comprises of rotor-stator combination with integrated air feed. Flotation cells can be divided into forced air and induced air cells in regard to the air flow mechanism (Deglon 2005). Integrated combination enables both the movement of slurry inside the flotation cell and creation of air bubbles and their dispersion throughout the cell. Thus impeller prevents sanding and allows particles to collide and attach to air bubbles. In addition to rotation speed the flotation cell's energy consumption is determined by the power transfer ratio of the drive mechanism and the air feed equipment (Rinne and Peltola 2008). (Wills and Napier-Munn 2006, p. 307; Yazar and Richter 2016, p. 25)

Rinne and Peltola (2008) were examining the total life cycle costs of flotation operations. The cost breakdown indicates that energy price forms 68% of all the flotation related costs over the product lifecycle of 25 years. Hence, the price of electricity and the energy efficiency of the flotation cell generate a significant share of total operational costs. The other costs taken into account in the study of Rinne and Peltola (2008) in addition to energy were capital, maintenance and reagents costs.

According to the study conducted by Rinne and Peltola (2008) minor reduction of the rotor tip speed is likely to have small effect on metallurgical performance of the cell but will lead to great savings on the energy consumption. This can be proven mathematically, see following equation 10,

$$P = N_p \rho N^3 D^5 \quad (10)$$

where P is the power dissipated in the tank (kW)

N_p is the power number

ρ is the slurry density (kg/m^3)

N is rotor tip speed (1/s)

D is diameter of rotor (m)

(Goel and Jameson 2012; Hemrajani and Tatterson 2004 cited by Tabosa et al. 2016)

as the power draw of the mixing mechanism is proportional to the third power of rotation speed. Thus, a minor reduction of the rotor tip speed may not have an effect on the flotation cell performance as the power draw and rotation speed are not directly

proportional. Rinne and Peltola (2008) calculated that 5% reduction of rotor tip speed results in savings of 15% in energy consumption. (Rinne and Peltola 2008)

Nevertheless, Lelinski et al. (2011) found a 3.14% increase in copper recovery by increasing a specific power input by 13.51% (kW/m^3). Similarly copper grade remained constant. In their study an extra investment of US\$500,000 in energy cost would produce additional US\$160 million in total revenue (Lelinski et al. 2011).

Variable speed drive allows adjustment of the rotor tip speed during normal operation (Rinne and Peltola 2008). Nowadays, many online analysis are made during the operation among others grade and recovery measurements. With the online data it would be possible to monitor the effect of rotor tip speed on the recovery and grade of the concentrate and properties of the cell feed and adjust the speed accordingly. According to Rinne and Peltola (2008) it is likely that every flotation cell in the same plant have a different optimal rotor tip speed. In order to optimize between the recovery and energy consumption it would be important to attach every individual cell into an automatized online control system.

3 DESIGN OF EXPERIMENTS

In this study the effect of rotor tip speed on flotation cell performance was examined via series of laboratory flotation tests conducted with Outotec GTK LabCell[®]. LabCell[®] is a laboratory scale batch flotation cell which is presented in detail in Figure 3. The design of experiments was constructed to represent industrial scale flotation plant conditions as well as possible. Outotec TankCell[®] e300 with 300 m³ of effective flotation volume was decided to use as a reference cell of industrial scale flotation.

In the study only the effect of rotor tip speed was monitored by its different levels. Other flotation parameters were kept as stable as possible. Air flow rate and pH were set to their target values and chemicals were dosed according to the recipe presented in appendix 1. The solids concentration of slurry was assumed to be constant in the beginning of every flotation test with the same amounts of feed within the flotation tests. Froth bed thickness varied in regard to the rotor tip speed. All the conditions were assumed to be similar between the reference tests that were executed with same rotation speeds. To ensure reasonable sample size for the scope of master's thesis the rotor tip speed was decided to be studied on four different levels. The values of rotor tip speeds used in laboratory tests were chosen based on industrial flotation plant conditions. The rotation speeds under examination were chosen by comparing the tangential speeds of Outotec TankCell[®] e300 1750 mm rotor and Outotec LabCell[®] 60 mm rotor. The tangential rotor tip speeds were calculated by equation 11:

$$v = 2\pi r\omega \quad (11)$$

where v is tangential speed (m/s)
 r is radial distance (m)
 ω is rotational speed (1/s).

Based on results presented in Table 1 and Table 2 such a rotor tip speeds were chosen to be used in laboratory tests that represent the Outotec TankCell[®] e300 motor power range 50% – 100%. Regular interval of tip speeds were chosen to be used and that is why rotor tip speeds 1100 rpm, 1400 rpm, 1700 rpm and 2000 rpm were chosen for laboratory tests. The rotor tip speeds used in the laboratory flotation tests are presented in Table 3. Higher (2300 rpm) and lower (900 rpm) tip speeds were tried to use but they

were found to be too high and low for the underlying conditions, primarily because of cell size and air flow rate.

Table 1. Tangential speed range of 60 mm rotor.

Rotor diameter 60 mm		
Rotor speed (rpm)	Rotor speed (1/s)	Rotor tip speed (m/s)
800	13.33	2.51
900	15.00	2.83
1000	16.67	3.14
1100	18.33	3.46
1200	20.00	3.77
1300	21.67	4.08
1400	23.33	4.40
1500	25.00	4.71
1600	26.67	5.03
1700	28.33	5.34
1800	30.00	5.65
1900	31.67	5.97
2000	33.33	6.28
2100	35.00	6.60
2200	36.67	6.91

Table 2. Tangential speed range of 1750 mm rotor.

Rotor diameter 1750 mm			
Motor control value (%)	Rotor speed (rpm)	Rotor speed (1/s)	Rotor tip speed (m/s)
0	0	0	0.00
10	7	0.12	0.64
20	14	0.23	1.28
30	21	0.35	1.92
40	28	0.47	2.57
50	35	0.58	3.21
60	42	0.70	3.85
70	49	0.82	4.49
80	56	0.93	5.13
85	59.5	0.99	5.45
90	63	1.05	5.77
100	70	1.17	6.41

Table 3. Comparison of rotor tip speed of laboratory flotation cell with industrial size flotation cell.

Tangential rotor tip speed (m/s)	Corresponding laboratory rotor tip speed (rpm)	Corresponding rotation speed of 1.75 m rotor (rpm)	Industrial flotation cell motor control value (%)
3.46	1100	37.7	53.90 %
4.40	1400	48.0	68.60 %
5.34	1700	58.3	83.30 %
6.28	2000	68.6	97.90 %

One of the rotor tip speeds under study represents the maximum motor control value of industrial flotation cell (i.e. reference level) and the rest of three represent slower rotation speeds. Previous studies have suggested that the high rotor tip speed is beneficial for the flotation rate (Deglon 2005). Many times flotation cells are operated with maximum power in everyday operation.

The execution order of test runs was randomized. One reference series of each flotation test was executed. If there was deviation in the circumstances of a flotation test a new replaceable test was performed. The sample size includes 8 flotation tests in total.

4 EXPERIMENTAL

4.1 Ore properties

The experiments were executed with Ni-Cu-PGE ore. Main sulphide mineral types of the ore are pyrrhotite, chalcopyrite and pentlandite. Copper and nickel concentrates are produced by froth flotation. Main copper mineral is chalcopyrite and nickel mineral pentlandite. Talc, serpentine and amphibole are the main gangue minerals. Pyrrhotite represents the main sulphide gangue mineral in the ore. Minerals appear in the ore in low concentrates which makes the operation challenging. The head grades of the examined ore are generally ~0.3% Cu and ~0.25% NiS and the approximate produced concentrate grades in industrial scale are ~25% and ~11% for copper and nickel, respectively. Total copper recovery in industrial scale is around 71% and nickel recovery around 60%.

4.2 Preparations

To prepare for the flotation tests Ni-Cu-PGE ore which had been delivered to the University of Oulu about six months before was crushed. Crushing was executed by Oulu Mining School Mini Pilot's jaw (Metso minerals Morse jaw crusher) and cone (Metso minerals Marcy gy-roll crusher) crushers into a < 4 mm particle size. After crushing, the material was homogenized and split into equal batches of 600 g each.

4.2.1 Grinding tests

Next, grinding tests were performed to examine the optimal grinding time. Wedag's rod mill was used to comminute the ore with 30 Hz frequency. The target grain size was P_{80} 75 μm . Particle size was analysed with optical Cilas 1190 particle size analyser. The results of grinding tests (Figure 2) shows that 40 minutes grinding time would be optimal for grinding of 600 g ore into particle size P_{80} 75 μm .

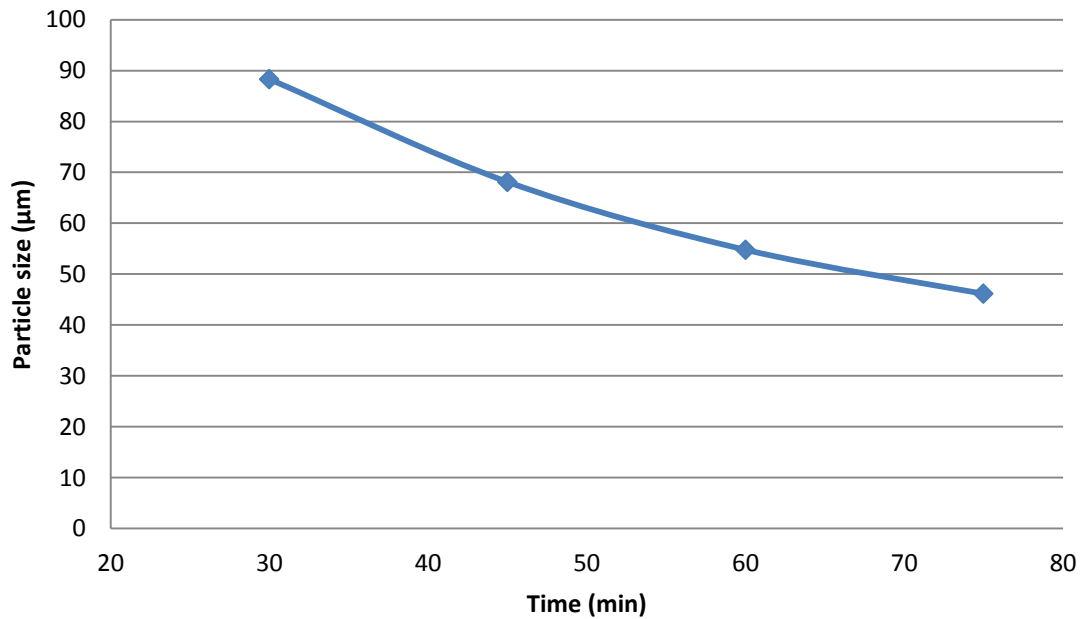


Figure 2. Results of the grinding tests performed with 600 g of crushed ore.

After initial grinding tests the amount feed was decided to increase by 100 grams in total in order to reach flotation feed of 1.9 kg and solids fraction by mass of 24.37%. According to the particle size analysis it was noticed that 40 minutes grinding time was not adequate and that is why 50 minutes of grinding time was used in order to comminute 633.33 g of crushed ore into the target P_{80} 75 µm particle size. Solids fraction of the grinding feed by mass was 61.29%. Particle size of the each flotation test feed was analysed with Cilas 1190 particle size analyser and the results are presented in Figure 32.

4.2.2 Accuracy of equipment

The rotation speed of the 60 mm rotor was checked by measuring it with tachometer. The results of measurements are presented in Table 4. It can be seen that the readings of Outotec LabCell[®] rotor tip speeds corresponds well with the measured values verified by tachometer with having the margin of error less than ± 10 rpm on the measured speeds. It should be remembered that there may be a slight error in the tachometer calibration as well.

Table 4. Rotation speed check-up of Outotec LabCell[®] 60 mm rotor.

Outotec LabCell [®]	Tachometer	Margin of error
200 rpm	198 rpm	1 %
1500 rpm	1494 rpm	0.40 %
1800 rpm	1793 rpm	0.39 %
2000 rpm	1992 rpm	0.4 %

Moreover, the accuracy of pH meter was checked with manufacturer's calibration solutions. The results presented in Table 5 show that the measuring device was performing with sufficient accuracy.

Table 5. pH meter check-up at 20.6 °C temperature.

Calibration solution	pH meter
10	10.2
7	7.2

4.2.3 Preparation of chemicals

In flotation tests carboxy methyl cellulose (CMC) was used as a depressant, Aerophine 3418A (sodium-diisobutyl dithiophosphate) as copper collector, sodium isopropyl xanthate (SIPX) as nickel collector and Dowfroth 250 (1-(1-methoxypropan-2-yloxy)propan-2-ol) as frother. Moreover, calcium oxide (CaO) was used for pH control.

Flotation chemicals were prepared in several occasions. All the chemicals were prepared with using deionized water. As xanthates decompose rapidly a new 1% SIPX solution was prepared on every Monday so that the chemical used on flotation tests was always prepared less than a week before. 1% CMC, 1% Aerophine 3418A and 10% CaO were prepared on 20.11.2018. When preparing CMC solution it was mixed for couple of hours with magnetic stirrer to dissolve the solid CMC with deionized water. Same CMC solution was used in all of the flotation tests. A new 1% Aerophine 3418A solution was prepared on 8.1.2019 and it was used on rest of the flotation tests. Dowfroth 250 was used as 100% solution and the same solution was used for all of the tests. Chemical solutions were stored in a fridge in between the flotation tests except 10% CaO was stored in room temperature.

4.3 Machinery

Outotec GTK LabCell[®] is a batch flotation machine for laboratory tests. There are 2 l, 4 l, 6.5 l and 8 l volume of cells available with equivalent rotors, stators and froth scrapers. The flotation cells are made of plastic. In the tests in question, 2 l and 6.5 l flotation cells were used with 45 mm and 60 mm rotors, respectively. The flotation machine is introduced in Figure 3 and rotor and stator designs are presented in Figure 4 and Figure 5.

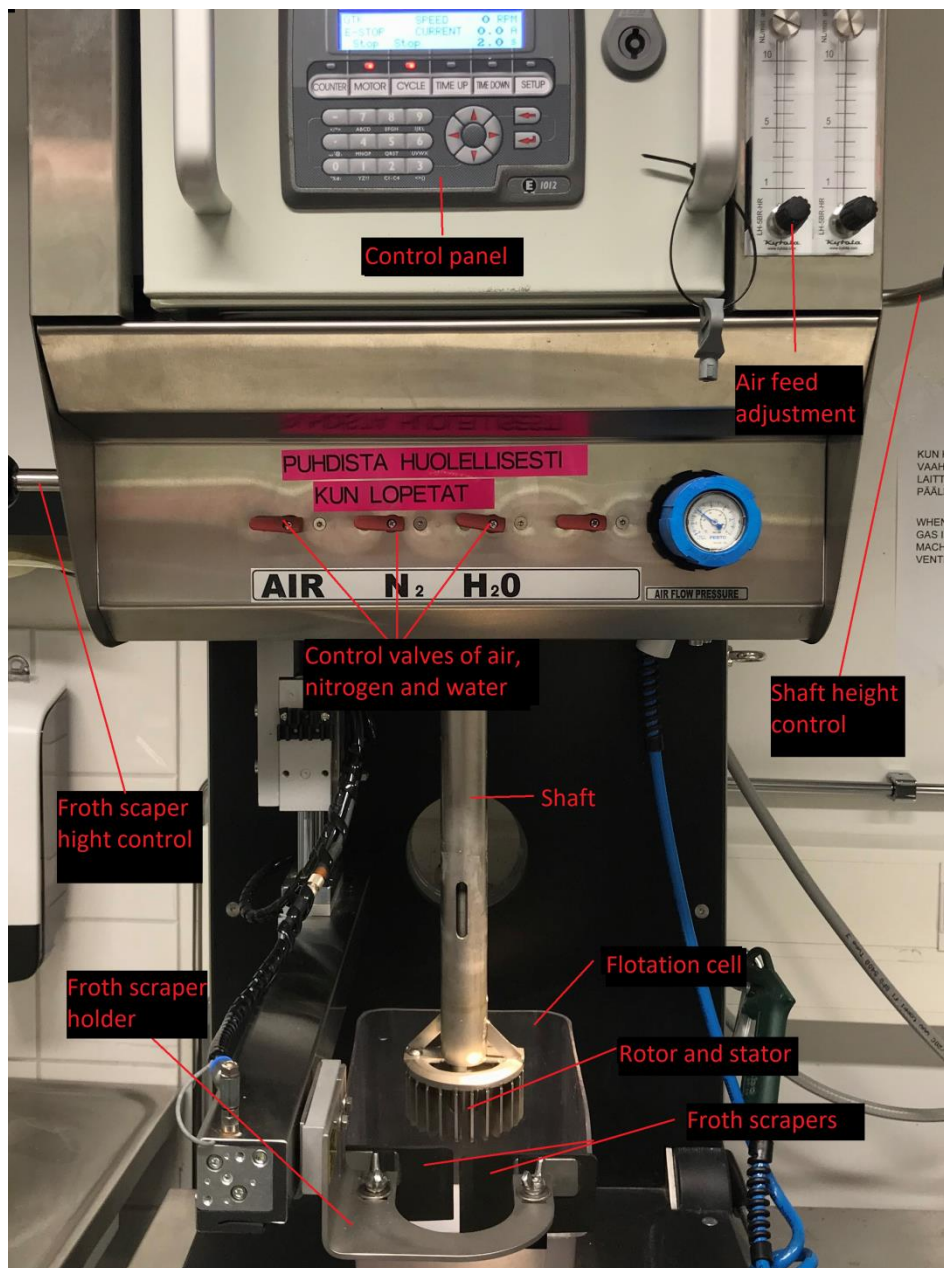


Figure 3. Introduction of the Outotec GTK LabCell[®] flotation machine.

The design of LabCell[®] is very similar to industrial scale flotation machine. For example the rotor and stator design are very similar to the industrial scale design of Outotec's products with only the scale being different. The biggest difference is the nature of batch process in laboratory conditions which creates some challenge in the operation. For example, the froth recovery differs in such a way that the froth is recovered with froth scrapers (Figure 4) into a separate collection dish. Thus, to ensure sufficient and uniform froth recovery the slurry level must be controlled precisely. The slurry level is controlled manually by water addition based on visual observation. Moreover, the recovery of concentrate decreases the solids concentration of slurry as a feed material is not added in this batch flotation test as the flotation proceeds. The water addition to maintain the slurry level further decreases the solids concentration. The conditions of laboratory flotation cell are examined further in chapter 6.5.



Figure 4. Outotec LabCell[®] froth scraper, rotor and stator designs.

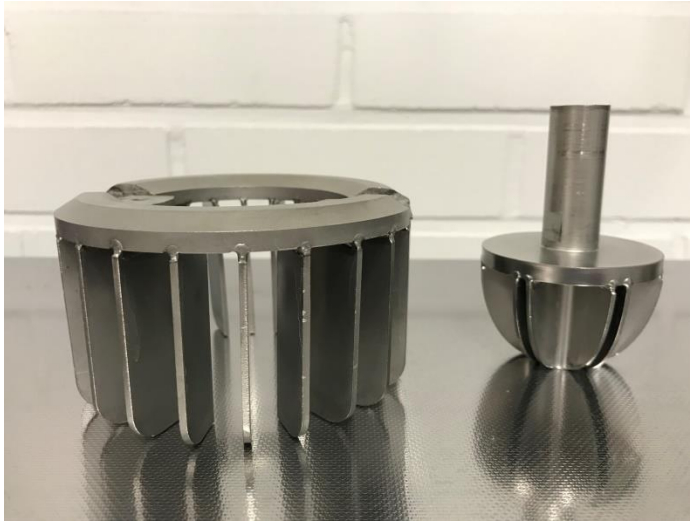


Figure 5. Outotec LabCell[®] rotor and stator design. There is 60 mm rotor with the applicable stator in the picture.

4.4 Flotation test procedure

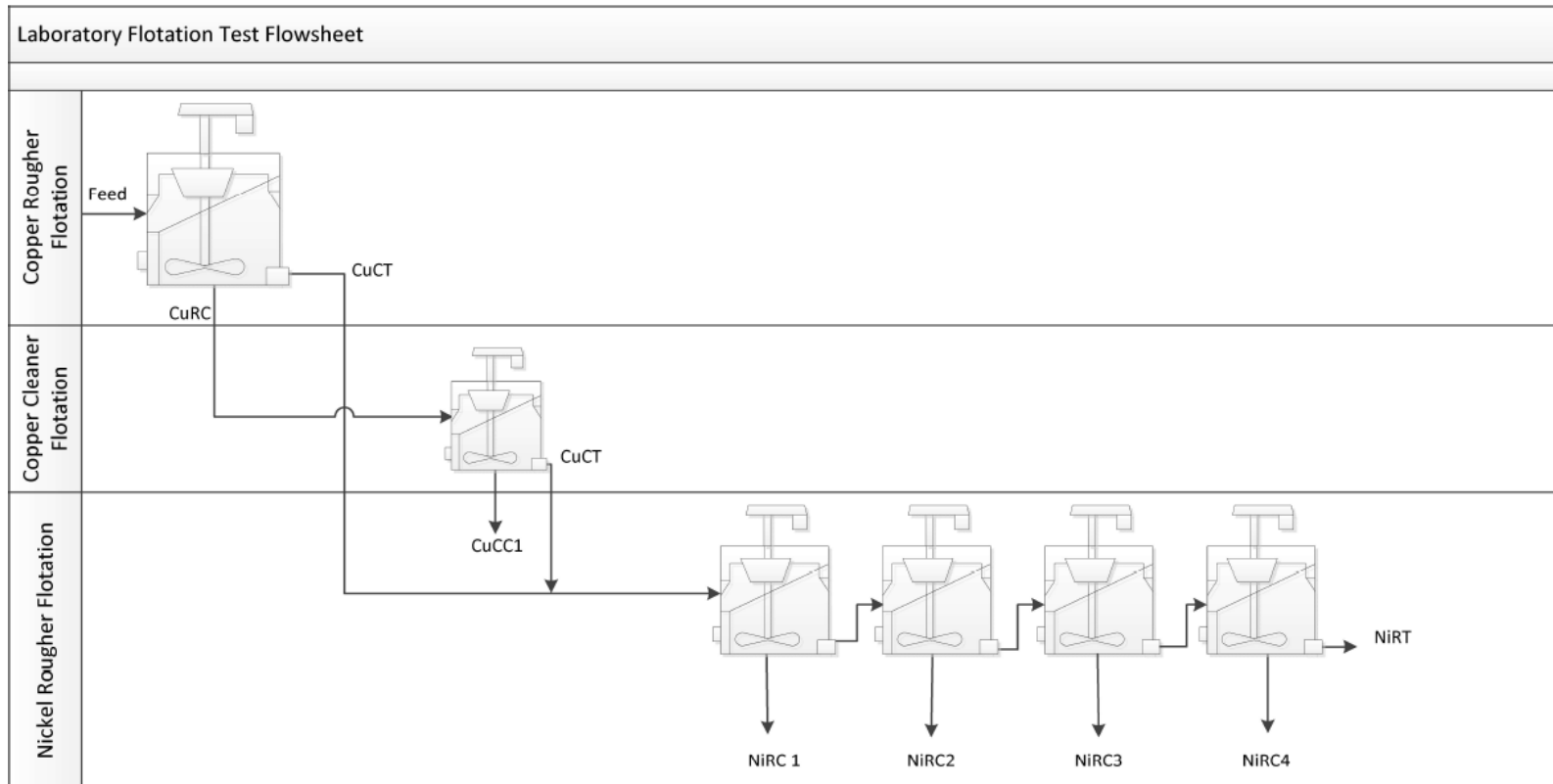


Figure 6. Laboratory flotation test flowsheet.

Flotation test was begun by grinding 1.9 kg of feed material into a particle size P_{80} 75 μm . Grinding was executed in three phases so that each of them contained 633.33 g crushed ore and 400 grams of water resulting solids concentration of slurry by mass 61.29%. All the water used in the tests was tap water of Oulu except chemical solutions were prepared with deionized water. Grinding mill was filled with 7 rods and grinding time of 50 minutes was used. Grinding was executed just prior to each flotation test to avoid oxidation.

The purpose of laboratory flotation tests was to simulate industrial scale flotation plant performance. Because of the properties of the ore every flotation test was begun by copper flotation even though the actual test was performed for nickel flotation. The flotation test was performed as sequential flotation where the tailings of copper flotation are the feed of nickel flotation. The complete flowsheet of laboratory flotation tests is presented in Figure 6. First, copper rougher flotation having solids concentration by mass 24.37% was performed in natural pH but the pH was measured and written down in the beginning of every flotation test. After pH testing 0.95 ml 1% Aerophine 3418A and 38 μl 100% Dowfroth 250 were added and conditioning time of 2 minutes was used with 1800 rpm rotor tip speed. Flotation was begun by opening the air valve into 4 l/min and starting the automatic froth scrapers. The waiting time of froth scrapers was set on 0.0 seconds in all of the flotation tests thus taking 10 seconds for one cycle. Flotation time of 10 minutes was used. The copper rougher flotation is illustrated in Figure 7.



Figure 7. Copper rougher flotation with 1800 rpm rotor tip speed and air flow 4 l/min.

The copper rougher concentrate (CuRC) was refloatated in cleaning flotation stage which increases the copper grade and provides more copper-free tailings for nickel flotation. In order to adjust the slurry level into a necessary level the copper cleaner concentrate was diluted with water from copper rougher tailings. The tailings flotation cell was let to settle down for a moment after which rather clear water was taken from the surface with decanter to adjust the slurry level. Thin layer of copper minerals was observed on the surface of settled water. Evidently, a small amount of copper has been added to the copper cleaner flotation feed manually and thus the copper recovery can be assumed to have improved slightly.

Adjusting slurry level with the settled tailings water was necessary as the amount of copper rougher concentrate was rather small and the reason for using particularly settled tailings water was that no fresh water can be added to the system as the copper rougher tailings and copper cleaner tailings were combined to form nickel rougher flotation feed. Adding fresh water would have both increased the volume too large and simultaneously it would have diluted the solids fraction of the nickel flotation feed.

For the copper cleaning flotation 0.95 ml 1% CMC was used as depressant, 0.95 ml 1% Aerophine 3418A was used as collector and 9.5 μ l 100% Dowfroth 250 was used as frother. Before adding the flotation chemicals pH was adjusted to 10.5 with 10% CaO. After one minute conditioning time flotation was begun by opening the air valve into 2 l/min. Copper cleaning flotation (Figure 8) was executed for 6 minutes in 2 l flotation cell with 45 mm rotor having a rotation speed of 1100 rpm. At the end of the flotation the copper cleaner flotation concentrate was filtered and washed with water.



Figure 8. Copper cleaning flotation in 2 l flotation cell with 45 mm rotor having the speed of 1100 rpm and air flow rate of 2 l/min.

Nickel rougher flotation was performed in 6.5 l flotation cell using 60 mm rotor with the applicable stator. At first the copper rougher flotation tailings (CuRT) and copper cleaner flotation tailings (CuCT) were combined as written previously. pH was adjusted to 9.8 with 10% CaO. Usual CaO dosage was about 1 ml. Next flotation chemicals including 2.85 ml 1% CMC, 9.5 ml 1% sodium isopropyl xanthate (SIPX) and 19 μ l 100% Dowfroth 250 were added in aforementioned order. Flotation was begun after 1 minute conditioning time with 4 l/min air flow and the rotation speed under

investigation. The tests were performed with rotation speeds 1100, 1400, 1700 and 2000 rpm.



Figure 9. NiRC1 flotation with 1400 rpm rotor tip speed and 4 l/min air flow rate. It can be visually estimated that there is chalcopyrite left in the feed of nickel flotation and it is concentrating in NiRC1 concentrate.

The nickel rougher flotation was carried out in four stages so that the tailings from a previous flotation phase were the feed of the next phase. To compare the laboratory test with industrial flotation plant the NiRC1 and NiRC2 were presenting rougher flotation cells in industrial scale and NiRC3 and NiRC4 were presenting the scavenger flotation cells. First stage of nickel rougher flotation is illustrated in Figure 9. After the first nickel rougher concentrate (NiRC1) had been collected for 7.5 minutes the tailings were continued to float (NiRC2) without add of any chemicals. NiRC2 flotation time was 7.5 minutes as well. NiRC2 flotation is illustrated in Figure 10.



Figure 10. NiRC2 flotation with 1700 rpm rotor tip speed and air flow rate 4 l/min.

In the beginning of NiRC3 flotation (Figure 11) xanthate was added to intensify the flotation. After dosing 5.70 ml 1% SIPX one minute conditioning time was applied after which flotation was begun by opening the air valve into 4 l/min and starting the froth scrapers. Flotation time of 12.5 minutes was used. Lastly, for nickel rougher flotation 4 (Figure 12) the tailings from NiRC3 flotation were continued to float yet another 12.5 minutes without add of any chemicals. The total active flotation time applied in nickel rougher flotation was 40 minutes. However, the total length of one flotation test series including copper flotation and all the preparations took about three hours.



Figure 11. NiRC3 flotation with 1700 rpm rotor tip speed and 4 l/min air flow rate.



Figure 12. NiRC4 flotation with 1700 rpm rotor tip speed and 4 l/min air flow rate.

After flotation tests all the concentrates and tailings were filtered and washed with water. Whatman grade 589/3 (retention $< 2 \mu\text{m}$) slow filter paper was used for all the concentrates and Whatman grade 1442-240 filter paper (retention $2,5\mu\text{m}$) for tailings. After filtration the concentrate cakes were dried in $80 \text{ }^\circ\text{C}$ oven over a night. On the following morning the dry materials were weighted and packed in plastic bags. The concentrates and tailings were stored in a freezer.

5 SAMPLE ANALYSIS

5.1 Methods, sample preparation and analysis procedure

Mineral grades were analyzed with X-ray fluorescence (XRF) spectrometer. Wavelength dispersive XRF spectrometer was used in the analysis to produce a reliable data because of its accurate detector. Energy dispersive portable XRF spectrometer is generally used in field conditions. (Gallhofer and Lottermoser 2018)

A XRF pellet was prepared by adding 6% of carbon wax to the sample and mixing them with wolfram-carbide-cobalt mortar. A 7 g briquette was prepared from the mixture with a hand press. The briquette may include some contamination from the mortar.

The produced concentrates and tailings were analyzed with Axios Max XRF analyze device produced by Panalytical. The device has a Rh-tube as X-ray generator with maximum power of 4 kW. SuperQ analysis program was used to analyze the pressed pellets. Magnesium (Mg), aluminum (Al), silicon (Si), calcium (Ca), chromium (Cr), iron (Fe), copper (Cu) and nickel (Ni) were analyzed. The analyses were done in The Center of Microscopy and Nanotechnology in the University of Oulu.

The results of XRF analyses are presented in appendix 2. Recoveries were calculated by the measured grades and masses of concentrates presented in Table 7. Recoveries were calculated by the equation 1.

The results presented in the study are based on measurements of wavelength dispersive X-ray fluorescence spectrometer (XRF). The method is considered to be reliable. The device informs the total amount of detected elements as percentage of the total amount of material. In none of the measurement the amount was 100%. There was fluctuation in the detection rate so that in part of the measurements the rate was close to 100% and in some it was significantly less. It would have been possible to transform the detection result to correspond 100%. However, it was not executed as it would have enlarged the grades of each element which was thought to cause more deviation in the results than without the transformation.

6 RESULTS AND DISCUSSION

The results of laboratory batch flotation tests are presented in this chapter. Majority of the results are presented either in regard to rotor tip speed with the date of testing or flotation phase. The tested rotor tip speeds with corresponding testing days are presented in Table 6. The effect of rotor tip speed was tested with four different speeds. One reference series was performed. Four nickel concentrates were collected in each of the flotation tests. The collected concentrates are designated as nickel rougher concentrate 1, 2, 3 and 4 with corresponding abbreviations NiRC1, NiRC2, NiRC3 and NiRC4. The flotation test series describe the performance of rougher flotation cells in a row so the results can be interpreted to describe individual flotation cells. The exact flotation test procedure is presented in chapter 4.4.

Calculations and graphs are based on calculated feed grade values. The grade of main feed is evaluated based on the sum of individual concentrates' grades and the total mass of concentrates and tailings in the test in question. The grade of nickel flotation feed is determined by subtracting the amount of nickel lost in copper flotation from the total nickel content in the feed. Moreover, the single cell performance is examined based on calculated feed grades of each of the cells. As the experiment was a batch flotation test it was not possible to take a sample of feed of each flotation cell because of the loss of material. The grade of each feed is estimated based on the total nickel recovery and amount of nickel recovered in each concentrate which gives more reliable result over the option that the actual analyzed feed grade would have given. The result is more reliable because the material losses are taken into account. The analyzed grades and all the calculations that the discussed figures are based on are provided in appendices 2, 3 and 4.

Table 6. Test arrangement

Date	8.1.2019	28.1.2019	14.12.2018	21.1.2019	10.12.2018	11.1.2019	3.12.2018	9.1.2019
Laboratory rotor tip speed (rpm)	1100 rpm	1100 rpm	1400 rpm	1400 rpm	1700 rpm	1700 rpm	2000 rpm	2000 rpm
Corresponding rotor tip speed (m/s)	3.46 m/s	3.46 m/s	4.40 m/s	4.4 m/s	5.34 m/s	5.34 m/s	6.28 m/s	6.28 m/s

6.1 Properties of nickel flotation feed

The properties of nickel flotation feed are determined based on the result of copper cleaning flotation. Unfortunately, it can be seen on the results that the feed properties were not equal between the different flotation tests. Thus, part of the deviation in latter nickel rougher flotation can be assumed to derive from the unequal contents of nickel and copper in the feed.

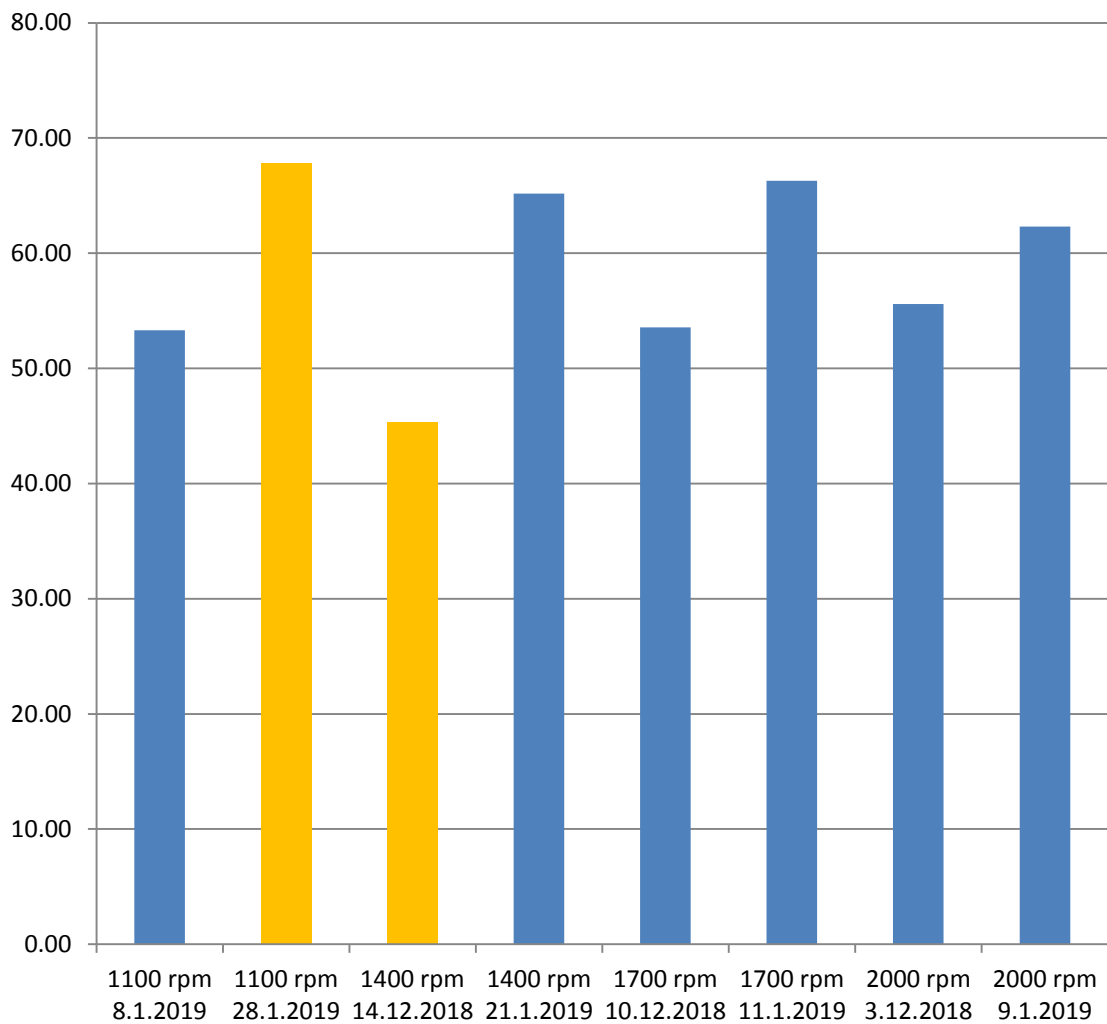


Figure 13. Copper recoveries (%) in copper cleaning flotation concentrates.

There is variation in the copper recoveries of different flotation tests as presented in Figure 13. The copper recovery is varying between 45%-68% in different flotation tests. This can be assumed to lead in variation in the copper content of nickel flotation feed as the main feed is assumed to be uniform in regard to nickel and copper content.

Moreover, the fluctuations in nickel recoveries to copper concentrates (Figure 14) are likely to cause variation in the nickel flotation feed.

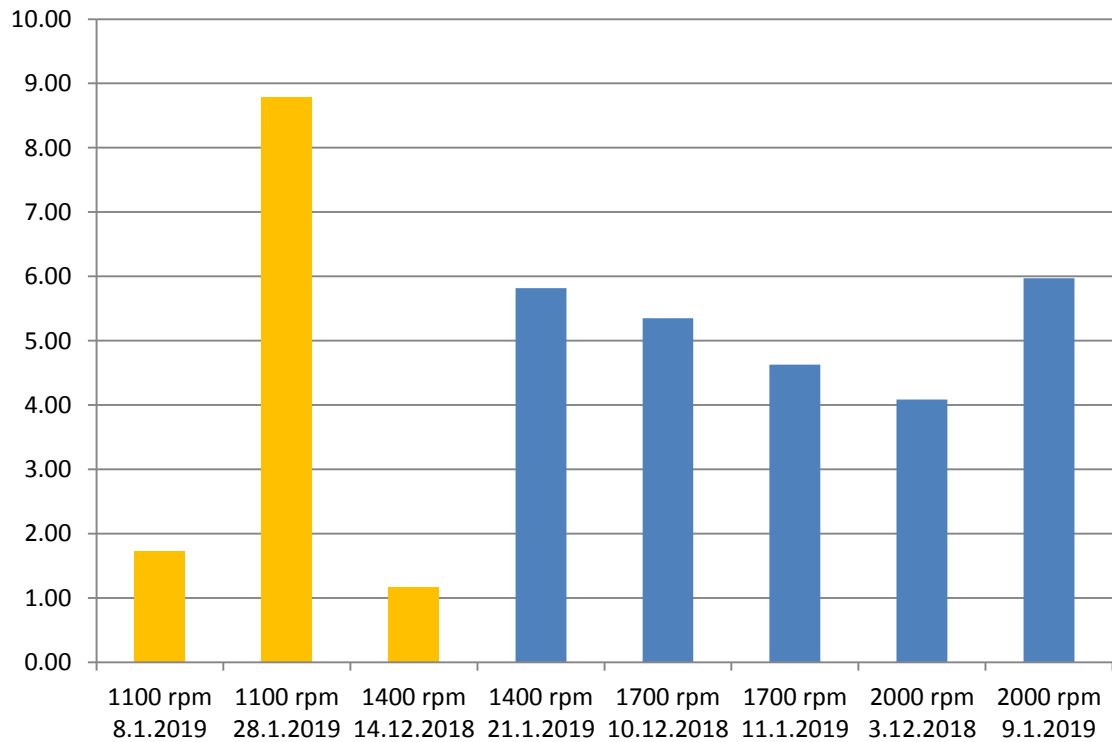


Figure 14. Nickel recoveries (%) in copper cleaning concentrates.

The Figure 14 shows that the nickel content is extremely low in two of the copper cleaning concentrates (8.1.2019 1100 rpm and 14.12.2018 1400 rpm) and exceptionally high in the concentrate 28.1.2019 1100 rpm.

It can be observed based on Figure 13 and Figure 14 that the copper and nickel recovery to the copper cleaning concentrate seems to have a slight interdependence as the copper and nickel recovery is the smallest (1100 rpm 8.1.2019 and 1400 rpm 14.12.2018) and highest (1100 rpm 28.1.2019) in the same tests in Figure 13 and Figure 14. When the copper recovery is low there is more copper and nickel left in the nickel flotation feed while copper recovery being high there is evidence that also nickel is recovered to copper concentrate resulting to smaller nickel content in the nickel flotation feed. Based on that can be assumed that the selectivity was not successful between nickel and copper in copper cleaning flotation.

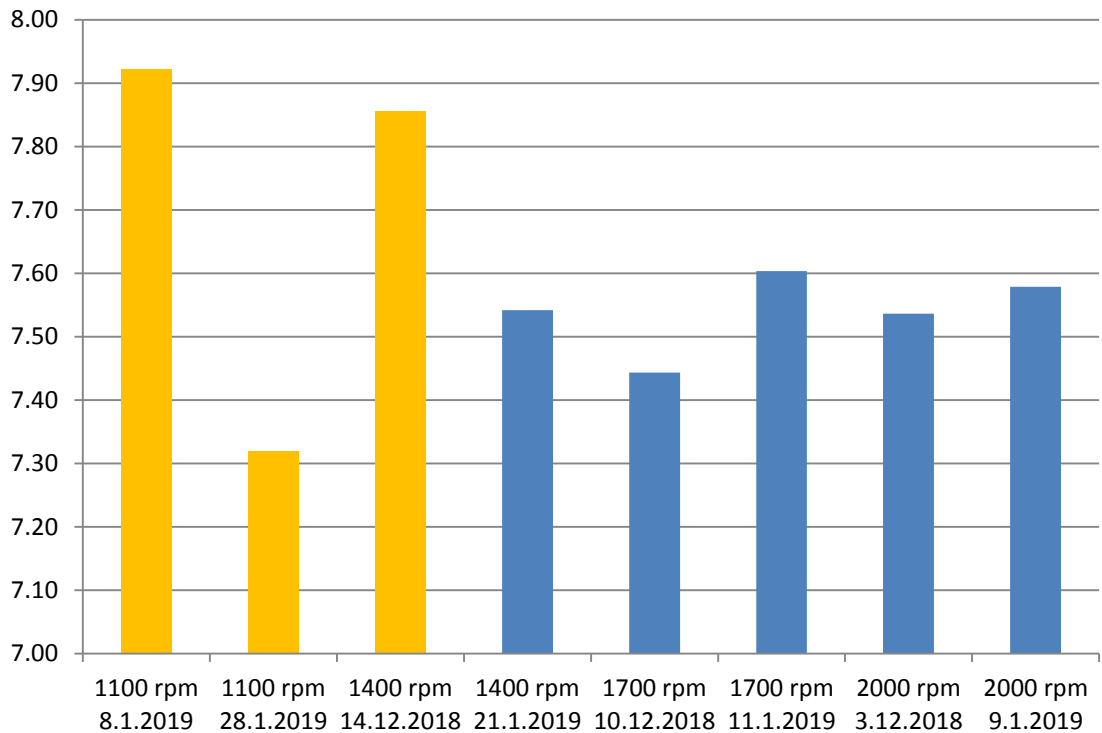


Figure 15. Nickel content of nickel flotation feed (g).

The nickel content of nickel flotation feed in grams presented in Figure 15 is calculated based on analysed nickel grades and masses of concentrates and tailings. There is variation in the nickel content of nickel flotation feed between the flotation tests. The flotation tests of 1100 rpm 8.1.2019, 1100 rpm 28.1.2019 and 1400 rpm 14.12.2018 are differentiating especially from the rest of the tests. The nickel content is fluctuating within 0.6 grams between the flotation tests which is around 8% of the average mass of pure nickel in the feed. The variation is considered to be rather significant and may cause divergence to the recovery values of nickel concentrates. If the increased nickel content in feed ended up in nickel concentrate for example in the case of 1100 rpm 8.1.2019 the additional 0.4 g would mean 5%-units increase in recovery and 0.4%-units increase in concentrate grade.

The fluctuation in Figure 15 can be concluded to originate from the selectivity differences in the copper cleaning flotation. When comparing the Figure 14 and Figure 15 there can be seen exactly inverse pattern of fluctuation between the nickel recovery in copper concentrate and nickel content of nickel flotation feed. The reason for that is the uniformity of main feed in regard to nickel content. The inverse pattern proves the accuracy of measurements.

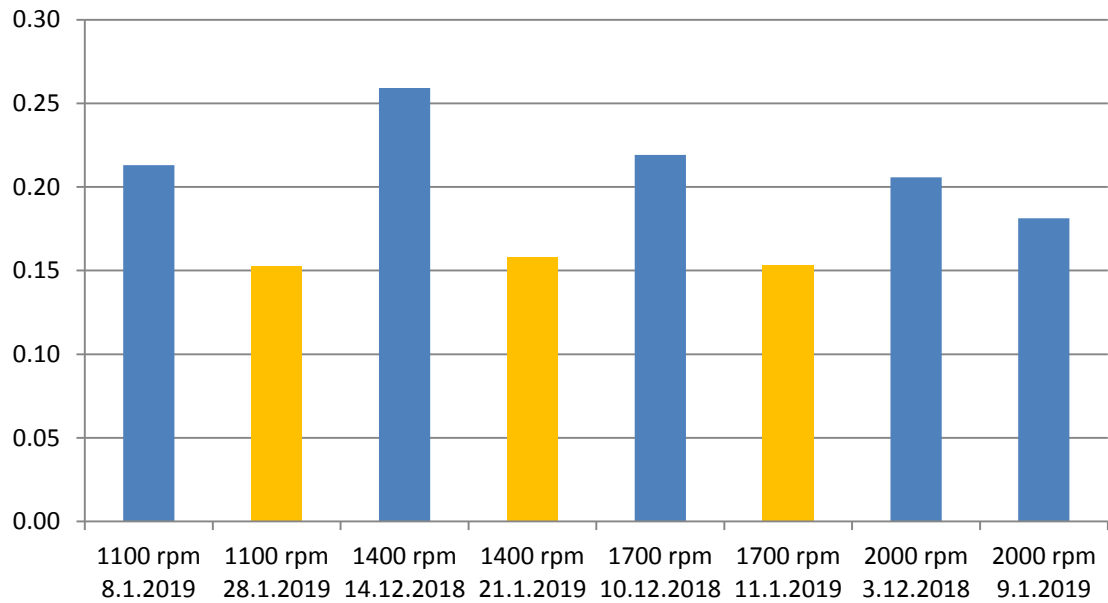


Figure 16. Copper grade of nickel flotation feed (%).

The Figure 16 shows that there are fluctuations in the copper content of nickel flotation feed which can be assumed to cause interference in the nickel rougher flotation. Biggest differences can be seen between the pairs of reference tests 1100 rpm, 1400 rpm and 1700 rpm. The conditions were rather uniform between the tests 2000 rpm in regard to copper content. As seen in Figure 16 the copper content was uniform between flotation tests 1100 rpm 28.1.2019, 1400 rpm 21.1.2019 and 1700 rpm 11.1.2019.

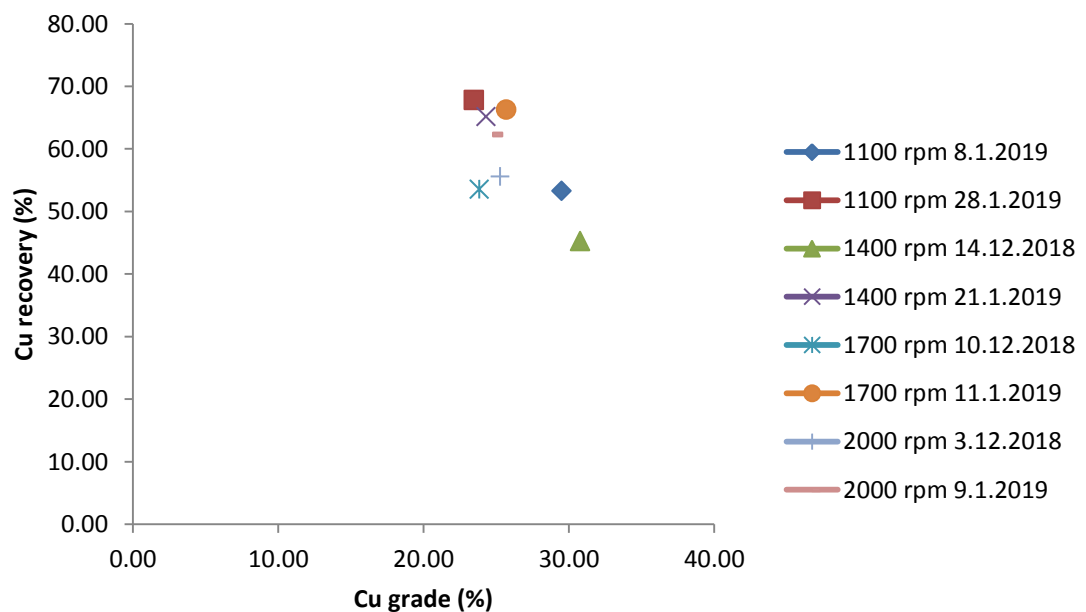


Figure 17. Copper recoveries vs. grades in copper concentrate (%).

The grade-recovery relationship of CuCC1 concentrates presented in Figure 17 describes the overall performance better than individual grade and recovery graphs. It can be seen in Figure 17 that there is fluctuation in the grade-recovery values of copper concentrates. The copper flotation was performed in similar conditions in all of the flotation tests and ideally there would not be any variation. Part of the variation can be explained by the mineralogical differences of the feed. It may be seen in Figure 17 that there is a conglomeration in regard to copper content with one series of each of the flotation conditions. The flotation tests of 1100 rpm 28.1.2019, 1400 rpm 21.1.2019, 1700 rpm 11.1.2019 and 2000 rpm 9.1.2019 are having similar values in regard to copper content of nickel flotation feed. Thus, it would be recommended to compare the series of mentioned tests when examining the performance of nickel flotation.

The reproducibility and the evenness of the nickel flotation conditions can be assessed by the results of copper flotation. Results of nickel flotation are disturbed by the rotor tip speed variation and sample size of two is not enough to assess the reproducibility reliably. The copper flotation results vary to a certain extent even though the conditions were kept uniform. As can be seen in Figure 13 the level of copper recoveries vary between 45.3% and 67.8% and the grades of copper cleaning concentrates presented in appendix 3 fluctuate between 23.5% and 30.8% in the eight performed flotation tests. The fluctuation in the values of copper flotation grades and recoveries can be considered to be significant and so the reproducibility of tests can be assumed to be rather low.

Table 7 presents the amounts of all the recovered concentrates and tailings. The masses of collected concentrates and tailings are illustrated in Figure 18 and the total amounts of collected material i.e. the calculated feeds are illustrated in Figure 19. The total sum of concentrates and tailings is used as a reference value for the amount of each flotation feed. All the recovery calculations are based on the total sums. There are no big fluctuations in the total amounts of collected material (Table 7, Figure 19) but there are moderate fluctuations in the sizes of individual concentrates (Figure 18). The masses of recovered concentrates presented in Table 7 are used when calculating the recoveries for example.

Table 7. Masses of concentrates and tailings (g).

Rotor tip speed	1100 rpm	1100 rpm	1400 rpm	1400 rpm	1700 rpm	1700 rpm	2000 rpm	2000 rpm
Date	8.1.2019	28.1.2019	14.12.2018	21.1.2019	10.12.2018	11.1.2019	3.12.2018	9.1.2019
CuCC1	15.14	25.16	12.66	22.27	19.19	21.48	18.33	21.95
NiRC1	25.21	50.20	43.59	52.60	46.99	81.15	88.99	102.05
NiRC2	21.69	26.57	31.91	35.25	41.73	29.97	27.16	33.70
NiRC3	34.25	36.26	27.32	39.74	30.97	35.33	39.68	41.72
NiRC4	23.66	25.39	17.52	34.49	33.38	22.14	42.90	30.57
NiRT	1732.03	1694.73	1696.63	1670.00	1657.24	1661.71	1599.44	1605.80
Total	1851.98	1858.31	1829.63	1854.35	1829.50	1851.77	1816.50	1835.78

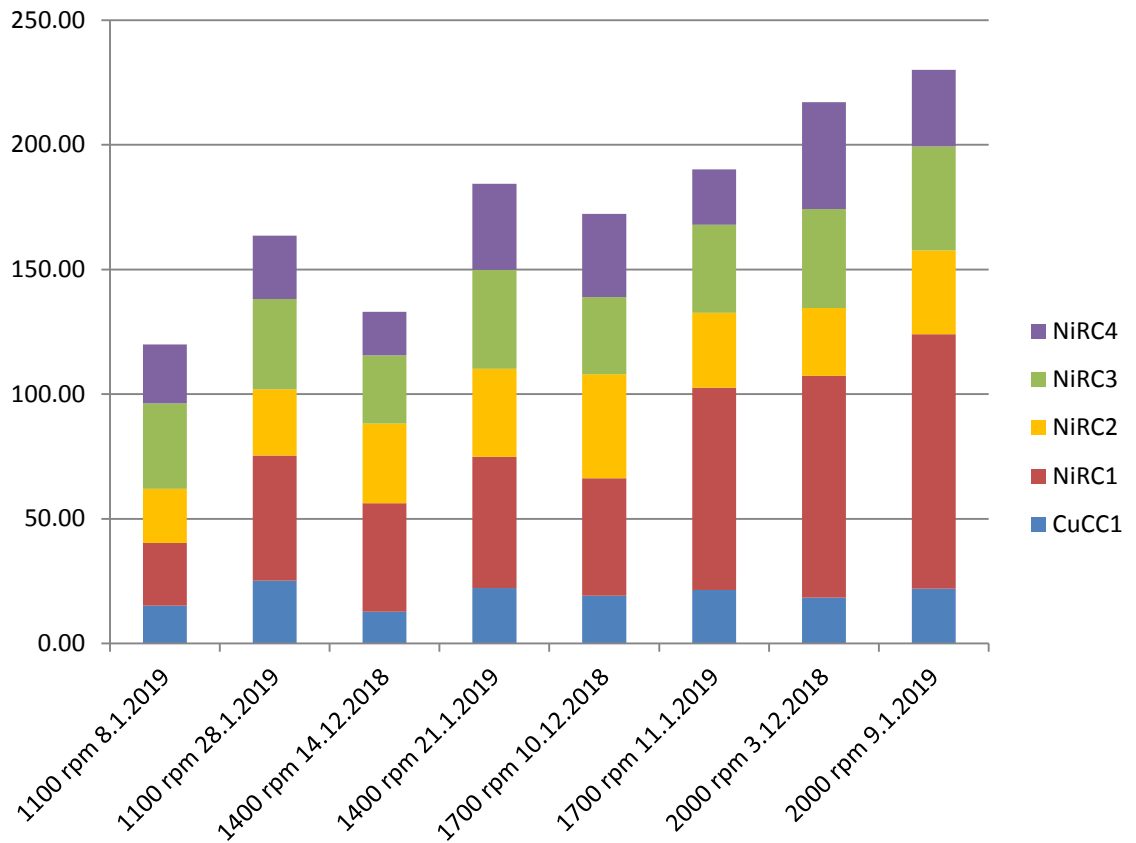


Figure 18. Masses of concentrates (g).

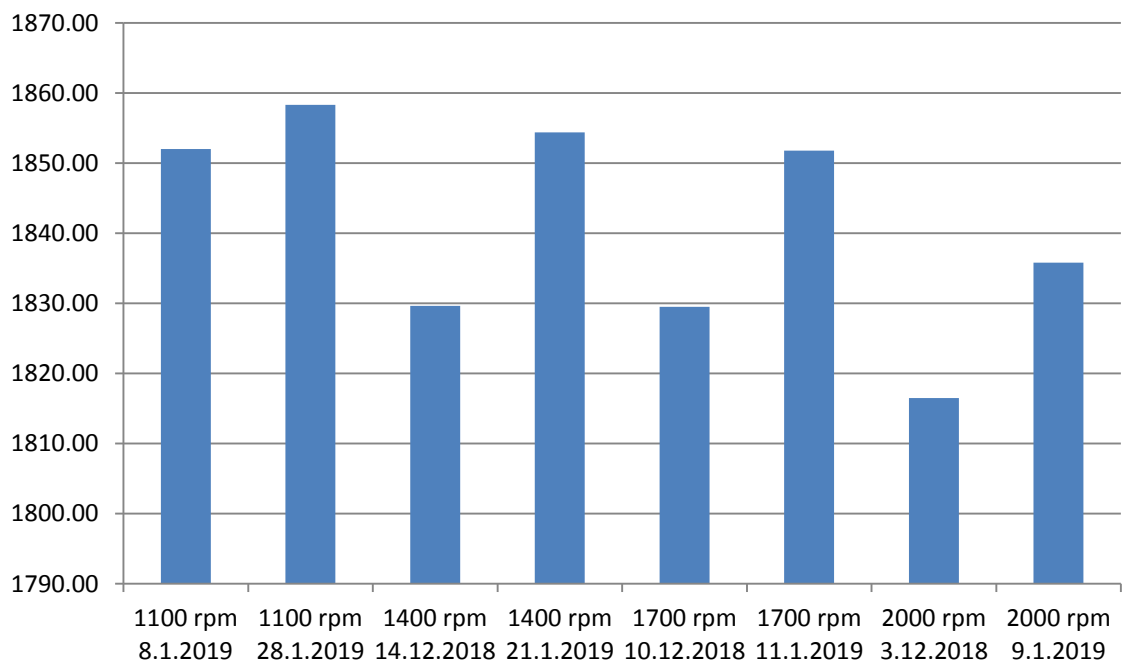


Figure 19. Total mass of collected material (g).

Based on information in Table 7 and Figure 18 can be seen that the amounts of copper cleaning concentrates (CuCC1) of flotation tests 1100 rpm 8.1.2019 and 1400 rpm 14.12.2018 were distinctly the smallest. The amount of recovered concentrate is affecting directly to the calculated recovery of mineral. As copper recovery in copper concentrate is the lowest in tests 1100 rpm 8.1.2019 and 1400 rpm 14.12.2018 (Figure 13) and the copper content of nickel flotation feed high compared to their reference tests (Figure 16) the increased copper content in nickel flotation feed is likely disturb the nickel flotation as copper is floated more easily than nickel.

Furthermore, the effect of rotor tip speed can be detected in Figure 18. There is a clear trend in the Figure 18 with the amount of collected concentrate (g) increasing with an increasing rotor tip speed. The total mass of collected material is almost two fold in flotation test 2000 rpm 9.1.2019 compared to 1100 rpm 8.1.2019. The biggest fluctuations can be seen in NiRC1 concentrates. The increase of rotor tip speed can be detected to improve especially the material recovery in the first phase of flotation.

6.2 Performance of nickel flotation

The analysis of nickel flotation tests are based on calculated nickel feed grades. When calculating the recovery of a nickel concentrate the amount of concentrate is compared to the detected amount of nickel in the nickel flotation feed after the copper flotation. The nickel collected in copper concentrate is excluded from the calculations. This approach takes into account the deviation of nickel flotation feed due to fluctuation in copper flotation and it describes well the actual enrichment conditions. However, when comparing the different flotation conditions the different contents of minerals in the feeds should be taken into account.

Cumulative recoveries and grades of each of the tests were calculated to evaluate the overall performance of individual flotation tests. For the cumulative recovery the individual values of recoveries NiRC1-NiRC4 were summed together. To calculate the cumulative grade the grades of individual concentrates NiRC1-NiRC4 were proportioned to the masses of recovered concentrates.

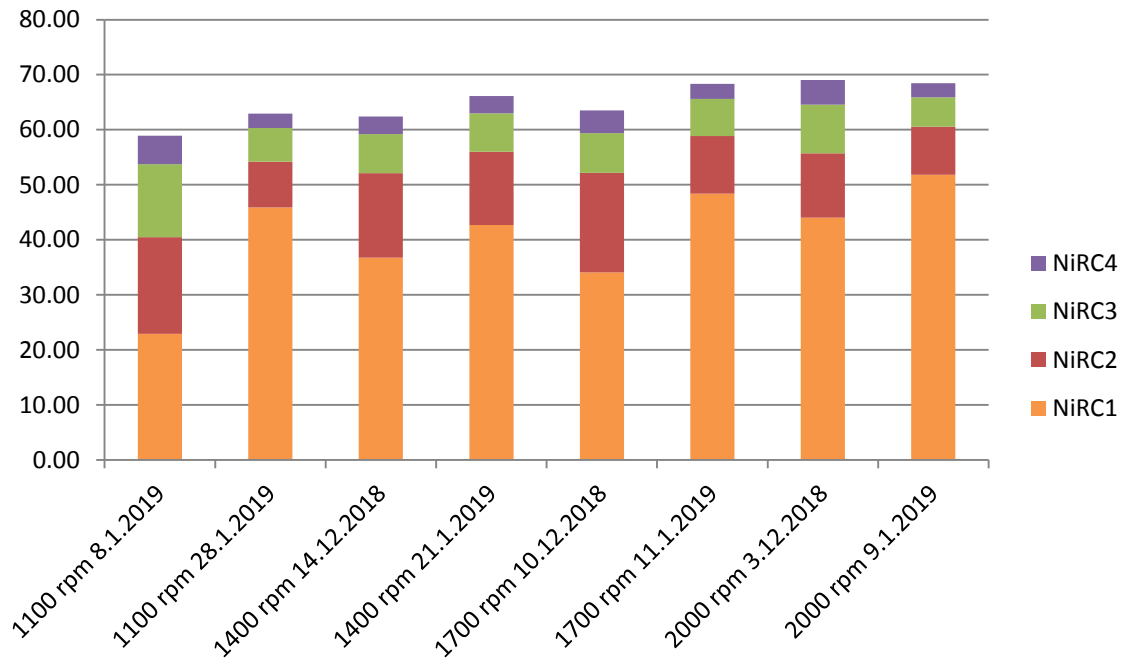


Figure 20. Cumulative nickel recoveries by flotation phases (%).

In the Figure 20 cumulative nickel recoveries are presented by flotation phases with all of the tested rotation speeds. There can be seen differences in the amount of nickel recovered in each phase of the flotation. The greatest fluctuations are within NiRC1 flotation recovery as the minimum value is 22.88% (1100 rpm 8.1.2019) and maximum 51.81% (2000 rpm 9.1.2019). It can be concluded that the rotor tip speed has a direct effect on the recovery of concentrate. Despite the variation of rotor tip speed the NiRC1 recovery is clearly the greatest in every flotation test (Figure 20, Figure 18 and Figure 23). The effect of rotor tip speed can be concluded to have a greatest effect on the fast floating material that is recovered in the first phase of flotation (Wills and Napier-Munn 2006, p. 296). On the contrary the feed of last flotation stage comprises of the most reluctant material and that is why in all of the flotation tests the recoveries of NiRC4 are the smallest. However, it can be seen in Figure 20 that the fluctuations between flotation phases even out as the flotation proceeds. This is logical as when there is a large amount of nickel left in the feed after for example NiRC1 flotation it is obvious that this nickel is likely to be recovered in the following stages of flotation (e.g. 1100 rpm 8.1.2019 and 1700 rpm 10.12.2018 in Figure 20). On the contrary when plenty of nickel is recovered already in the first phase of flotation there is not much left to recover in the rest of the stages and that is why the recoveries of e.g. NiRC2, NiRC3 and NiRC4 concentrates are relatively small in 1100 rpm 28.1.2019 and 2000 rpm 9.1.2019 in Figure 20.

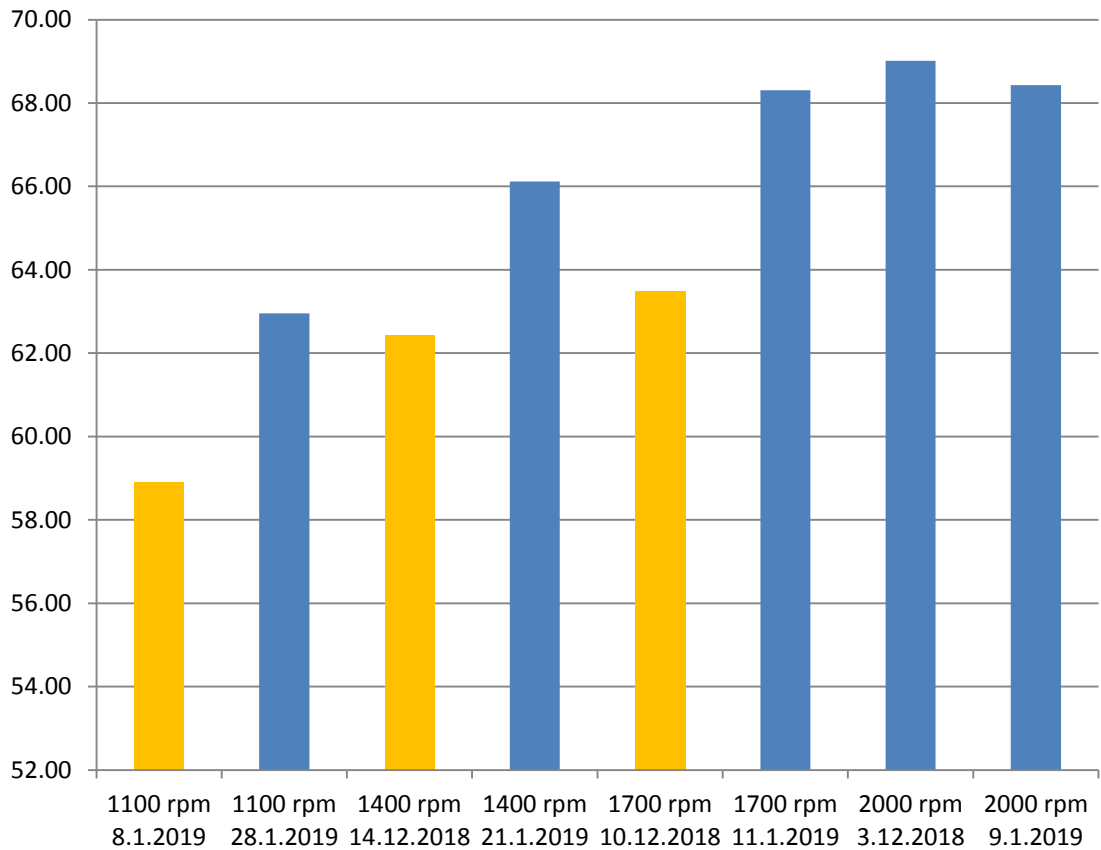


Figure 21. Cumulative nickel recoveries of each flotation test (%).

Cumulative nickel recoveries are presented in Figure 21. As the scale of coordinate axes is different than in Figure 20 the fluctuations can be observed more distinctly in Figure 21. A clear trend of increasing nickel recovery with increase in rotor tip speed can be observed in the figure.

There is fluctuation in the performance between each pair of flotation tests executed in similar conditions. Ideally, there would not be a big difference between similar conditions. When comparing the Figure 21 with Figure 16 can be seen that there is clear interdependence between the copper content of feed with the nickel recovery. Thus, it can be concluded that the increased copper content in nickel flotation feed is disturbing the nickel flotation.

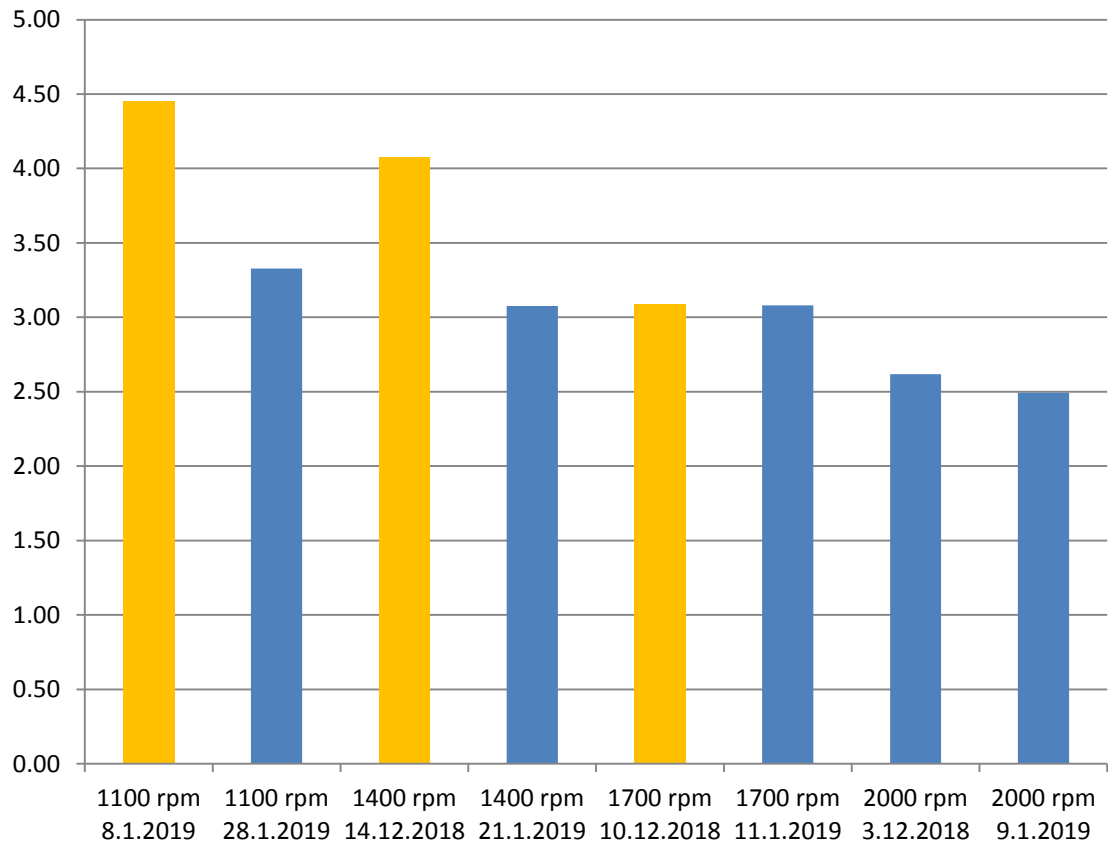


Figure 22. Total cumulative nickel grades (%).

Based on Figure 21 and Figure 22 can be seen that the flotation tests of 1100 rpm and 1400 rpm behave logically in such a way that 1100 rpm 8.1.2019 and 1400 rpm 14.12.2018 having a decreased recovery compared to their reference test in Figure 21 are to be compensated with increased concentrate grade in Figure 22. However, the 1700 rpm 10.12.2018 is behaving exceptionally as the decreased recovery compared to 1700 rpm 11.1.2019 is not to be compensated with increased concentrate grade but the grades of the two tests are equal (Figure 22). That is weakening the performance of flotation test 1700 rpm 10.12.2018. The flotation conditions can be evaluated to have been uniform between the both of flotation tests of 2000 rpm as both the cumulative recoveries (Figure 21) and cumulative grades (Figure 22) are in uniform levels. Potential reason for the decreased variation in the performance of the two 2000 rpm flotation tests could be equally performed copper flotation (Figure 17) or the optimal flotation conditions. The optimal flotation conditions were assumed to be around rotor tip speed of 2000 rpm.

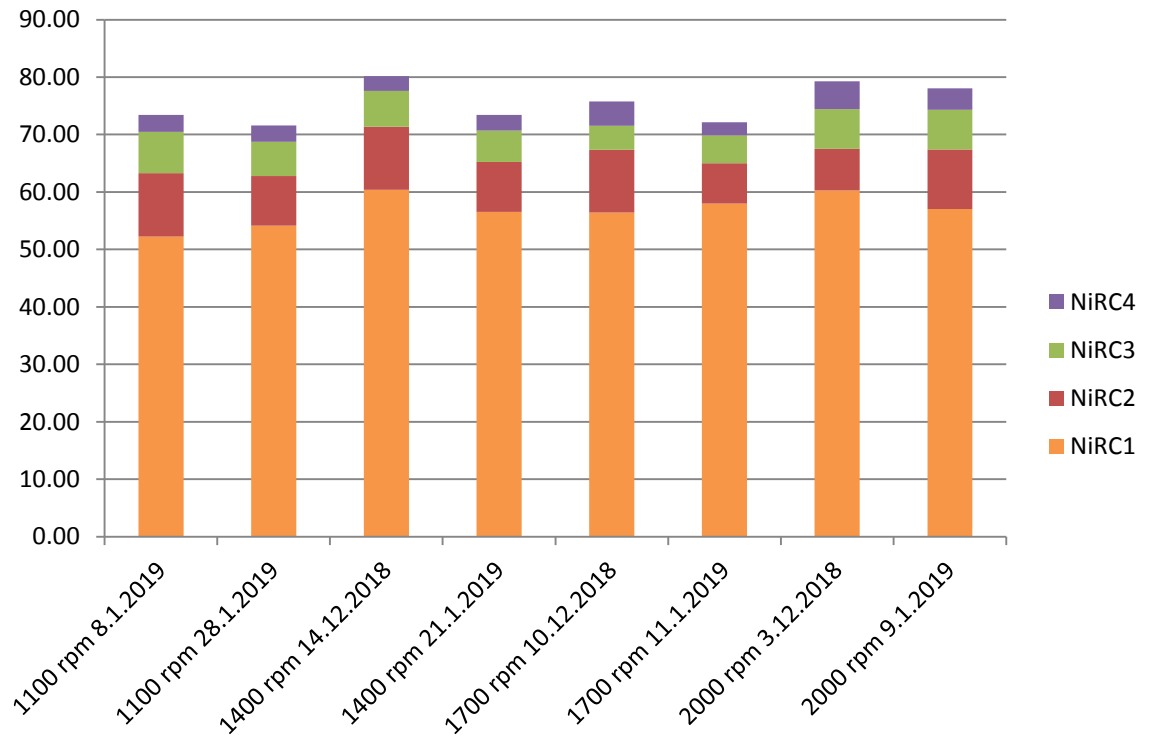


Figure 23. Cumulative recovery of copper (%) in nickel concentrate.

Figure 23 presents the copper recovery in nickel concentrate. The fluctuation in copper recovery between flotation phases NiRC1-NiRC4 of different flotation tests is not as big as in nickel recoveries (Figure 20). However, there is fluctuation in overall cumulative recovery between the different flotation tests. There is a slight trend of increasing copper recovery as a function of rotor tip speed observed in Figure 23. However, the cumulative recovery of flotation test 1400 rpm 14.12.2018 is the greatest. The cumulative recovery of copper in nickel concentrate seems to have an inverse fluctuation compared to cumulative nickel recovery in nickel concentrate (Figure 20, Figure 21) when comparing the performance of reference tests. The copper recovery in nickel concentrate is increased in flotation tests 1100 rpm 8.1.2019, 1400 rpm 14.12.2018 and 1700 rpm 10.12.2018 compared to their reference tests. The copper content of nickel flotation feed was increased in the tests in question (Figure 16). The poor cumulative nickel recoveries of flotation tests 1100 rpm 8.1.2019, 1400 rpm 14.12.2018 and 1700 rpm 10.12.2018 observed in Figure 21 can be concluded to derive from increased copper content in feed. Thus copper is found to be concentrated to the nickel concentrate more likely over nickel. Furthermore, the poor performance might be due to insufficiently performing collector chemicals. The purpose of collector chemicals is to change the natural behaviour of minerals. 1% Aerophine 3418A was used as a copper collector and 1% sodium isopropyl xanthate as nickel collector.

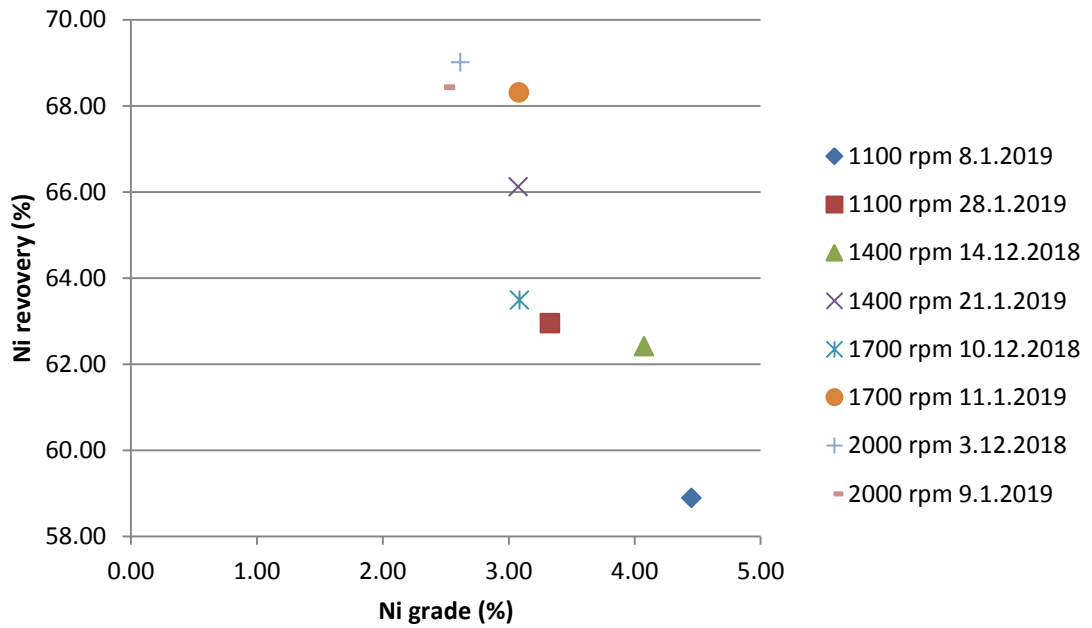


Figure 24. Total cumulative nickel grades and recoveries (%).

To examine both the nickel grade and recovery similarly gives a better impression of the actual flotation response. It can be seen in Figure 24 that the differences in the nickel recoveries are much larger than in cumulative nickel grades. Moreover, the results of reference tests differ a lot. For example, performance of flotation test 1100 rpm 28.1.2019 and 1700 rpm 10.12.2018 are close to each other but both of them differ a lot from their reference tests. Only the two tests performed with 2000 rpm rotor tip speed have rather equal performance in regard to concentrate grade and recovery relationship.

With every tested rotor tip speed another test was showing notably better performance in recovery over the other test of the same tip speed. Only with rotor tip speed 2000 rpm there was not much difference. To combine the results of the tests with same tip speeds the formation of average is one way to examine the results. However, combining might distort the results as the errors of both of the tests are also combined. The other way to assess the results is to compare the individual values that are presented in Figure 25.

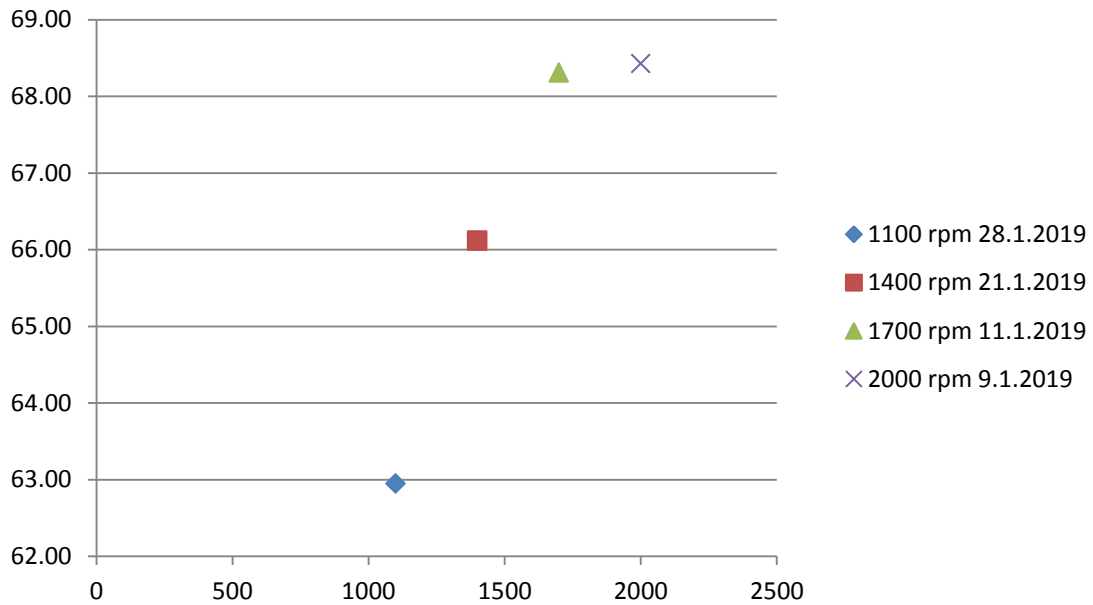


Figure 25. Cumulative nickel recoveries (%) with uniform copper content in feed.

One series of tests was selected based on the information of Figure 17 with a principle of copper content being as uniform as possible between the selected flotation tests. The selection was made based on the copper content as it was assumed to be the main factor of interfere based on the previously presented graphs. With the results shown in Figure 25 it can be assumed that a minor reduction of rotor tip speed may not influence on the recovery of nickel notably negatively. The Figure 25 supports a viewpoint that the reduction of rotor tip speed may not have linear effect on the flotation cell performance but a reduction of rotor tip speed on higher tip speed might decrease the recovery of valuable mineral to a lesser extend compared to a similar size of reduction in lower rotor tip speed. Similarly, as the rotor tip speed is reduced the energy consumption of a flotation cell is decreased which creates savings. The topic is discussed in more detail in the following chapter 6.3.

6.3 Profitability of flotation in regard to rotor tip speed

The profitability of rotor tip speed reduction is evaluated based on the performance of laboratory flotation tests scaled into industrial cell size. The energy consumption was estimated by measuring the current intake of industrial scale flotation cell motor with each of the corresponding rotor tip speeds used in laboratory conditions. The laboratory flotation tests were used to simulate the performance of an industrial scale rougher-scavenger flotation cell bank. For the profitability calculations similar performance was

assumed to be reached with seven cell rougher-scavenger flotation bank in industrial scale. Thus, the energy consumption of an individual industrial scale cell was multiplied by seven to assess the energy consumption of a flotation bank.

The motor power was calculated with each of the corresponding rotor tip speeds with following equation 12

$$P = \sqrt{3} \cdot U \cdot I \cdot \cos \varphi \quad (12)$$

where P is motor power (W)
 U is voltage (V)
 I is current (A)
 φ is power ratio (%)

by using the values mentioned in a motor nameplate and the measured current intakes. One of the calculations is illustrated in equation 13.

$$P = \sqrt{3} \cdot 690 \text{ V} \cdot 0.364 \cdot 323 \text{ A} \cdot \cos 0.958 = 80\,817 \text{ W} \quad (13)$$

The results are presented in Table 8.

Table 8. Motor power (kW) of industrial flotation cell with each of the tested rotor tip speeds.

Laboratory rotor tip speed (rpm)	Corresponding rotor tip speed (m/s)	Motor current intake (%)	Current (A)	Power (kW)
1100 rpm	3.46	36.40 %	117.57	80.82
1400 rpm	4.40	45.60 %	147.29	101.24
1700 rpm	5.34	59.40 %	191.86	131.88
2000 rpm	6.28	76.30 %	246.45	169.40

Secondly, the amount of produced concentrate was evaluated based on the performance of laboratory flotation tests. The 300 m³ flotation cell is 46,153.85-fold the size of 6.5 l flotation cell. Thus, the amount of concentrates were assumed to be 46,153.85-fold the amount of concentrates produced in laboratory scale when scaled into industrial size. The volume based scaling is very approximate method and includes error. It was

decided to be used because of the difficulty to scale a laboratory batch conditions into continuous industrial conditions. The scaling based on residence time could have been more precise. Nevertheless, there would have been error deriving from the difference between continuously operated process and batch process which is examined in chapter 6.5. For the simplicity reasons volume based scaling was used. It should be taken into account that the results are suggestive.

The economic value of each concentrate was evaluated by the concentrate grade and current price of nickel. Finally, the profitability of each flotation condition was evaluated as a sum of concentrate value and energy consumption. The results were examined with several scenarios of electricity and nickel price presented in the following figures.

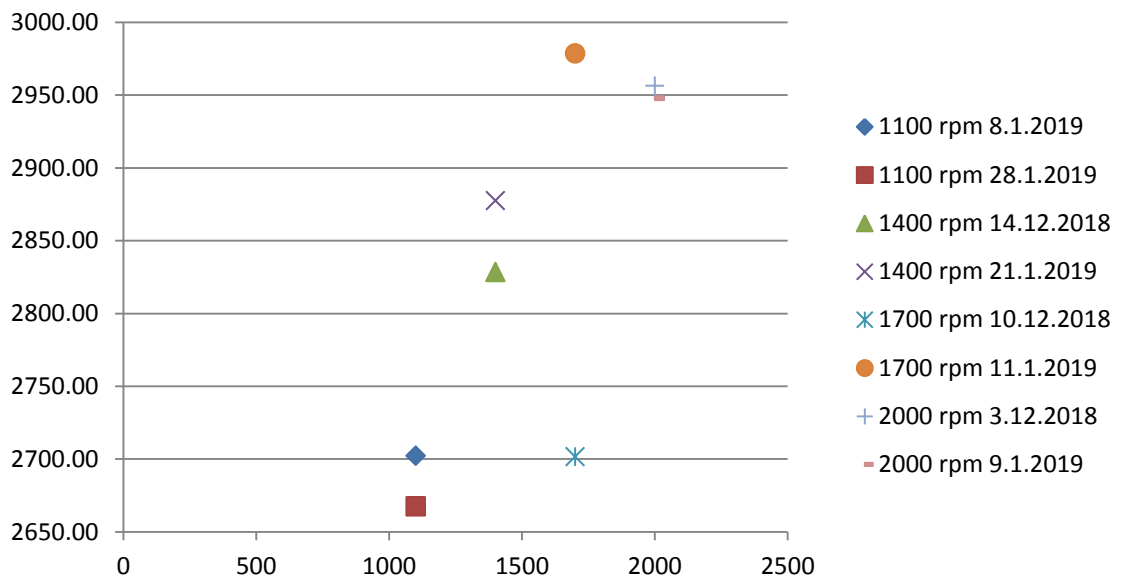


Figure 26. Profit of processing (US\$) when energy consumption is taken into account. Energy price of US\$ 0.1/kWh and current nickel price US\$ 12,810/ton are used in the calculations.

In Figure 26 is presented the profit of processing based on concentrate grades and recoveries with today's value of nickel and price of electricity. It can be seen that the pairs of each reference tests are rather close to each other so that there is a trend of increasing profit with increasing rotor tip speed. Flotation test 1700 rpm 11.1.2019 can be detected to be the most profitable in the conditions of Figure 26. Exceptionally, there is a huge difference between the values of two concentrates produced with 1700 rpm rotor tip speed with the profit of test 10.12.2018 being extraordinary low. The flotation

test 1700 rpm 10.12.2018 had a distinctly lower recovery compared to its reference test and also to other flotation tests which was seen in Figure 21. The recovery of flotation test 1700 rpm 10.12.2018 was approximately in the level of recoveries of 1400 rpm flotation tests in Figure 21. However, as the concentrate grade and especially energy consumption is taken into account it can be seen that the profitability of processing in flotation test 1700 rpm 10.12.2018 is collapsing to the level of 1100 rpm concentrates in Figure 26. The weak performance of flotation test 1700 rpm 10.12.2018 can be concluded to derive from weak concentrate grade and recovery combined with rather high energy consumption. The low recovery of flotation test 1700 rpm 10.12.2018 can be assumed to derive from increased copper grade of nickel flotation feed (Figure 16) and increased recovery of copper to the nickel concentrate compared to its reference test (Figure 23)

It can be detected by comparing the information in Figure 21, Figure 22 and Figure 24 with Figure 26 that the fluctuations in concentrate grades and recoveries between the reference tests seem to even out when the profitability is taken into account. There is not remarkable difference between reference tests observed in Figure 26 (except 1700 rpm 10.12.2018). The differences in profitability are greater between different processing conditions than between reference tests if 1700 rpm 10.12.2018 is not taken into account. Thus, the rotor tip speed can be detected to have an effect to the profitability of produced concentrate.

If the result of 1700 rpm 10.12.2018 is assumed to be an outlier and 1700 rpm 11.1.2019 representing the actual performance of 1700 rpm rotor tip speed it may be concluded that 1700 rpm is the most profitable condition of producing nickel concentrate with energy price of US\$ 0.1/kWh. The situation in profitability of different conditions changes while energy price is varying. In Figure 27 is presented the situation with energy price of US\$ 0.2/kWh.

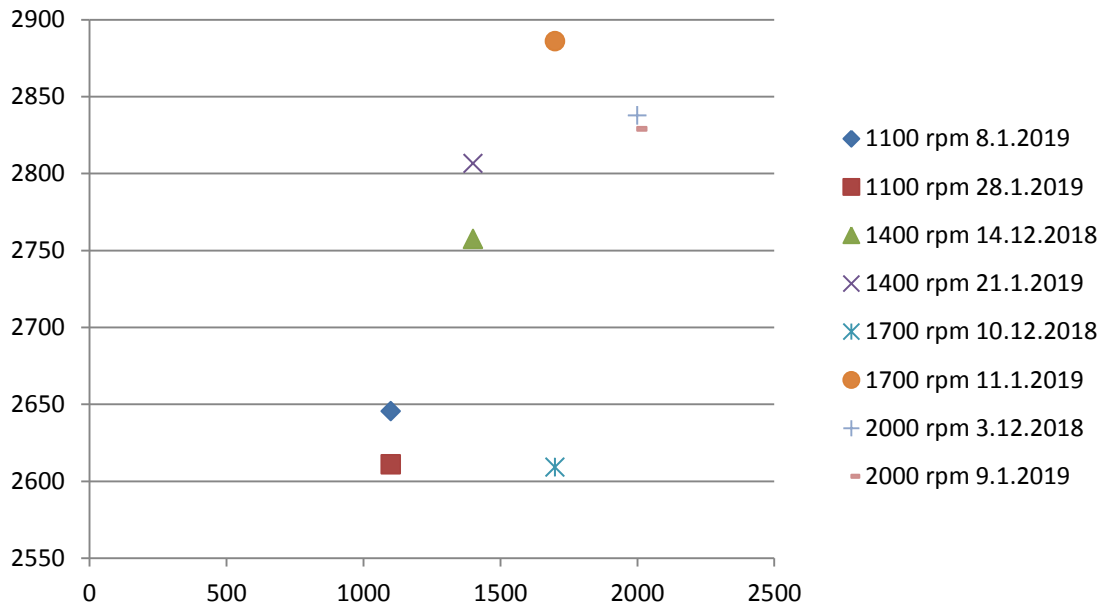


Figure 27. Profit of processing (US\$) with energy price of US\$ 0.2/kWh and current nickel price US\$ 12,810/ton.

The Figure 27 is presenting the similar scenario as Figure 26 but the energy price used in the calculations is double compared to a previous graph. It can be seen in Figure 27 that the profitability of all the processing conditions is naturally decreasing while energy price is increasing. The one concentrate produced with 1700 rpm rotor tip speed is still the most valuable as in the conditions presented in Figure 26. Moreover, the difference in profitability between the 2000 rpm concentrates and 1700 rpm 11.1.2019 can be detected to increase so that 1700 rpm 11.1.2019 presents the most profitable processing condition more distinctly than in Figure 26. Also the value of concentrates produced with rotor tip speeds 1100 rpm and 1400 rpm is slightly improved when comparing to concentrate 1700 rpm 11.1.2019. As the energy price keeps on increasing (Figure 30 and Figure 31) the condition of 2000 rpm is getting more and more unprofitable.

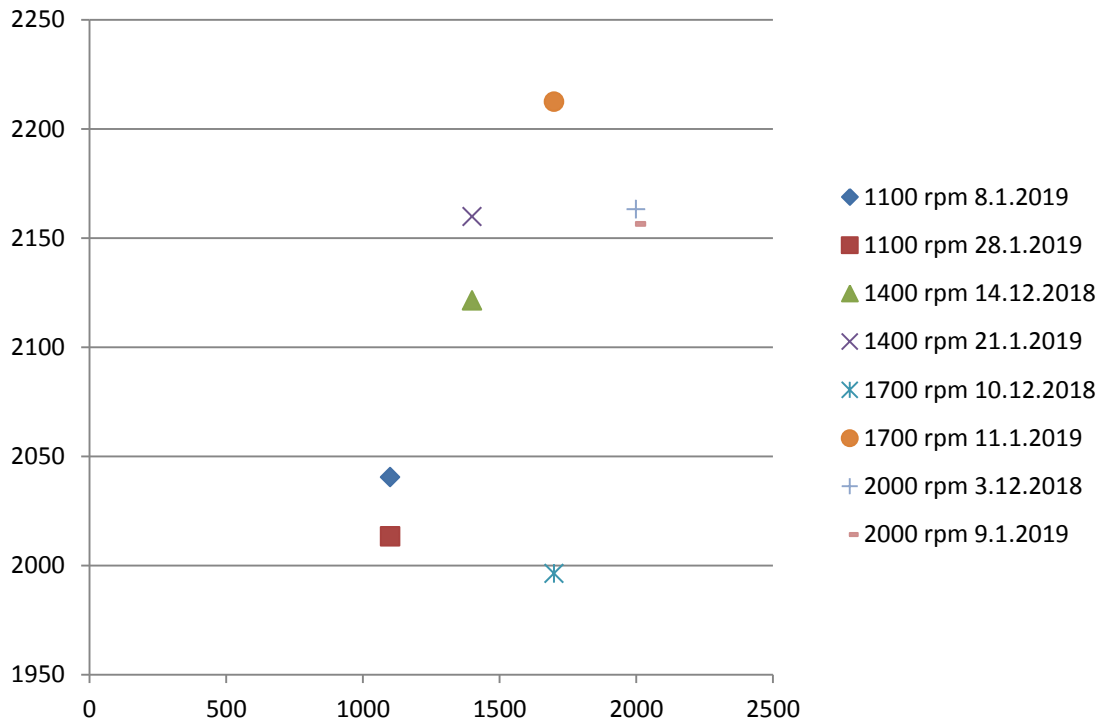


Figure 28. Profit of processing (US\$) with energy price US\$ 0.2/kWh and nickel price US\$ 10,000/ton.

Figure 28 presents a scenario of decreased nickel price but cost of electricity staying constant compared to Figure 27. First of all, in the scenario of reduced nickel value (US\$ 10,000/ton) it can be observed, that the value of all the concentrates is declining outstandingly. In the Figure 27 the value of all the concentrates is above US\$ 2,600 whereas in the Figure 28 the value of all the concentrates is below US\$ 2,250. Profitability is mostly dependent on the value of nickel. Moreover, it can be observed in Figure 27 and Figure 28 that the difference in value between concentrates 1100 rpm, 1400 rpm and 1700 rpm (11.1.2019) is declining. Also the profitability of processing with 2000 rpm tip speed seems to decrease as it is in the same level with flotation test 1400 rpm 21.1.2019.

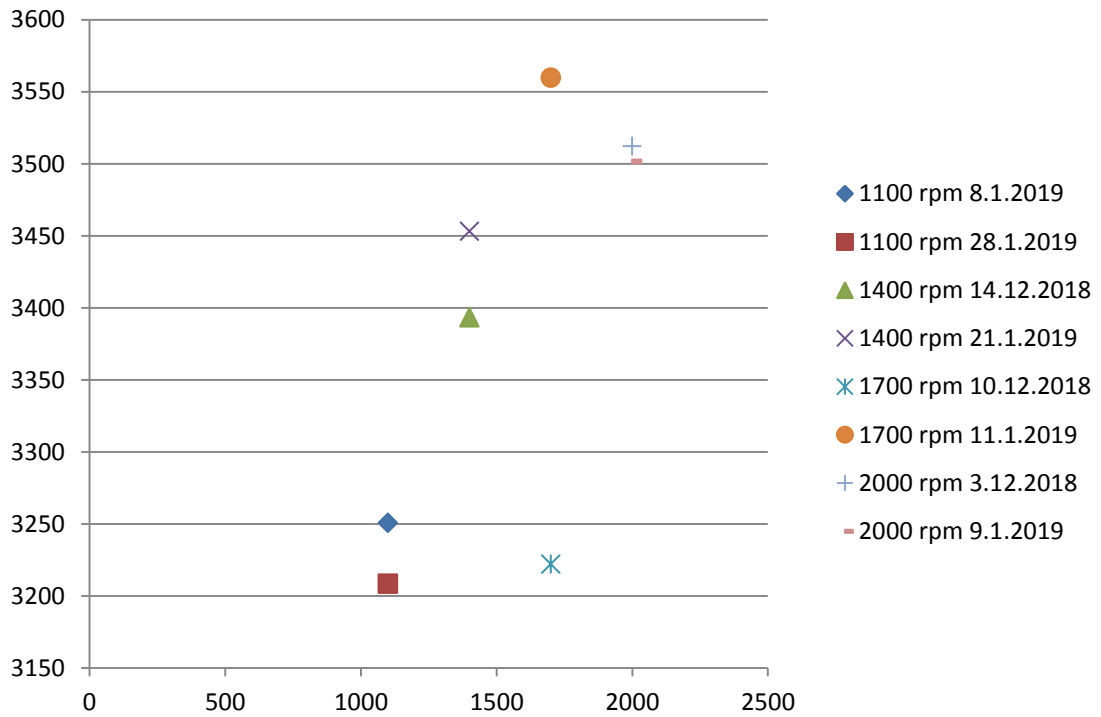


Figure 29. Profit of processing (US\$) with energy price US\$ 0.2/kWh and nickel price US\$ 15,620/ton.

Figure 29 presents the scenario of increased nickel value while energy price is in the same level as in the Figure 27 and Figure 28. The nickel price is increased in the calculations as much as it is decreased in Figure 28 compared to Figure 27. Thus, Figure 28 and Figure 29 present the scenarios of nickel price \pm US\$ 2,810 compared to Figure 27 which presents the current value of nickel.

It can be seen in Figure 29 that the concentrate 1700 rpm (11.1.2019) is again the most valuable concentrate. Moreover, it can be detected that the difference in value of concentrate 1700 rpm (11.1.2019) is increasing compared to lower rotor tip speeds but staying rather constant compared to concentrates of 2000 rpm in the Figure 27 and Figure 28. Also it can be seen that the profitability of processing with 2000 rpm rotor tip speed is again distinctly the second profitable condition as it is Figure 26 and Figure 27.

By comparing the information in Figure 27, Figure 28 and Figure 29 can be detected that the higher the nickel price is the greater becomes the differences between different flotation conditions. In Figure 28 where the nickel price is the lowest the values of all the concentrates are within US\$ 200 if 1700 rpm 10.12.2019 is excluded. While in a Figure 29 where the nickel price is the highest the values of concentrates are within US\$ 350. The behavior is due to different nickel contents of the concentrates.

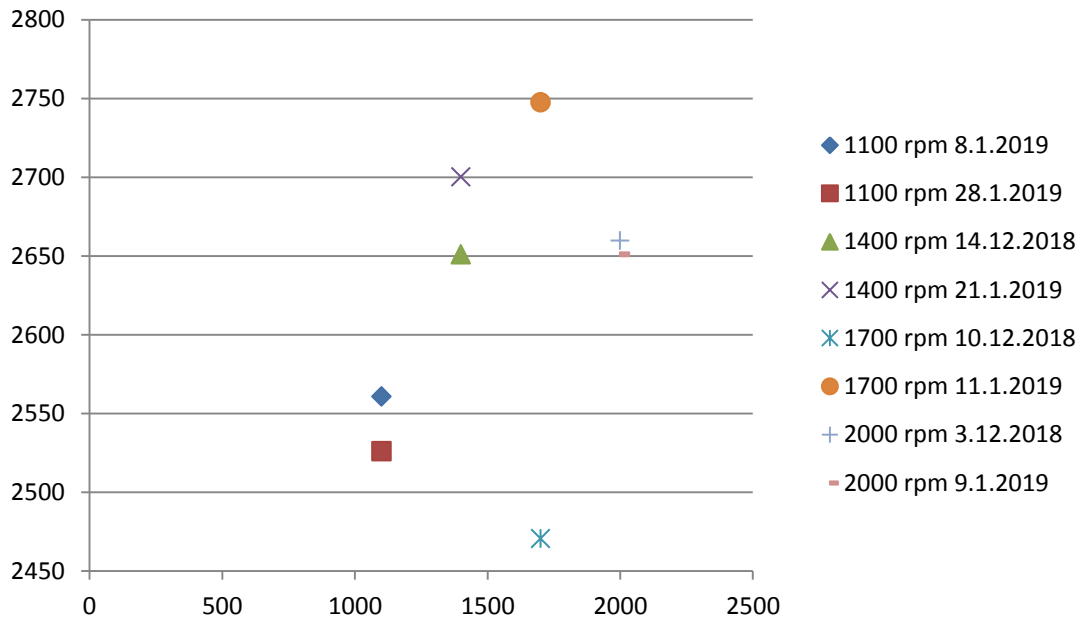


Figure 30. Profit of processing (US\$) with energy price US\$ 0.35/kWh and current nickel price US\$ 12,810/ton.

In Figure 30 is presented the profit of processing with increased energy price US\$ 0.35/kWh and current nickel price US\$ 12,810/ton. In Figure 30 the trend between lower rotor tip speeds and the condition of 1700 rpm 11.1.2019 is very similar to previous graphs. However, in Figure 30 the profitability of concentrates 2000 rpm is declining compared to Figure 27 and now profitability of processing is clearly in the similar level of 1400 rpm concentrates and even below the test 1400 rpm 21.1.2019. Thus, it can be concluded that the increase in energy price improves the profitability of concentrates produced with low rotor tip seeds.

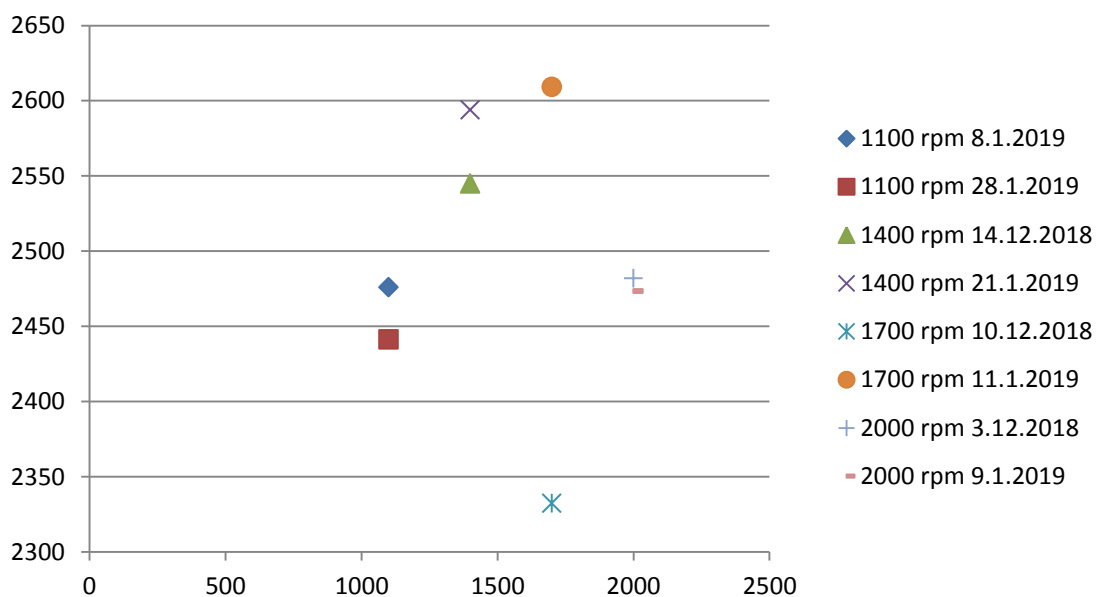


Figure 31. Profit of processing (US\$) with energy price US\$ 0.5/kWh and current nickel price US\$ 12,810/ton.

Figure 31 presents a rather extreme scenario with energy price of US\$ 0.5/kWh and current nickel price US\$ 12,810/ton. As the energy price is furthermore increased in the calculations it can be observed in the Figure 31 that the values of concentrates produced with rotor tip speeds of 1100 rpm, 1400 rpm and 1700 rpm (11.1.2019) are getting closer to each other. Moreover, the profitability of concentrates produced with 2000 rpm rotor tip speed is notably decreased compared to Figure 30. In the Figure 30 the profit of processing with rotor tip speed 2000 rpm is in the level of 1400 rpm concentrates but in a Figure 31 it is close to the level of 1100 rpm concentrates.

The profitability differences between different flotation conditions are reducing as the energy price is increasing and nickel price is staying constant. In the first scenario of energy price US\$ 0.1 kW/h and nickel price US\$ 12,810/ton the values of all the concentrates are approximately within US\$ 300 (Figure 26). Whereas in the scenario of energy price US\$ 0.5/kWh and similar nickel price the values of concentrates are within US\$ 170 (Figure 31) when 1700 rpm 10.12.2018 is excluded. Thus, it can be concluded that the profitability of processing with lower rotor tip speeds is increased as the energy price is increasing. However, the trend between different flotation conditions stays rather similar despite the fluctuation in energy and nickel price so that the concentrate of flotation test 1700 rpm 11.1.2019 attains the highest profit in all the conditions. However, it can be evaluated that if the energy price was further increased compared to Figure 31 the concentrate of flotation test 1400 rpm 21.1.2019 would soon become the most profitable.

6.4 Discussion on particle size

Particle size must be optimized in flotation so that it is neither too large nor too small. Usually, large particles do not comprise purely of valuable minerals (Wills and Napier-Munn 2006, p. 7-8). Thus recovery of them would decrease the concentrate grade (Wills and Napier-Munn 2006, p. 7-8). Moreover, large particles might be too heavy to be collected by air bubbles which would decrease recovery (Wills and Napier-Munn 2006, p. 268). Small particles are more improbable to attach to an air bubble and thus recovery of small particles is generally poor (Grano 2006; Safari et al. 2016; Tabosa et al. 2016). Furthermore, grinding consumes significant amounts of energy and thus profitability of

operation can be increased by leaving the particle size rather slightly large than small. Particle size P_{80} 75 μm is generally assumed to be optimal in froth flotation.

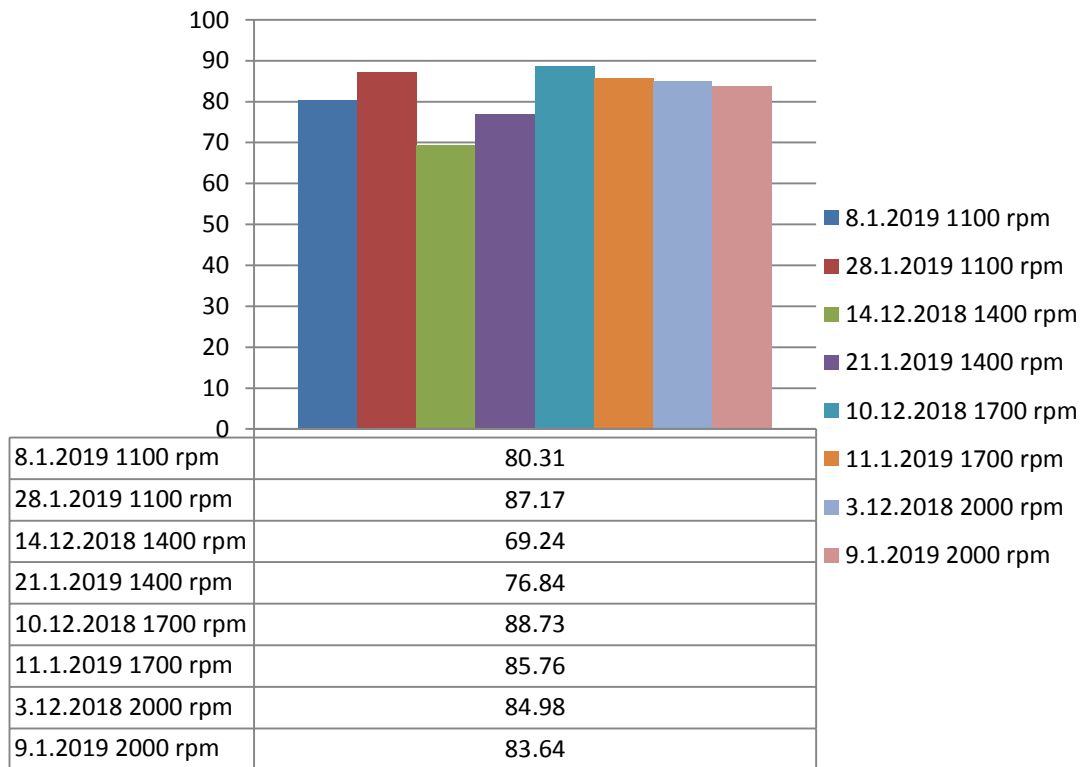


Figure 32. Particle size (μm) of the flotation feed.

The Figure 32 illustrates the particle size in the each of flotation test feeds. The P_{80} particle size is varying between 69.2 μm (1400 rpm 14.12.2018) and 88.7 μm (1700 rpm 10.12.2018). The original particle size analysis reports are presented in appendix 5. The target particle size of grinding was P_{80} 75 μm which is assumed to be an optimal. Particle size of feed was measured from a sample taken manually from the flotation feed. The feed was mixed prior to sampling. As the size of sample was tiny, few grams, compared to the size of feed the particle size measurement cannot be assumed to describe the characteristics of entire feed completely perfectly. There is a risk that either large amount of larger particles than average are to be collected in the sample or large amount of smaller particles than average are to be collected. In both of the situations the result of measurement would be skewed when comparing to the actual performance.

There is fluctuation in the particle size of the flotation feeds as can be seen in Figure 32. The creation of equal grinding result is difficult because of the variation in ore quality. The grinding feeds were homogenized and precisely measured and thus grinding conditions were assumed to be equal. However, the result of grinding is not equal. A

reason for the inequalities is most probably the variation in the hardness of the ore which creates differences to the impact response. Moreover, a slight leak of slurry was observed during the grinding as there was a small gap between a lid and grinding mill. However, the leakage was rather uniform over all of the tests and therefore it can be assumed that the leakage cannot have created a significant difference to the particle size via the loss of material and improved energy input to the rest of the material. Also, when comparing the total masses of the calculated flotation feeds (Table 7) it can be seen that there is only 41.8 g of difference between the biggest (1858.3g in 1100 rpm 28.1.2019) and smallest (1816.5g in 2000 rpm 3.12.2018) feed. The particle size was clearly the smallest (P_{80} 69.24 μm) in flotation test 1400 rpm 14.12.2018. Mass of the flotation test 1400 rpm 14.12.2018 feed was slightly below the average of all the feeds and thus part of the deviation in particle size could be explained by the increased leak of slurry and increased energy input to the remaining material.

It can be seen based on Figure 13, Figure 14 and Figure 21 that the recoveries seem to be the smallest in flotation tests 1100 rpm 8.1.2019 and 1400 rpm 14.12.2018 in which also the particle size is among the smallest and closest to assumed optimum P_{80} 75 μm (Figure 32). The observed relationship between recovery and particle size is opposite that would be expected based on the optimal particle size (Wills and Napier-Munn 2006, p. 268). On the contrary, it is proposed that small particles have decreased probability to attach an air bubble (Grano 2006; Wills and Napier-Munn 2006, p. 7; Safari et al. 2016; Tabosa et al. 2016) which might explain the phenomenon. However, the particle size $P_{80} \sim 70 \mu\text{m}$ what is not what is generally meant with fine particle size on flotation (- 20 μm) (Amini et al. 2016; Safari et al. 2016). Particle size is the greatest in flotation test 1700 rpm 10.12.2018. The same flotation test has a significantly decreased performance in nickel recovery which is not compensated by increase of concentrate grade compared to its reference test. That leads to a collapse of performance in the profitability examination in chapter 6.3. Large particle size of flotation feed 1700 rpm 10.12.2018 might have reduced the degree of liberation of minerals. Thus particles may have included copper minerals which are diminishing the recovery of nickel concentrate. Smaller particle size would have ensured higher degree of liberation and could have improved the flotation cell performance. The same phenomenon is assumed to cause the fluctuation in performance of other flotation tests. Based on the results can be proposed that the copper content of particles is likely to define the performance more than physical particle size. It can be proposed that actually particle size smaller than P_{80}

75 μm could have ensured the enhanced performance of flotation cell via improved degree of liberation.

It has been proved in several studies (Grano 2006; Schubert 2008; Amini et al. 2016; Safari et al. 2016; Jameson 2013 cited by Tabosa 2016) that different particle sizes in flotation feed need different hydrodynamic conditions for optimum recovery. It would have been very interesting to examine the flotation response in regard to particle size by fractioning the produced concentrates into different particle sizes. However, it was unfortunately not possible with the small amounts of concentrates produced in flotation tests. About 10 grams of material is needed for conducting of reliable XRF analysis to examine the concentrate grade. The smallest concentrates being less than 20 grams could thus not be divided into particle size fractions. The only method to enable the classification would have been to combine the corresponding concentrates of two or more flotation tests. However, combining different flotation tests would presumably contort the results. Especially, when examining the fluctuation between the pairs of reference tests in several figures in chapter 6.2 the distortion effect would have been obvious. As the study represents preliminary research of the topic, concerning the resources available and the scope of thesis it was decided to execute the XRF analysis without fractioning the samples to be able to observe the overall effect of rotor tip speed on flotation cell performance and thus avoid the risk of distortion of results. The amount of produced concentrate and possibility for analysis of several particle size fractions should be taken into account in the future studies.

6.5 Laboratory flotation cell performance and reliability of results

In flotation operations there are lots of sources of deviation which leads into difficulties in creation of equal conditions that would allow neutral comparison of results. All the variation must be considered when comparing the results. First of all, there are differences in the feed ore in regard to grade and behavior in accordance with comminution. That leads to a deviation in grinding circumstances and differences in particle size distribution in the flotation feed. The effect of particle size in flotation is discussed in chapters 2.4.1 and 6.4. During flotation there are differences in solids concentration, chemical concentrations, pH and temperature that may cause variation in the flotation cell performance.

There is even more deviation in the circumstances of nickel flotation compared to copper flotation as the nickel flotation feed is emerged from copper flotation. There is fluctuation in the copper concentration of nickel flotation feed. Large amounts of copper in nickel flotation feed were shown to disturb the nickel flotation (chapter 6.2) because copper is floated more likely than nickel. That may decrease nickel concentrate grade and recovery alike. The performance and effect of copper flotation in the executed tests is discussed in detail in chapters 6.1 and 6.2.

As laboratory tests were executed as batch flotation tests there is more deviation, or the origins of deviation are different compared to continuously operated circumstances in industrial scale. Moreover, as the scale being smaller the deviation in results is more apparent when it comes to contamination or chemicals' concentrations for example.

The conditions in Outotec LabCell[®] flotation cell are illustrated in Figure 33 where the flotation cell is filled with water and both rotor and air flow are turned on.

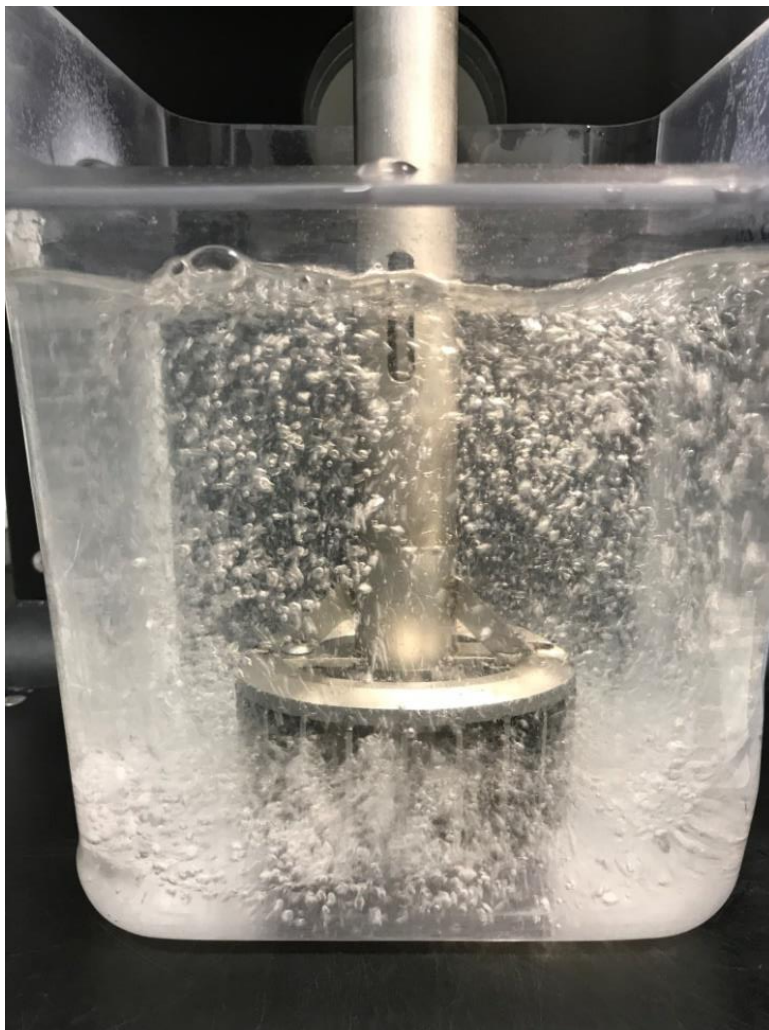


Figure 33. Conditions in Outotec LabCell[®] flotation cell when filled with water and rotor and air flow are turned on.

The performance of a laboratory flotation machine was observed during the flotation tests and it was examined to compare it with industrial scale performance. To compare for example a 300 m³ flotation cell with laboratory size cell the scale is very different as the industrial scale flotation cell is some 46,150-fold bigger compared to a laboratory cell. The basic principle of operation is very similar except of the nature of batch reaction in laboratory flotation machine. It forms some challenges for the operation and creation of equivalent conditions between the flotation tests. For example the control of froth bed thickness, slurry level and the solids concentration of the slurry are challenging in the batch conditions. The topics are examined in detail in the following chapters.

The control of froth bed thickness would have been possible by rotor tip speed and air flow rate adjustment. However, the froth bed thickness could not be intentionally controlled in the tests as the rotor tip speed was changed according to the research plan and air flow rate was kept constant in order to be able to observe purely the effect of rotor tip speed. There were remarkable differences in the thickness of froth bed that were derived from rotor tip speed adjustment. In order to attain thicker froth bed and presumably better recovery in lower rotation speeds an increase of air flow rate would be recommended.

The slurry level in a flotation cell was controlled during the test in order to achieve maximal recovery. In a batch flotation test slurry level is decreasing when flotation is proceeding as the concentrate is recovered from the flotation cell. Thus water must be added to maintain the desired froth level for recovery. In a laboratory flotation test the control of slurry level is fully based on visual observation.

Flotation tests were performed within large range of rotor tip speeds. As the slurry flow conditions fluctuate considerably whether the rotor tip speed is 1100 rpm or 2000 rpm the slurry level had to be controlled accordingly. When performing flotation tests with high rotor tip speeds some settled, clear water was taken on side before the beginning of nickel flotation to avoid slurry overflow and loss in recovery. On the other hand, when performing tests with low rotor tip speeds some extra water had to be added in the very beginning of nickel flotation to enable a sufficient level of slurry and froth recovery. As

mentioned in previous paragraph, some water addition was necessary in all of the flotation tests when the flotation was proceeding to compensate the volume of recovered concentrate. The amount of water addition could not be measured because there was only one person executing the flotation tests. Moreover, the froth scrapers and walls of the flotation cell were rinsed actively as some concentrate was accumulating on them. The latter can be assumed to enhance the recovery.

In a batch process the control of slurry level goes in parallel with the control of solids concentration of slurry as the water addition both increases the slurry level but similarly decreases the solids concentration. Thus, the solids concentration of slurry fluctuates between the flotation tests and could not be kept constant. This is due to the nature of batch process where no feed material is added as the flotation proceeds. As mentioned in chapter 2.4.4 the solids concentration of slurry has been found to have an effect on selectivity of flotation (Wills and Napier-Munn 2006, p. 290). Thus, the differences in solids concentrations of slurry between different flotation tests might cause variation in performance of flotation. Moreover, the relationship between solids and water recovered to the concentrate might vary in between the different flotation tests which may cause some deviation to the solids concentration of slurry. However, the latter effect is assumed to be negligible.

The water addition has also an effect on pH and the flotation chemicals' concentrations. The concentrations were not controlled according to the amount of water addition. pH was set in the beginning of each flotation test according to the initial amount of water and chemicals were added with the measures mentioned in the recipe (Appendix 1). To assure the equal conditions chemicals should be added with equal concentrations and pH should be controlled with the water addition.

Furthermore, when operating a batch process compared to a continuous process there is some increased loss of material in the operation. That is due to use of number of separate dishes where the material is treated. Rinsing cannot be performed perfectly and thus there will be losses. The amount of material losses can be seen in Table 7 where both the amounts of individual concentrates are presented with the sum of collected concentrates and tailings. When comparing the total amount of material with the measured feed of 1.9 kg of solids in Table 7 can be observed that the amount of losses

are fluctuating approximately between 40 to 85 grams. The main sources of losses are grinding, spilling in flotation, filtration and material handling.

It was clearly observed that there are different hydrodynamic conditions in different parts of the flotation cell which can be seen in chapter 4.4 in Figure 7 -Figure 12. As visualized in aforementioned figures the rotor creates eddies in flotation cells that are not covered with froth. The phenomenon might derive from disturbance of froth zone by increase of energy input as mentioned in chapter 2.4.7. The instability of froth zone decreases recovery (Deglon 2005; Schubert 2008; Tabosa et al. 2016).

Furthermore, some differences were detected between the smaller 2 l and larger 6.5 l flotation cell used. In the 2 l flotation cell froth was packing against the back wall of the flotation cell indicating that the froth scrapers did not reach to recover all the froth from the very back of the flotation cell. The same phenomenon was not observed in larger 6.5 l flotation cell. There might have been a slight difference in the position of the froth scrapers between the cells. The difference might also be due to mineralogical differences of copper and nickel concentrates rather than the cell design. The copper cleaning flotation was performed in 2 l flotation cell while 6.5 l cell was used in nickel flotation tests.

The rotor and stator design of Outotec GTK LabCell[®] is similar to industrial scale rotor and stator produced by Outotec. Air distribution in Outotec's FloatForce[®] mixing mechanism is done via six ports that are connected to the shaft (Coleman and Rinne 2011). Air flows into individual air dispersion slots outside the rotor (Coleman and Rinne 2011). Thus, rotor can be filled with slurry which prevents reduction of power consumption in the increase of air flow rate (Coleman and Rinne 2011). The aspect ratio of rotor to the flotation tank diameter (Pinto et al. 2018) is examined based on the information of Outotec brochure (Outotec 2016) and measurements taken of the 6.5 l flotation cell. The rotor to tank diameter in 300 m³ flotation cell is 0.21.

$$\frac{1.75 \text{ m}}{8.5 \text{ m}} = 0.21 \quad (14)$$

While in laboratory cell the aspect ratio is 0.22.

$$\frac{6 \text{ cm}}{27 \text{ cm}} = 0.22 \quad (15)$$

Based on the results there is not much of a difference in the rotor to flotation cell diameters of the two different scales. The laboratory cell diameter was measured as the diameter of a rectangular flotation cell while the industrial cell is round.

The height of a flotation cell is one of the biggest differences between the laboratory and industrial scale. In a 6.5 l laboratory flotation cell the distance from the bottom to the cell lip is 20 cm so the bubble-particle aggregates must transfer only 20 cm to reach the froth level while in the industrial flotation cell the distance is several meters. Because of increased distance there is more time for numerous reactions to take place. However, the bubble and particle properties are similar in both of the scales and for example the aggregates are not any stronger in industrial scale. There is bubble-particle attachment, detachment and reattachment taken place in addition to entrapment and entrainment in a flotation cell. It is hard to estimate the total effect of these reactions compared to laboratory scale where they are taken place in smaller extent. In similar conditions the performance of industrial flotation cell could be similar, better or worse depending on the extent of each mentioned sub-reaction.

Scale of tested rotor tip speeds was rather wide. Wide scale was chosen to be able to detect the potential effect of rotor tip speed distinctly. However, the hydrodynamic conditions differ in between the tested rotor tip speeds and there might appear some hydrodynamic processes with lower speeds that do not occur with higher speeds. Moreover, the nature of hydrodynamic processes and for example the proportional sizes of different hydrodynamic areas might vary between the different scales. However, the meaning of the study was to observe the effect of rotor tip speed on overall performance so the differences in hydrodynamic processes do not effect on this study other than creating the desired performance difference. It should be remembered that the response might not be equal in industrial scale.

7 CONCLUSIONS

In the examination of the effect of rotor tip speed on flotation cell performance was found that cumulative nickel recovery is increasing while simultaneously cumulative nickel grade is decreasing with increasing rotor tip speed. The decreased concentrate grade with increase of rotor tip speed can be concluded to derive from nature of grade-recovery relationship. Recovery of low grade particles and entrainment are increased with the increase in rotor tip speed which increases the recovery but decreases the concentrate grade.

Based on the results it can be concluded that the copper traces in nickel flotation feed are disturbing the performance of nickel flotation. There was found an interdependence between copper content of nickel flotation feed and nickel recovery. There is an increased copper recovery in such a nickel flotation tests where the copper content is increased in the nickel flotation feed i.e. where copper flotation was performed poorly. Copper was found to be recovered more easily over nickel and thus the nickel recovery is disturbed. It may be concluded based on the results that selectively performed copper flotation is a base for successful nickel flotation as the copper content of nickel flotation feed defines the performance of nickel recovery.

Nickel recovery was examined as a function of rotor tip speed in terms of uniform copper content. There was observed that nickel recovery is not acting linearly as a function of rotor tip speed. Based on the results it can be assumed that minor reduction in rotor tip speed is not likely to have a remarkable effect in recovery. An equal extent of reduction of rotor tip speed can be observed to have smaller effect on nickel recovery at higher speeds compared to lower speeds. However, the concentrate produced with lower rotor tip speed has an increased concentrate grade. There was only one series of samples indicating the effect. More research is needed for the generalization of the results.

Based on the results reduction of rotor tip speed on the level of 1700 rpm (5.34 m/s) would be the most optimal with several investigated scenarios of nickel and electricity price when concentrate grade, recovery and energy consumption of flotation cell are taken into account. In the comparative calculations may be seen that the profitability of processing increases with low rotor tip speeds (1100 rpm = 3.46 m/s and 1400 rpm =

4.4 m/s) when the energy price is increased i.e. the differences in profitability of different conditions decrease. On the other hand, the increase in nickel price affects in such a way that the profitability differences increase between different flotation conditions. Based on the results it can be concluded that with high electricity price the lower rotor tip speeds are likely to be more profitable over maximum speed. On the other hand, with high nickel price the high rotor tip speeds are assumed to be the most profitable. Minor changes in metal grade, recovery and price and in cost of electricity may change the most profitable flotation condition.

There is variation between the results of tests executed in similar conditions. The total fluctuation in results is considered to be rather significant. Larger sample size would be needed in order to evaluate the effect of rotor tip speed more reliably. However, in profitability evaluation the variation is greater between different conditions than between the pairs of reference tests. Thereof it may be concluded that the rotor tip speed has reliably an effect on flotation cell performance. Even though there is variation between individual flotation tests the overall trends in results are assumed to be reliable. Flotation test 1700 rpm 10.12.2018 is assumed to be an outlier resulting from high copper content of nickel flotation feed and low nickel recovery that is not compensated by increase of concentrate grade. Main factor of variation is assumed to be the heterogeneous performance of copper flotation. Especially the fluctuation in copper flotation is proposed to decrease the reproducibility of results. Other sources of variation can be differences in particle size, ore properties and used chemicals' concentrates. Furthermore, there might be minor defects in the operation of machinery and there might be traces of other minerals in the used laboratory instruments. Moreover, there is some inaccuracy deriving from the sample preparation and analysis of samples.

7.1 Recommendations

Based on the research it would be recommended to impugn the rotor tips speeds used in industrial flotation plants and further investigate whether savings could be created by the speed reduction. Based on the results, the rotor tip speed of 5.34 m/s would be recommended to be applied in nickel flotation with current electricity US\$ 0.1/kWh and nickel price US\$ 12,810/t to enable the best profit. However, further investigation is needed before generalization of the results.

Effect of rotor tip speed is recommended to be examined in an industrial scale. There are differences in the operation of laboratory flotation cell compared to industrial flotation cell and thus the results of laboratory experiments cannot be assumed to transform directly into industrial scale. Moreover, there might be different responses into the change of rotor speed with regard to ore type. Therefore, before generalization of the results it would be important to examine the effect with several ore types and larger sample sizes. Larger sample sizes are recommended in all the future studies to assure the reliability of results.

Secondly, it would be recommended to define individually optimal flotation conditions on every flotation cell of a flotation plant in regard to rotor tip speed. The optimization of rotor tip speed could be connected into the continuous analysis of flotation feed properties. Thus the rotor tip speed could be automatically controlled that the produced concentrate had always the most optimal properties in regard to profitability of the operation. The study of individually optimal rotor tip speed could be demonstrated in laboratory scale so that the rotor tip speed was changed in the middle of batch flotation series. The simplest test would be an increase of rotor tip speed either in the rougher or scavenger cells. In rougher cells the increase of recovery of valuable minerals is assumed to be limited by the froth carrying capacity i.e. the ability of air bubbles to carry solids (Deglon 2005; Lelinski et al. 2011). Therefore, the increased energy input is assumed to have the most significant effect in the scavenger cells where the most reluctant material is to be recovered. The recovery is assumed to increase in scavenger cells as the rotor tip speed is increased. On the other hand, there is an assumption that the fast floating material in rougher cells could be floated even with lesser energy input. There is an energy saving potential in the rougher cells if the rotor tip speed could be decreased without significant effect on flotation cell performance. However, the performance should be examined to assure of the effect.

8 SUMMARY

In the theory part the results of previous studies about the effects of different flotation parameters were examined. The effect of particle size, bubble size, air flow rate, slurry properties, froth depth, chemicals dosage and power input were examined in detail in separate sub-chapters. Furthermore, the role of energy input in froth flotation and results of previous studies were examined in the theory part.

Based on the theory survey can be said that the attachment of particles on the air bubbles is in the most important role in flotation is as it is the basis of true flotation. The bubble-particle attachment can be improved by decrease of bubble size, increased air dispersion, increased amount of air bubbles, decreased solids concentration of slurry, shallow froth depth, add of collector chemicals and increase of energy input in the flotation cell. The increase of energy input effects on the bubble-particle contacting but it also decreases the bubble size, improves air dispersion and increases the amount of air bubbles by creation of smaller bubbles. However, there is a limit up to which rotor tip speed can be increased without disturbance of froth zone and decrease of recovery.

Froth flotation is a complex phenomenon where the interaction of sub-processes defines the overall performance. Effect of rotor tip speed was studied in laboratory conditions with Outotec GTK LabCell[®] flotation machine. The performance of nickel flotation was studied with four different rotor tip speeds while keeping the other process conditions stable. By analyse of concentrates there was found an increase of nickel recovery and decrease of concentrate grade with the increase of the rotor tip speed. The increased rate of recovery can be concluded to derive from decreased bubble size, increased bubble-particle contact and increased rate of entrainment. The decreased rate of concentrate grade can be concluded to derive from the increased recovery of low grade particles. Moreover, physical collection methods (entrainment and entrapment) are enhanced as power input is increased and the increased floatability of gangue might decrease the concentrate grade. Furthermore, a relationship between the copper content of nickel flotation feed and recovery of nickel was found. The recovery of nickel was found to be decreased by the high traces of copper in the nickel flotation feed. Thus, selectively performed copper flotation could be concluded to be important for the performance of latter nickel flotation.

The rotor tip speed was found to have a non-linear relationship with nickel recovery. The relationship was examined in uniform conditions of copper content in nickel flotation feed. It was found that a reduction of rotor tip speed on higher tip speed might decrease the recovery of valuable mineral to a lesser extent compared to a similar size of reduction in lower rotor tip speed. Similarly, savings are created as the energy consumption of flotation cell is decreased.

The performance of each flotation condition was evaluated in regard to grade, recovery and energy consumption. The results of laboratory tests were scaled into industrial scale based on volumes and an energy consumption of industrial flotation cell was measured to conduct the profitability calculations. Different scenarios of nickel and electricity prices were examined. It was found that the increase of electricity price decreased the profitability differences of tested rotor tip speeds. On the other hand, with the increase of nickel value the profitability differences of different conditions increased. Today's conditions the circumstances of rotor tip speed 5.34 m/s (1700 rpm) were the most profitable. In profitability assessment there was greater variation between different flotation conditions than between the pairs of reference tests. Thus, the overall trend in results is thought to be reliable despite the moderate variation between reference tests.

9 REFERENCES

- Amini, E., Bradshaw, D.J., Finch J.A. and Brennan, M., 2013. Influence of turbulence kinetic energy on bubble size in different scale flotation cells. *Minerals Engineering*, 45, 146-150
- Amini, E., Bradshaw, D.J. and Xie, W., 2016. Influence of flotation cell hydrodynamics on the flotation kinetics and scale up, Part 1: Hydrodynamic parameter measurements and ore property determination. *Minerals Engineering*, 99, 40-51.
- Coleman, R. and Rinne, A., 2011. Flotation mechanism design for improved metallurgical and energy performance. *Metallurgical plant design and operating strategies (MetPlant 2011)*, Perth, WA, Australia, August, 8-9, 2011. 405-418.
- Deglon, D.A., Egya-Mensah, D. and Franzidis, J.P., 2000. Review of hydrodynamics and gas dispersion in flotation cells on South African platinum concentrators. *Minerals Engineering*, 13 (3), 235-244.
- Deglon, D.A., 2005. The effect of agitation on the flotation of platinum ores. *Minerals Engineering*, 18, 839-844.
- Evans, G.M., Doroodchi, E., Lane G.L., Koh, P.T.L. and Schwarz, M.P., 2008. Mixing and gas dispersion in mineral flotation cells. *Chemical Engineering research and design*, 86, 1350-1362.
- FLSmidth, 2019. Products, Flotation [online document]. Denmark, FLSmidth. Available: <https://www.flsmidth.com/en-gb/products/flotation> [referred 2.5.2019].
- Gallhofer, D and Lottermoser, B.G., 2018. The Influence of Spectral Interferences on Critical Element Determination with Portable X-Ray Fluorescence (pXRF). *Minerals* 2018, 8, 320.
- Goel, S. and Jameson G.J., 2012. Detachment of particles from bubbles in an agitated vessel. *Minerals Engineering*, 36-38, 324-330.

Gorain, B.K., Franzidis, J.P. and Manlapig, E.V., 1995a. Studies on impeller type, impeller speed and air flow rate in an industrial scale flotation cell. Part 1: Effect on bubble size distribution. *Minerals Engineering*, 8 (6), 615-635.

Gorain, B.K., Franzidis, J.P. and Manlapig, E.V., 1995b. Studies on impeller type, impeller speed and air flow rate in an industrial scale flotation cell. Part 2: Effect on gas holdup. *Minerals Engineering*, 8 (12), 1557-1570.

Gorain, B.K., Franzidis, J.P. and Manlapig, E.V., 1996. Studies on impeller type, impeller speed and air flow rate in an industrial scale flotation cell. Part 3: Effect on superficial gas velocity. *Minerals Engineering*, 9 (6), 639-654.

Gorain, B.K., Franzidis, J.P. and Manlapig, E.V., 1997. Studies on impeller type, impeller speed and air flow rate in an industrial scale flotation cell. Part 4: Effect of bubble surface area flux on flotation performance. *Minerals Engineering*, 10 (4), 367-379.

Gorain, B.K., Napier-Munn, T.J., Franzidis, J.P. and Manlapig, E.V., 1998a. Studies on impeller type, impeller speed and air flow rate in an industrial scale flotation cell. Part 5: Validation of $k-S_b$ relationship and effect of froth depth. *Minerals Engineering*, 11 (7), 615-626.

Gorain, B.K., Harris, M.C., Franzidis, J.P. and Manlapig, E.V., 1998b. The effect of froth residence time on the kinetics of flotation. *Minerals Engineering*, 11 (7), 627-638.

Grano, S., 2006. Effect of impeller rotational speed on the size dependent flotation rate of galena in full scale plant cells. *Minerals Engineering*, 19, 1307-1318.

Grau, R.A. and Heiskanen, K., 2003. Gas dispersion measurements in a flotation cell. *Minerals Engineering*, 16, 1081-1089.

Hadler, K., Greyling, M., Plint, N. and Cilliers, J.J., 2012. The effect of froth depth on air recovery and flotation performance. *Minerals Engineering* 36-38, 248-253.

Kerfoot, D. G. E., 2012, Nickel, Ullmann's encyclopedia of industrial chemistry, Electronic release. Weinheim, Germany, Wiley-VCH.

Lelinski, D., Govender, D., Dabrowski, B., Traczyk, F. and Mulligan, M., 2011, Effective use of energy in the flotation process. 6th Southern African Base Metals Conference 2011. The Southern African Institute of Mining and Metallurgy, 137-148.

Liu, H-J., Zhang, W. and Sun, C-B., 2014. Experiences in using gas dispersion measurements to evaluate metallurgical performance of scavenger cleaner and recleaner circuit at Vale's Thompson Mill. *J. Cent. South Univ.* 21, 3955–3962.

London Metal Exchange, 2019. Metals, Non-ferrous [online document]. London: London Metal Exchange. Available: <https://www.lme.com/Metals/Non-ferrous/Nickel#tabIndex=0> [referred 28.2.2019].

Maldonado, M., Araya, R. and Finch, J., 2011. Optimizing flotation bank performance by recovery profiling. *Minerals Engineering*, 24, 939-943.

Nesset, J.E., Hernandez-Aguilar, H.R., Acuna, C., Gomez, C.O. and Finch, J.A., 2006. Some gas dispersion characteristics of mechanical flotation machines. *Minerals Engineering* 19, 807-815.

Outotec, 2016. Outotec flotation TankCell e-series [online document]. Finland: Outotec. Available: https://www.outotec.com/globalassets/products/flotation/ote_outotec_tankcell_e-series_en.pdf [referred 13.2.2019].

Pinto, T.C.S., Braga, A.S. Filho, L.S.L. and Deglon, D.A., 2018. Analysis of key mixing parameters in industrial Wemco mechanical flotation cells. *Minerals Engineering*, 123, 167-172.

Rinne, A. and Peltola, A., 2008. On lifetime costs of flotation operations. *Minerals Engineering*, 21, 846-850.

Safari M., Harris, M., Deglon, D., Filho, L.L. and Testa, F., 2016. The effect of energy input on flotation kinetics. *International Journal of Mineral Processing*, 156, 108-115.

Safari, M. and Deglon, D., 2018. An attachment-detachment kinetic model for the effect of energy input on flotation. *Minerals Engineering*, 117, 8-13.

Schubert, H., 2008. On the optimization of hydrodynamics in fine particle flotation. *Minerals Engineering*, 21, 930-936.

Tabosa, E., Runge, K., Holtham, P. and Duffy, K., 2016. Improving flotation energy efficiency by optimizing cell hydrodynamics. *Minerals Engineering*, 96-97, 194-202.

Wills B.A. and Napier-Munn, T.J., 2006. *Will's Mineral Processing Technology*. 7th edition. Oxford, Great Britain: Elsevier Ltd, pp. 444. ISBN 0-7506-4450-8.

Yarar, B and Richter, R.B., 2016. Flotation. *Ullmann's encyclopedia of industrial chemistry*, Electronic release. Weinheim, Germany, Wiley-VCH, pp. 56.

Yianatos, J.B., 2007. Fluid flow and kinetic modelling in flotation related processes Columns and Mechanically Agitated Cells – A Review. *Chemical Engineering Research and Design*, 85 (A12), 1591-1603.

Date		Sample
Test N°		Water type
Pulp density (g/lt)		Test objective
Grind size (μ)		

Sample (kg)	1,90
Volume (L)	6,5

Reagent Scheme

STAGE	Mixing rpm	time (min)		pH	E (mV)	CMC g/t / [ml]	Aerophine 3418A g/t / [ml]	Dowfroth 250 g/t / [μl]	SIPX g/t / [ml]	Product	
		cond.	flot.							Name	weight [g]
						1,0 %	1,0 %	100 %	1,0 %		
MFF, 6.5L kenno	1800										
Ilma 4l/h	"										
	"	2					5 0,95	20 38,0			
	"		10								CuRC
	"										CuRT
CuCC1 (feed CuRC),	1100										
1.5L kenno	"			10,5							
Ilma 2l/h	"	1				5 0,95	5 0,95	5 9,50			
	"		6								CuCC1
											CuCT1
Feed CuRT+CuCT1+CuCT2	X										
6.5L kenno	"			9,8							
Ilma 4l/h	"	1				15 2,85		10 19,0	50 9,50		
	"		7,5								NiRC1
	"		7,5								NiRC2
	"	1							30 5,70		
	"		12,5								NiRC3
			12,5								NiRC4
											NiRT
Total		5	56			20 3,8	10 1,9	35 66,5	80 15,2		

12.2.2019 12:32

Microscopy and Nanotechnology Centre

Quantification of sample Kauppila 1100 rpm CuCC1_8.1.2019

R.M.S.: 0,14
 Result status:
 Sum: 97,20 %
 Sample type: Pressed powder
 Initial sample weight (g): 13,16
 Weight after pressing (g): 14
 Correction applied for medium: No
 Correction applied for film: No
 Used Compound list: Geology EOL
 Results database: omnian
 Results database in: c:\panalytical\superq\userdata

Element	Conc. (%)
1 O	5,41
2 Mg	2,763
3 Al	0,17
4 Si	2,76
5 S	25,885
6 Ca	0,739
7 Cr	0,03
8 Fe	29,054
9 Ni	0,918
10 Cu	29,51

Binder

Chemical formula Weight (g)
 C18H36O2N2 0,84

12.2.2019 12:52

Microscopy and Nanotechnology Centre

Quantification of sample Kauppila 1100 rpm NiRC1_8.1.2019

R.M.S.: 0,144
 Result status:
 Sum: 97,30 %
 Sample type: Pressed powder
 Initial sample weight (g): 13,16
 Weight after pressing (g): 14
 Correction applied for medium: No
 Correction applied for film: No
 Used Compound list: Geology EOL
 Results database: omnian
 Results database in: c:\panalytical\superq\userdata

Element	Conc. (%)
1 O	15,062
2 Mg	6,492
3 Al	0,436
4 Si	8,186
5 S	19,618
6 Ca	2,691
7 Cr	0,096
8 Fe	29,427
9 Ni	7,191
10 Cu	8,109

Binder

Chemical formula Weight (g)
 C18H36O2N2 0,84

12.2.2019 12:55

Microscopy and Nanotechnology Centre

Quantification of sample Kauppila 1100 rpm NiRC2_8.1.2019

R.M.S.: 0,061
 Result status:
 Sum: 96,80 %
 Sample type: Pressed powder
 Initial sample weight (g): 13,16
 Weight after pressing (g): 14
 Correction applied for medium: No
 Correction applied for film: No
 Used Compound list: Geology EOL
 Results database: omnian
 Results database in: c:\panalytical\superq\userdata

Element	Conc. (%)
1 O	16,881
2 Mg	7,14
3 Al	0,51
4 Si	9,199
5 S	18,376
6 Ca	3,121
7 Cr	0,129
8 Fe	33,037
9 Ni	6,415
10 Cu	1,984

Binder

Chemical formula Weight (g)
 C18H36O2N2 0,84

12.2.2019 12:58

Microscopy and Nanotechnology Centre

Quantification of sample Kauppila 1100 rpm NiRC3_8.1.2019

R.M.S.: 0,056
 Result status:
 Sum: 96,60 %
 Sample type: Pressed powder
 Initial sample weight (g): 13,16
 Weight after pressing (g): 14
 Correction applied for medium: No
 Correction applied for film: No
 Used Compound list: Geology EOL
 Results database: omnian
 Results database in: c:\panalytical\superq\userdata

Element	Conc. (%)
1 O	18,294
2 Mg	7,578
3 Al	0,545
4 Si	9,99
5 S	17,622
6 Ca	3,607
7 Cr	0,152
8 Fe	34,952
9 Ni	3,077
10 Cu	0,823

Binder

Chemical formula Weight (g)
 C18H36O2N2 0,84

12.2.2019 12:59

Microscopy and Nanotechnology Centre

Quantification of sample Kauppila 1100 rpm NiRC4_8.1.2019

R.M.S.: 0,101
 Result status:
 Sum: 96,50 %
 Sample type: Pressed powder
 Initial sample weight (g): 13,16
 Weight after pressing (g): 14
 Correction applied for medium: No
 Correction applied for film: No
 Used Compound list: Geology EOL
 Results database: omnian
 Results database in: c:\panalytical\superq\userdata

Element	Conc. (%)
1 O	23,935
2 Mg	9,596
3 Al	0,745
4 Si	13,133
5 S	13,221
6 Ca	4,992
7 Cr	0,209
8 Fe	28,491
9 Ni	1,725
10 Cu	0,49

Binder

Chemical formula Weight (g)
 C18H36O2N2 0,84

12.2.2019 13:05

Microscopy and Nanotechnology Centre

Quantification of sample Kauppila 1100 rpm NiRT_8.1.2019

R.M.S.: 0,036
 Result status:
 Sum: 91,70 %
 Sample type: Pressed powder
 Initial sample weight (g): 13,16
 Weight after pressing (g): 14
 Correction applied for medium: No
 Correction applied for film: No
 Used Compound list: Geology EOL
 Results database: omnian
 Results database in: c:\panalytical\superq\userdata

Element	Conc. (%)
1 O	37,484
2 Mg	13,217
3 Al	1,109
4 Si	21,113
5 S	0,736
6 Ca	9,375
7 Cr	0,291
8 Fe	8,088
9 Ni	0,188
10 Cu	0,06

Binder

Chemical formula Weight (g)
 C18H36O2N2 0,84

13.2.2019 7:50
Microscopy and Nanotechnology Centre
Quantification of sample Kauppila 1100 rpm CuCC1_28.01.2019

R.M.S.: 0,136
Result status:
Sum: 97,50 %
Sample type: Pressed powder
Initial sample weight (g): 13,16
Weight after pressing (g): 14
Correction applied for medium: No
Correction applied for film: No
Used Compound list: Geology EOL
Results database: omnian
Results database in: c:\panalytical\superq\userdata

Element	Conc. (%)
1 O	8,739
2 Mg	4,158
3 Al	0,253
4 Si	4,594
5 S	23,69
6 Ca	1,362
7 Cr	0,05
8 Fe	28,409
9 Ni	2,802
10 Cu	23,456

Binder
Chemical formula Weight
(g)
C18H36O2N2 0,84

13.2.2019 7:52
Microscopy and Nanotechnology Centre
Quantification of sample Kauppila 1100 rpm NiRC1_28.01.2019

R.M.S.: 0,076
Result status:
Sum: 97,10 %
Sample type: Pressed powder
Initial sample weight (g): 13,16
Weight after pressing (g): 14
Correction applied for medium: No
Correction applied for film: No
Used Compound list: Geology EOL
Results database: omnian
Results database in: c:\panalytical\superq\userdata

Element	Conc. (%)
1 O	16,875
2 Mg	7,13
3 Al	0,504
4 Si	9,2
5 S	18,481
6 Ca	3,133
7 Cr	0,134
8 Fe	31,925
9 Ni	6,691
10 Cu	3,022

Binder
Chemical formula Weight
(g)
C18H36O2N2 0,84

13.2.2019 7:55
Microscopy and Nanotechnology Centre
Quantification of sample Kauppila 1100 rpm NiRC2_28.01.2019

R.M.S.: 0,076
Result status:
Sum: 96,30 %
Sample type: Pressed powder
Initial sample weight (g): 13,16
Weight after pressing (g): 14
Correction applied for medium: No
Correction applied for film: No
Used Compound list: Geology EOL
Results database: omnian
Results database in: c:\panalytical\superq\userdata

Element	Conc. (%)
1 O	20,427
2 Mg	8,38
3 Al	0,623
4 Si	11,201
5 S	15,947
6 Ca	3,994
7 Cr	0,176
8 Fe	32,403
9 Ni	2,289
10 Cu	0,909

Binder
Chemical formula Weight
(g)
C18H36O2N2 0,84

13.2.2019 7:56
Microscopy and Nanotechnology Centre
Quantification of sample Kauppila 1100 rpm NiRC3_28.01.2019

R.M.S.: 0,106
Result status:
Sum: 95,70 %
Sample type: Pressed powder
Initial sample weight (g): 13,16
Weight after pressing (g): 14
Correction applied for medium: No
Correction applied for film: No
Used Compound list: Geology EOL
Results database: omnian
Results database in: c:\panalytical\superq\userdata

Element	Conc. (%)
1 O	25,188
2 Mg	10,052
3 Al	0,777
4 Si	13,871
5 S	11,907
6 Ca	5,201
7 Cr	0,214
8 Fe	26,82
9 Ni	1,235
10 Cu	0,464

Binder
Chemical formula Weight
(g)
C18H36O2N2 0,84

13.2.2019 7:58
Microscopy and Nanotechnology Centre
Quantification of sample Kauppila 1100 rpm NiRC4_28.01.2019

R.M.S.: 0,097
Result status:
Sum: 94,30 %
Sample type: Pressed powder
Initial sample weight (g): 13,16
Weight after pressing (g): 14
Correction applied for medium: No
Correction applied for film: No
Used Compound list: Geology EOL
Results database: omnian
Results database in: c:\panalytical\superq\userdata

Element	Conc. (%)
1 O	32,279
2 Mg	12,249
3 Al	1,029
4 Si	17,948
5 S	5,854
6 Ca	7,144
7 Cr	0,278
8 Fe	16,401
9 Ni	0,759
10 Cu	0,311

Binder
Chemical formula Weight
(g)
C18H36O2N2 0,84

13.2.2019 7:59
Microscopy and Nanotechnology Centre
Quantification of sample Kauppila 1100 rpm NiRT_28.01.2019

R.M.S.: 0,034
Result status:
Sum: 91,70 %
Sample type: Pressed powder
Initial sample weight (g): 13,16
Weight after pressing (g): 14
Correction applied for medium: No
Correction applied for film: No
Used Compound list: Geology EOL
Results database: omnian
Results database in: c:\panalytical\superq\userdata

Element	Conc. (%)
1 O	37,755
2 Mg	13,269
3 Al	1,128
4 Si	21,283
5 S	0,542
6 Ca	9,44
7 Cr	0,299
8 Fe	7,798
9 Ni	0,16
10 Cu	0,047

Binder
Chemical formula Weight
(g)
C18H36O2N2 0,84

12.2.2019 13:08

Microscopy and Nanotechnology Centre

Quantification of sample Kauppila 1400 rpm CuCC1_14.12.2018

R.M.S.: 0,137
 Result status:
 Sum: 97,00 %
 Sample type: Pressed powder
 Initial sample weight (g): 13,16
 Weight after pressing (g): 14
 Correction applied for medium: No
 Correction applied for film: No
 Used Compound list: Geology EOL
 Results database: omnian
 Results database in: c:\panalytical\superq\userdata

Element	Conc. (%)
1 O	4,455
2 Mg	2,328
3 Al	0,142
4 Si	2,234
5 S	26,438
6 Ca	0,628
7 Cr	0,025
8 Fe	29,255
9 Ni	0,733
10 Cu	30,785

Binder

Chemical formula	Weight (g)
C18H36O2N2	0,84

12.2.2019 13:10

Microscopy and Nanotechnology Centre

Quantification of sample Kauppila 1400 rpm NiRC1_14.12.2018

R.M.S.: 0,117
 Result status:
 Sum: 98,00 %
 Sample type: Pressed powder
 Initial sample weight (g): 13,16
 Weight after pressing (g): 14
 Correction applied for medium: No
 Correction applied for film: No
 Used Compound list: Geology EOL
 Results database: omnian
 Results database in: c:\panalytical\superq\userdata

Element	Conc. (%)
1 O	15,489
2 Mg	6,728
3 Al	0,479
4 Si	8,372
5 S	19,44
6 Ca	2,745
7 Cr	0,117
8 Fe	31,456
9 Ni	6,618
10 Cu	6,521

Binder

Chemical formula	Weight (g)
C18H36O2N2	0,84

12.2.2019 13:11

Microscopy and Nanotechnology Centre

Quantification of sample Kauppila 1400 rpm NiRC2_14.12.2018

R.M.S.: 0,049
 Result status:
 Sum: 96,60 %
 Sample type: Pressed powder
 Initial sample weight (g): 13,16
 Weight after pressing (g): 14
 Correction applied for medium: No
 Correction applied for film: No
 Used Compound list: Geology EOL
 Results database: omnian
 Results database in: c:\panalytical\superq\userdata

Element	Conc. (%)
1 O	17,576
2 Mg	7,367
3 Al	0,537
4 Si	9,578
5 S	17,958
6 Ca	3,347
7 Cr	0,157
8 Fe	34,653
9 Ni	3,792
10 Cu	1,622

Binder

Chemical formula	Weight (g)
C18H36O2N2	0,84

12.2.2019 13:12

Microscopy and Nanotechnology Centre

Quantification of sample Kauppila 1400 rpm NiRC3_14.12.2018

R.M.S.: 0,08
 Result status:
 Sum: 96,30 %
 Sample type: Pressed powder
 Initial sample weight (g): 13,16
 Weight after pressing (g): 14
 Correction applied for medium: No
 Correction applied for film: No
 Used Compound list: Geology EOL
 Results database: omnian
 Results database in: c:\panalytical\superq\userdata

Element	Conc. (%)
1 O	21,021
2 Mg	8,581
3 Al	0,656
4 Si	11,518
5 S	15,391
6 Ca	4,173
7 Cr	0,19
8 Fe	31,635
9 Ni	2,027
10 Cu	1,076

Binder

Chemical formula	Weight (g)
C18H36O2N2	0,84

12.2.2019 13:14

Microscopy and Nanotechnology Centre

Quantification of sample Kauppila 1400 rpm NiRC4_14.12.2018

R.M.S.: 0,108
 Result status:
 Sum: 96,00 %
 Sample type: Pressed powder
 Initial sample weight (g): 13,16
 Weight after pressing (g): 14
 Correction applied for medium: No
 Correction applied for film: No
 Used Compound list: Geology EOL
 Results database: omnian
 Results database in: c:\panalytical\superq\userdata

Element	Conc. (%)
1 O	25,733
2 Mg	10,199
3 Al	0,803
4 Si	14,164
5 S	11,541
6 Ca	5,429
7 Cr	0,24
8 Fe	25,727
9 Ni	1,455
10 Cu	0,696

Binder

Chemical formula	Weight (g)
C18H36O2N2	0,84

12.2.2019 13:15

Microscopy and Nanotechnology Centre

Quantification of sample Kauppila 1400 rpm NiRT_14.12.2018

R.M.S.: 0,035
 Result status:
 Sum: 91,70 %
 Sample type: Pressed powder
 Initial sample weight (g): 13,16
 Weight after pressing (g): 14
 Correction applied for medium: No
 Correction applied for film: No
 Used Compound list: Geology EOL
 Results database: omnian
 Results database in: c:\panalytical\superq\userdata

Element	Conc. (%)
1 O	37,613
2 Mg	13,204
3 Al	1,131
4 Si	21,17
5 S	0,627
6 Ca	9,506
7 Cr	0,291
8 Fe	7,903
9 Ni	0,174
10 Cu	0,055

Binder

Chemical formula	Weight (g)
C18H36O2N2	0,84

13.2.2019 8:00

Microscopy and Nanotechnology Centre

Quantification of sample Kauppila 1400 rpm CuCC1_21.01.2019

R.M.S.: 0,138
 Result status:
 Sum: 97,50 %
 Sample type: Pressed powder
 Initial sample weight (g): 13,16
 Weight after pressing (g): 14
 Correction applied for medium: No
 Correction applied for film: No
 Used Compound list: Geology EOL
 Results database: omnian
 Results database in: c:\panalytical\superq\userdata

Element	Conc. (%)
1 O	8,629
2 Mg	4,152
3 Al	0,251
4 Si	4,523
5 S	23,762
6 Ca	1,299
7 Cr	0,054
8 Fe	28,454
9 Ni	2,091
10 Cu	24,308

Binder

Chemical formula Weight
(g)
 C18H36O2N2 0,84

13.2.2019 8:01

Microscopy and Nanotechnology Centre

Quantification of sample Kauppila 1400 rpm NiRC1_21.01.2019

R.M.S.: 0,087
 Result status:
 Sum: 96,70 %
 Sample type: Pressed powder
 Initial sample weight (g): 13,16
 Weight after pressing (g): 14
 Correction applied for medium: No
 Correction applied for film: No
 Used Compound list: Geology EOL
 Results database: omnian
 Results database in: c:\panalytical\superq\userdata

Element	Conc. (%)
1 O	18,962
2 Mg	7,78
3 Al	0,557
4 Si	10,403
5 S	16,839
6 Ca	3,742
7 Cr	0,151
8 Fe	29,035
9 Ni	6,123
10 Cu	3,11

Binder

Chemical formula Weight
(g)
 C18H36O2N2 0,84

13.2.2019 8:03

Microscopy and Nanotechnology Centre

Quantification of sample Kauppila 1400 rpm NiRC2_21.01.2019

R.M.S.: 0,066
 Result status:
 Sum: 96,60 %
 Sample type: Pressed powder
 Initial sample weight (g): 13,16
 Weight after pressing (g): 14
 Correction applied for medium: No
 Correction applied for film: No
 Used Compound list: Geology EOL
 Results database: omnian
 Results database in: c:\panalytical\superq\userdata

Element	Conc. (%)
1 O	19,316
2 Mg	7,925
3 Al	0,585
4 Si	10,574
5 S	16,872
6 Ca	3,836
7 Cr	0,167
8 Fe	33,791
9 Ni	2,842
10 Cu	0,713

Binder

Chemical formula Weight
(g)
 C18H36O2N2 0,84

13.2.2019 8:04

Microscopy and Nanotechnology Centre

Quantification of sample Kauppila 1400 rpm NiRC3_21.01.2019

R.M.S.: 0,109
 Result status:
 Sum: 95,70 %
 Sample type: Pressed powder
 Initial sample weight (g): 13,16
 Weight after pressing (g): 14
 Correction applied for medium: No
 Correction applied for film: No
 Used Compound list: Geology EOL
 Results database: omnian
 Results database in: c:\panalytical\superq\userdata

Element	Conc. (%)
1 O	25,468
2 Mg	10,012
3 Al	0,792
4 Si	14,031
5 S	11,715
6 Ca	5,48
7 Cr	0,234
8 Fe	26,291
9 Ni	1,324
10 Cu	0,396

Binder

Chemical formula Weight
(g)
 C18H36O2N2 0,84

13.2.2019 8:05

Microscopy and Nanotechnology Centre

Quantification of sample Kauppila 1400 rpm NiRC4_21.01.2019

R.M.S.: 0,091
 Result status:
 Sum: 93,70 %
 Sample type: Pressed powder
 Initial sample weight (g): 13,16
 Weight after pressing (g): 14
 Correction applied for medium: No
 Correction applied for film: No
 Used Compound list: Geology EOL
 Results database: omnian
 Results database in: c:\panalytical\superq\userdata

Element	Conc. (%)
1 O	32,805
2 Mg	12,268
3 Al	1,02
4 Si	18,277
5 S	5,21
6 Ca	7,512
7 Cr	0,29
8 Fe	15,394
9 Ni	0,69
10 Cu	0,233

Binder

Chemical formula Weight
(g)
 C18H36O2N2 0,84

13.2.2019 8:06

Microscopy and Nanotechnology Centre

Quantification of sample Kauppila 1400 rpm NiRT_21.01.2019

R.M.S.: 0,033
 Result status:
 Sum: 91,50 %
 Sample type: Pressed powder
 Initial sample weight (g): 13,16
 Weight after pressing (g): 14
 Correction applied for medium: No
 Correction applied for film: No
 Used Compound list: Geology EOL
 Results database: omnian
 Results database in: c:\panalytical\superq\userdata

Element	Conc. (%)
1 O	37,754
2 Mg	13,27
3 Al	1,134
4 Si	21,266
5 S	0,449
6 Ca	9,472
7 Cr	0,303
8 Fe	7,697
9 Ni	0,153
10 Cu	0,046

Binder

Chemical formula Weight
(g)
 C18H36O2N2 0,84

12.2.2019 13:17

Microscopy and Nanotechnology Centre

Quantification of sample Kauppila 1700 rpm CuCC1_10.12.2018

R.M.S.: 0,14
 Result status:
 Sum: 97,30 %
 Sample type: Pressed powder
 Initial sample weight (g): 13,16
 Weight after pressing (g): 14
 Correction applied for medium: No
 Correction applied for film: No
 Used Compound list: Geology EOL
 Results database: omnian
 Results database in: c:\panalytical\superq\userdata

Element	Conc. (%)
1 O	9,295
2 Mg	4,494
3 Al	0,269
4 Si	4,863
5 S	23,265
6 Ca	1,396
7 Cr	0,058
8 Fe	27,657
9 Ni	2,192
10 Cu	23,834

Binder

Chemical formula	Weight (g)
C18H36O2N2	0,84

12.2.2019 13:52

Microscopy and Nanotechnology Centre

Quantification of sample Kauppila 1700 rpm NiRC1_10.12.2018

R.M.S.: 0,103
 Result status:
 Sum: 96,60 %
 Sample type: Pressed powder
 Initial sample weight (g): 13,16
 Weight after pressing (g): 14
 Correction applied for medium: No
 Correction applied for film: No
 Used Compound list: Geology EOL
 Results database: omnian
 Results database in: c:\panalytical\superq\userdata

Element	Conc. (%)
1 O	19,014
2 Mg	7,86
3 Al	0,579
4 Si	10,356
5 S	16,593
6 Ca	3,822
7 Cr	0,149
8 Fe	28,107
9 Ni	5,4
10 Cu	4,763

Binder

Chemical formula	Weight (g)
C18H36O2N2	0,84

12.2.2019 14:04

Microscopy and Nanotechnology Centre

Quantification of sample Kauppila 1700 rpm NiRC2_10.12.2018

R.M.S.: 0,102
 Result status:
 Sum: 96,30 %
 Sample type: Pressed powder
 Initial sample weight (g): 13,16
 Weight after pressing (g): 14
 Correction applied for medium: No
 Correction applied for film: No
 Used Compound list: Geology EOL
 Results database: omnian
 Results database in: c:\panalytical\superq\userdata

Element	Conc. (%)
1 O	21,433
2 Mg	8,651
3 Al	0,668
4 Si	11,725
5 S	14,988
6 Ca	4,423
7 Cr	0,191
9 Fe	29,921
10 Ni	3,228
11 Cu	1,042

Binder

Chemical formula	Weight (g)
C18H36O2N2	0,84

12.2.2019 14:28

Microscopy and Nanotechnology Centre

Quantification of sample Kauppila 1700 rpm NiRC3_10.12.2018

R.M.S.: 0,105
 Result status:
 Sum: 95,60 %
 Sample type: Pressed powder
 Initial sample weight (g): 13,16
 Weight after pressing (g): 14
 Correction applied for medium: No
 Correction applied for film: No
 Used Compound list: Geology EOL
 Results database: omnian
 Results database in: c:\panalytical\superq\userdata

Element	Conc. (%)
1 O	24,253
2 Mg	9,619
3 Al	0,754
4 Si	13,288
5 S	12,676
6 Ca	5,288
7 Cr	0,209
8 Fe	27,229
9 Ni	1,727
10 Cu	0,535

Binder

Chemical formula	Weight (g)
C18H36O2N2	0,84

12.2.2019 15:28

Microscopy and Nanotechnology Centre

Quantification of sample Kauppila 1700 rpm NiRC4_10.12.2018

R.M.S.: 0,109
 Result status:
 Sum: 94,40 %
 Sample type: Pressed powder
 Initial sample weight (g): 13,16
 Weight after pressing (g): 14
 Correction applied for medium: No
 Correction applied for film: No
 Used Compound list: Geology EOL
 Results database: omnian
 Results database in: c:\panalytical\superq\userdata

Element	Conc. (%)
1 O	30,046
2 Mg	11,386
3 Al	0,922
4 Si	16,652
5 S	7,647
6 Ca	6,908
7 Cr	0,254
8 Fe	19,156
9 Ni	0,917
10 Cu	0,504

Binder

Chemical formula	Weight (g)
C18H36O2N2	0,84

12.2.2019 15:30

Microscopy and Nanotechnology Centre

Quantification of sample Kauppila 1700 rpm NiRT_10.12.2018

R.M.S.: 0,034
 Result status:
 Sum: 91,40 %
 Sample type: Pressed powder
 Initial sample weight (g): 13,16
 Weight after pressing (g): 14
 Correction applied for medium: No
 Correction applied for film: No
 Used Compound list: Geology EOL
 Results database: omnian
 Results database in: c:\panalytical\superq\userdata

Element	Conc. (%)
1 O	37,603
2 Mg	13,26
3 Al	1,114
4 Si	21,188
5 S	0,563
6 Ca	9,377
7 Cr	0,294
8 Fe	7,773
9 Ni	0,164
10 Cu	0,058

Binder

Chemical formula	Weight (g)
C18H36O2N2	0,84

13.2.2019 9:05

Microscopy and Nanotechnology Centre

Quantification of sample Kauppila 1700 rpm CuCC1_11.01.2019

R.M.S.: 0,139
 Result status:
 Sum: 97,40 %
 Sample type: Pressed powder
 Initial sample weight (g): 13,16
 Weight after pressing (g): 14
 Correction applied for medium: No
 Correction applied for film: No
 Used Compound list: Geology EOL
 Results database: omnian
 Results database in: c:\panalytical\superq\userdata

Element	Conc. (%)
1 O	7,632
2 Mg	3,759
3 Al	0,232
4 Si	3,951
5 S	24,348
6 Ca	1,127
7 Cr	0,043
8 Fe	28,882
9 Ni	1,717
10 Cu	25,695

Binder

Chemical formula	Weight (g)
C18H36O2N2	0,84

13.2.2019 9:06

Microscopy and Nanotechnology Centre

Quantification of sample Kauppila 1700 rpm NiRC1_11.01.2019

R.M.S.: 0,101
 Result status:
 Sum: 96,80 %
 Sample type: Pressed powder
 Initial sample weight (g): 13,16
 Weight after pressing (g): 14
 Correction applied for medium: No
 Correction applied for film: No
 Used Compound list: Geology EOL
 Results database: omnian
 Results database in: c:\panalytical\superq\userdata

Element	Conc. (%)
1 O	23,303
2 Mg	9,212
3 Al	0,697
4 Si	12,812
5 S	13,576
6 Ca	5,063
7 Cr	0,188
8 Fe	25,389
9 Ni	4,532
10 Cu	2,006

Binder

Chemical formula	Weight (g)
C18H36O2N2	0,84

13.2.2019 10:37

Microscopy and Nanotechnology Centre

Quantification of sample Kauppila 1700 rpm NiRC2_11.01.2019

R.M.S.: 0,075
 Result status:
 Sum: 96,70 %
 Sample type: Pressed powder
 Initial sample weight (g): 13,16
 Weight after pressing (g): 14
 Correction applied for medium: No
 Correction applied for film: No
 Used Compound list: Geology EOL
 Results database: omnian
 Results database in: c:\panalytical\superq\userdata

Element	Conc. (%)
1 O	20,625
2 Mg	8,396
3 Al	0,634
4 Si	11,302
5 S	15,757
6 Ca	4,151
7 Cr	0,187
8 Fe	32,349
9 Ni	2,665
10 Cu	0,657

Binder

Chemical formula	Weight (g)
C18H36O2N2	0,84

13.2.2019 10:39

Microscopy and Nanotechnology Centre

Quantification of sample Kauppila 1700 rpm NiRC3_11.01.2019

R.M.S.: 0,103
 Result status:
 Sum: 96,20 %
 Sample type: Pressed powder
 Initial sample weight (g): 13,16
 Weight after pressing (g): 14
 Correction applied for medium: No
 Correction applied for film: No
 Used Compound list: Geology EOL
 Results database: omnian
 Results database in: c:\panalytical\superq\userdata

Element	Conc. (%)
1 O	24,546
2 Mg	9,776
3 Al	0,762
4 Si	13,503
5 S	12,538
6 Ca	5,129
7 Cr	0,225
8 Fe	27,876
9 Ni	1,452
10 Cu	0,385

Binder

Chemical formula	Weight (g)
C18H36O2N2	0,84

13.2.2019 10:40

Microscopy and Nanotechnology Centre

Quantification of sample Kauppila 1700 rpm NiRC4_11.01.2019

R.M.S.: 0,107
 Result status:
 Sum: 94,80 %
 Sample type: Pressed powder
 Initial sample weight (g): 13,16
 Weight after pressing (g): 14
 Correction applied for medium: No
 Correction applied for film: No
 Used Compound list: Geology EOL
 Results database: omnian
 Results database in: c:\panalytical\superq\userdata

Element	Conc. (%)
1 O	30,025
2 Mg	11,631
3 Al	0,952
4 Si	16,586
5 S	7,683
6 Ca	6,577
7 Cr	0,27
8 Fe	19,828
9 Ni	0,923
10 Cu	0,29

Binder

Chemical formula	Weight (g)
C18H36O2N2	0,84

13.2.2019 10:45

Microscopy and Nanotechnology Centre

Quantification of sample Kauppila 1700 rpm NiRT_11.01.2019

R.M.S.: 0,032
 Result status:
 Sum: 91,40 %
 Sample type: Pressed powder
 Initial sample weight (g): 13,16
 Weight after pressing (g): 14
 Correction applied for medium: No
 Correction applied for film: No
 Used Compound list: Geology EOL
 Results database: omnian
 Results database in: c:\panalytical\superq\userdata

Element	Conc. (%)
1 O	37,749
2 Mg	13,256
3 Al	1,133
4 Si	21,272
5 S	0,431
6 Ca	9,467
7 Cr	0,289
8 Fe	7,643
9 Ni	0,145
10 Cu	0,047

Binder

Chemical formula	Weight (g)
C18H36O2N2	0,84

12.2.2019 15:39

Microscopy and Nanotechnology Centre

Quantification of sample Kauppila 2000 rpm CuCC1_03.12.2018

R.M.S.: 0,142
 Result status:
 Sum: 97,40 %
 Sample type: Pressed powder
 Initial sample weight (g): 13,16
 Weight after pressing (g): 14
 Correction applied for medium: No
 Correction applied for film: No
 Used Compound list: Geology EOL
 Results database: omnian
 Results database in: c:\panalytical\superq\userdata

Element	Conc. (%)
1 O	8,309
2 Mg	4,104
3 Al	0,246
4 Si	4,273
5 S	23,917
6 Ca	1,302
7 Cr	0,046
8 Fe	28,195
9 Ni	1,751
10 Cu	25,262

Binder

Chemical formula Weight
(g)
 C18H36O2N2 0,84

12.2.2019 16:03

Microscopy and Nanotechnology Centre

Quantification of sample Kauppila 2000 rpm NiRC1_03.12.2018

R.M.S.: 0,114
 Result status:
 Sum: 95,90 %
 Sample type: Pressed powder
 Initial sample weight (g): 13,16
 Weight after pressing (g): 14
 Correction applied for medium: No
 Correction applied for film: No
 Used Compound list: Geology EOL
 Results database: omnian
 Results database in: c:\panalytical\superq\userdata

Element	Conc. (%)
1 O	24,726
2 Mg	9,649
3 Al	0,742
4 Si	13,636
5 S	12,24
6 Ca	5,458
7 Cr	0,195
8 Fe	23,027
9 Ni	3,729
10 Cu	2,505

Binder

Chemical formula Weight
(g)
 C18H36O2N2 0,84

13.2.2019 7:44

Microscopy and Nanotechnology Centre

Quantification of sample Kauppila 2000 rpm NiRC2_03.12.2018

R.M.S.: 0,078
 Result status:
 Sum: 96,50 %
 Sample type: Pressed powder
 Initial sample weight (g): 13,16
 Weight after pressing (g): 14
 Correction applied for medium: No
 Correction applied for film: No
 Used Compound list: Geology EOL
 Results database: omnian
 Results database in: c:\panalytical\superq\userdata

Element	Conc. (%)
1 O	21,216
2 Mg	8,645
3 Al	0,659
4 Si	11,595
5 S	15,177
6 Ca	4,33
7 Cr	0,196
8 Fe	30,427
9 Ni	3,239
10 Cu	0,993

Binder

Chemical formula Weight
(g)
 C18H36O2N2 0,84

13.2.2019 7:45

Microscopy and Nanotechnology Centre

Quantification of sample Kauppila 2000 rpm NiRC3_03.12.2018

R.M.S.: 0,105
 Result status:
 Sum: 97,30 %
 Sample type: Pressed powder
 Initial sample weight (g): 13,16
 Weight after pressing (g): 14
 Correction applied for medium: No
 Correction applied for film: No
 Used Compound list: Geology EOL
 Results database: omnian
 Results database in: c:\panalytical\superq\userdata

Element	Conc. (%)
1 O	24,854
2 Mg	9,94
3 Al	0,782
4 Si	13,611
5 S	12,659
6 Ca	5,279
7 Cr	0,235
8 Fe	27,578
9 Ni	1,684
10 Cu	0,64

Binder

Chemical formula Weight
(g)
 C18H36O2N2 0,84

13.2.2019 7:47

Microscopy and Nanotechnology Centre

Quantification of sample Kauppila 2000 rpm NiRC4_03.12.2018

R.M.S.: 0,102
 Result status:
 Sum: 94,30 %
 Sample type: Pressed powder
 Initial sample weight (g): 13,16
 Weight after pressing (g): 14
 Correction applied for medium: No
 Correction applied for film: No
 Used Compound list: Geology EOL
 Results database: omnian
 Results database in: c:\panalytical\superq\userdata

Element	Conc. (%)
1 O	31,476
2 Mg	11,908
3 Al	0,978
4 Si	17,484
5 S	6,474
6 Ca	7,132
7 Cr	0,28
8 Fe	17,406
9 Ni	0,78
10 Cu	0,418

Binder

Chemical formula Weight
(g)
 C18H36O2N2 0,84

13.2.2019 7:48

Microscopy and Nanotechnology Centre

Quantification of sample Kauppila 2000 rpm NiRT_03.12.2018

R.M.S.: 0,033
 Result status:
 Sum: 91,50 %
 Sample type: Pressed powder
 Initial sample weight (g): 13,16
 Weight after pressing (g): 14
 Correction applied for medium: No
 Correction applied for film: No
 Used Compound list: Geology EOL
 Results database: omnian
 Results database in: c:\panalytical\superq\userdata

Element	Conc. (%)
1 O	37,793
2 Mg	13,314
3 Al	1,135
4 Si	21,271
5 S	0,434
6 Ca	9,479
7 Cr	0,291
8 Fe	7,628
9 Ni	0,146
10 Cu	0,048

Binder

Chemical formula Weight
(g)
 C18H36O2N2 0,84

13.2.2019 13:51

Microscopy and Nanotechnology Centre

Quantification of sample Kauppila 2000 rpm CuCC1_09.01.2019

R.M.S.: 0,138
 Result status:
 Sum: 97,50 %
 Sample type: Pressed powder
 Initial sample weight (g): 13,16
 Weight after pressing (g): 14
 Correction applied for medium: No
 Correction applied for film: No
 Used Compound list: Geology EOL
 Results database: omnian
 Results database in: c:\panalytical\superq\userdata

Element	Conc. (%)
1 O	8,167
2 Mg	3,933
3 Al	0,242
4 Si	4,292
5 S	24,067
6 Ca	1,187
7 Cr	0,041
8 Fe	28,609
9 Ni	2,193
10 Cu	24,779

Binder

Chemical formula Weight (g)
 C18H36O2N2 0,84

13.2.2019 13:52

Microscopy and Nanotechnology Centre

Quantification of sample Kauppila 2000 rpm NiRC1_09.01.2019

R.M.S.: 0,104
 Result status:
 Sum: 96,30 %
 Sample type: Pressed powder
 Initial sample weight (g): 13,16
 Weight after pressing (g): 14
 Correction applied for medium: No
 Correction applied for film: No
 Used Compound list: Geology EOL
 Results database: omnian
 Results database in: c:\panalytical\superq\userdata

Element	Conc. (%)
1 O	24,067
2 Mg	9,507
3 Al	0,739
4 Si	13,242
5 S	12,875
6 Ca	5,171
7 Cr	0,198
8 Fe	24,853
9 Ni	3,848
10 Cu	1,839

Binder

Chemical formula Weight (g)
 C18H36O2N2 0,84

13.2.2019 13:53

Microscopy and Nanotechnology Centre

Quantification of sample Kauppila 2000 rpm NiRC2_09.01.2019

R.M.S.: 0,094
 Result status:
 Sum: 96,70 %
 Sample type: Pressed powder
 Initial sample weight (g): 13,16
 Weight after pressing (g): 14
 Correction applied for medium: No
 Correction applied for film: No
 Used Compound list: Geology EOL
 Results database: omnian
 Results database in: c:\panalytical\superq\userdata

Element	Conc. (%)
1 O	22,966
2 Mg	9,294
3 Al	0,715
4 Si	12,573
5 S	13,961
6 Ca	4,727
7 Cr	0,222
8 Fe	29,231
9 Ni	1,963
10 Cu	1,011

Binder

Chemical formula Weight (g)
 C18H36O2N2 0,84

13.2.2019 13:54

Microscopy and Nanotechnology Centre

Quantification of sample Kauppila 2000 rpm NiRC3_09.01.2019

R.M.S.: 0,111
 Result status:
 Sum: 95,50 %
 Sample type: Pressed powder
 Initial sample weight (g): 13,16
 Weight after pressing (g): 14
 Correction applied for medium: No
 Correction applied for film: No
 Used Compound list: Geology EOL
 Results database: omnian
 Results database in: c:\panalytical\superq\userdata

Element	Conc. (%)
1 O	28,409
2 Mg	11,071
3 Al	0,9
4 Si	15,699
5 S	9,257
6 Ca	6,098
7 Cr	0,258
8 Fe	22,238
9 Ni	0,976
10 Cu	0,545

Binder

Chemical formula Weight (g)
 C18H36O2N2 0,84

13.2.2019 13:55

Microscopy and Nanotechnology Centre

Quantification of sample Kauppila 2000 rpm NiRC4_09.01.2019

R.M.S.: 0,09
 Result status:
 Sum: 93,60 %
 Sample type: Pressed powder
 Initial sample weight (g): 13,16
 Weight after pressing (g): 14
 Correction applied for medium: No
 Correction applied for film: No
 Used Compound list: Geology EOL
 Results database: omnian
 Results database in: c:\panalytical\superq\userdata

Element	Conc. (%)
1 O	32,944
2 Mg	12,357
3 Al	1,045
4 Si	18,336
5 S	5,014
6 Ca	7,489
7 Cr	0,3
8 Fe	15,057
9 Ni	0,624
10 Cu	0,399

Binder

Chemical formula Weight (g)
 C18H36O2N2 0,84

13.2.2019 13:57

Microscopy and Nanotechnology Centre

Quantification of sample Kauppila 2000 rpm NiRT_09.01.2019

R.M.S.: 0,032
 Result status:
 Sum: 91,20 %
 Sample type: Pressed powder
 Initial sample weight (g): 13,16
 Weight after pressing (g): 14
 Correction applied for medium: No
 Correction applied for film: No
 Used Compound list: Geology EOL
 Results database: omnian
 Results database in: c:\panalytical\superq\userdata

Element	Conc. (%)
1 O	37,727
2 Mg	13,266
3 Al	1,129
4 Si	21,258
5 S	0,365
6 Ca	9,446
7 Cr	0,292
8 Fe	7,476
9 Ni	0,149
10 Cu	0,045

Binder

Chemical formula Weight (g)
 C18H36O2N2 0,84

13.2.2019 13:58

Microscopy and Nanotechnology Centre

Quantification of sample Kauppila Feed

R.M.S.: 0,058
 Result status:
 Sum: 92,50 %
 Sample type: Pressed powder
 Initial sample weight (g): 13,16
 Weight after pressing (g): 14
 Correction applied for medium: No
 Correction applied for film: No
 Used Compound list: Geology EOL
 Results database: omnian
 Results database in: c:\panalytical\superq\userdata

Element	Conc. (%)
1 O	36,132
2 Mg	12,906
3 Al	1,086
4 Si	20,272
5 S	2,074
6 Ca	8,952
7 Cr	0,279
8 Fe	9,827
9 Ni	0,467
10 Cu	0,503

Binder

Chemical formula

Weight
(g)

C18H36O2N2

0,84

Appendix 3 (1)

	Total mass (g)	Cumulative mass (g)	Ni grade (%)	Ni mass (g)	Pure nickel recovery (g)	Ni recovery (%)	Single cell Ni recovery (%)	Cumulative Ni recovery (%)	Cumulative Ni grade (%)	Recovered nickel (%), cumulative
1100 CuCC1_8.1.2019	15,14		0,92	0,14		1,72				
NIRC1_8.1.2019	25,21	25,21	7,19	1,81		22,88		22,88	7,19	38,85
NIRC2_8.1.2019	21,69	46,90	6,42	1,39		17,56	22,77	40,44	6,83	68,67
NIRC3_8.1.2019	34,25	81,15	3,08	1,05		13,30	22,34	53,75	5,25	91,25
NIRC4_8.1.2019	23,66	104,81	1,73	0,41	4,67	5,15	11,14	58,90	4,45	100,00
NIRT_8.1.2019	1732,03		0,19	3,26						
Calculated feed	1851,98	100,15	0,44	8,06						
Calculated nickel feed	1836,84		0,43	7,92						
1100 CuCC1_28.1.2019	25,16		2,80	0,70		8,79				
NIRC1_28.1.2019	50,20	50,20	6,69	3,36		45,89	45,89	45,89	6,69	72,90
NIRC2_28.1.2019	26,57	76,77	2,29	0,61		8,31	15,36	54,20	5,17	86,10
NIRC3_28.1.2019	36,26	113,03	1,24	0,45		6,12	13,36	60,32	3,91	95,82
NIRC4_28.1.2019	25,39	138,42	0,76	0,19	4,61	2,63	6,64	62,95	3,33	100,00
NIRT_28.1.2019	1694,73		0,16	2,71						
Calculated feed	1858,31	133,81		8,02						
Calculated nickel feed	1833,15		0,40	7,32						
1400 CuCC1_14.12.2018	12,66		0,73	0,09		1,17				
NIRC1_14.12.2018	43,59	43,59	6,62	2,88		36,72	36,72	36,72	6,62	58,83
NIRC2_14.12.2018	31,91	75,50	3,79	1,21		15,40	24,34	52,13	5,42	83,51
NIRC3_14.12.2018	27,32	102,82	2,03	0,55		7,05	14,72	59,17	4,52	94,80
NIRC4_14.12.2018	17,52	120,34	1,46	0,25	4,90	3,25	7,95	62,42	4,07	100,00
NIRT_14.12.2018	1696,63		0,17	2,95						
Calculated feed	1829,63	115,44		7,95						
Calculated nickel feed	1816,97		0,43	7,86						
1400 CuCC1_21.1.2019	22,27		2,09	0,47		5,82				
NIRC1_21.1.2019	52,60	52,60	6,12	3,22		42,70	42,70	42,70	6,12	64,59
NIRC2_21.1.2019	35,25	87,85	2,84	1,00		13,28	23,18	55,99	4,81	84,68
NIRC3_21.1.2019	39,74	127,59	1,32	0,53		6,98	15,85	62,97	3,72	95,23
NIRC4_21.1.2019	34,49	162,08	0,69	0,24	4,99	3,16	8,52	66,12	3,08	100,00
NIRT_21.1.2019	1670,00		0,15	2,56						
Calculated feed	1854,35	157,09		8,01						
Calculated nickel feed	1832,08		0,41	7,54						

Appendix 3 (3)

	Calculated feed (g)	Ni in feed (g)	Ni in feed (%)	Copper content in nickel flotation feed (%)	Cu grade (%)	Cu weight (g)	Cu recovery (%)	Cu in feed (g)	Cu in feed (%)
1100 CuCC1_8.1.2019	1851,98				29,51	4,47	53,32	8,38	100
NiRC1_8.1.2019	1836,84	7,92	0,43		0,21	8,11	2,04	52,26	46,68
NiRC2_8.1.2019	1811,63	6,11	0,34			1,98	0,43	11,00	22,29
NiRC3_8.1.2019	1789,94	4,72	0,26			0,82	0,28	7,21	1,44
NiRC4_8.1.2019	1755,69	3,66	0,21			0,49	0,12	2,96	13,79
NiRT_8.1.2019	1732,03	3,26	0,19			0,06	1,04	26,57	12,40
Calculated feed						0,45	8,38		
Calculated nickel feed							3,91		
1100 CuCC1_28.1.2019	1858,31				23,46	5,90	67,80	8,70	100
NiRC1_28.1.2019	1833,15	7,32	0,40		0,15	3,02	1,52	54,14	32,20
NiRC2_28.1.2019	1782,95	3,96	0,22			0,91	0,24	8,62	14,77
NiRC3_28.1.2019	1756,38	3,35	0,19			0,46	0,17	6,00	11,99
NiRC4_28.1.2019	1720,12	2,90	0,17			0,31	0,08	2,82	10,06
NiRT_28.1.2019	1694,73	2,71	0,16			0,05	0,80	28,42	9,15
Calculated feed						0,47	8,70		
Calculated nickel feed							2,80		
1400 CuCC1_14.12.2018	1829,63				30,79	3,90	45,29	8,61	100
NiRC1_14.12.2018	1816,97	7,86	0,43		0,26	6,52	2,84	60,36	54,71
NiRC2_14.12.2018	1773,38	4,97	0,28			1,62	0,52	10,99	21,69
NiRC3_14.12.2018	1741,47	3,76	0,22			1,08	0,29	6,24	13,35
NiRC4_14.12.2018	1714,15	3,21	0,19			0,70	0,12	2,59	12,26
NiRT_14.12.2018	1696,63	2,95	0,17			0,06	0,93	19,82	10,84
Calculated feed						0,47	8,61		
Calculated nickel feed							4,71		
1400 CuCC1_21.1.2019	1854,35				24,31	5,41	65,17	8,31	100
NiRC1_21.1.2019	1832,08	7,54	0,41		0,16	3,11	1,64	56,54	34,83
NiRC2_21.1.2019	1779,48	4,32	0,24			0,71	0,25	8,69	15,14
NiRC3_21.1.2019	1744,23	3,32	0,19			0,40	0,16	5,44	12,11
NiRC4_21.1.2019	1704,49	2,79	0,16			0,23	0,08	2,78	10,22
NiRT_21.1.2019	1670,00	2,56	0,15			0,05	0,77	26,55	9,25
Calculated feed						0,45	8,31		
Calculated nickel feed							2,89		

Appendix 3 (4)

	Calculated feed (g)	Ni in feed (g)	Ni in feed (%)	Copper content in nickel flotation feed (%)	Cu grade (%)	Cu weight (g)	Cu recovery (%)	Cu in feed (g)	Cu in feed (%)
1700 CuCC1 10.12.	1829,50				23,83	4,57	53,55	8,54	100
NiRC1 10.12.	1810,31	7,44	0,41	0,22	4,76	2,24	56,40	3,97	46,45
NiRC2 10.12.	1763,32	4,91	0,28		1,04	0,43	10,96	1,73	20,25
NiRC3 10.12.	1721,59	3,56	0,21		0,54	0,17	4,18	1,30	15,16
NiRC4 10.12.	1690,63	3,02	0,18		0,50	0,17	4,24	1,13	13,22
NiRT 10.12.	1657,24	2,72	0,16		0,06	0,96	24,22	0,96	11,25
Calculated feed					0,47	8,54			
Calculated nickel feed						3,97			
1700 CuCC1_11.1.2019	1851,77				25,70	5,52	66,30	8,33	100
NiRC1_11.1.2019	1830,29	7,60	0,42	0,15	2,01	1,63	58,01	2,81	33,70
NiRC2_11.1.2019	1749,14	3,93	0,22		0,66	0,20	7,02	1,18	14,15
NiRC3_11.1.2019	1719,17	3,13	0,18		0,39	0,14	4,85	0,98	11,79
NiRC4_11.1.2019	1683,84	2,61	0,16		0,29	0,06	2,29	0,85	10,15
NiRT_11.1.2019	1661,71	2,41	0,15		0,05	0,78	27,83	0,78	9,38
Calculated feed					0,45	8,33			
Calculated nickel feed						2,81			
2000 CuCC1 3.12.	1816,50				25,26	4,63	55,59	8,33	100
NiRC1 3.12.	1798,16	7,54	0,42	0,21	2,51	2,23	60,25	3,70	44,41
NiRC2 3.12.	1709,18	4,22	0,25		0,99	0,27	7,29	1,47	17,65
NiRC3 3.12.	1682,01	3,34	0,20		0,64	0,25	6,86	1,20	14,41
NiRC4 3.12.	1642,34	2,67	0,16		0,42	0,18	4,85	0,95	11,37
NiRT 3.12.	1599,44	2,34	0,15		0,05	0,77	20,75	0,77	9,22
Calculated feed					0,46	8,33			
Calculated nickel feed						3,70			
2000 CuCC1_9.1.2019	1835,782				24,78	5,44	62,32	8,73	100
NiRC1_9.1.2019	1813,83	7,58	0,42	0,18	1,84	1,88	57,05	3,29	37,68
NiRC2_9.1.2019	1711,78	3,65	0,21		1,01	0,34	10,36	1,41	16,18
NiRC3_9.1.2019	1678,09	2,99	0,18		0,55	0,23	6,91	1,07	12,28
NiRC4_9.1.2019	1636,37	2,58	0,16		0,40	0,12	3,71	0,84	9,68
NiRT_9.1.2019	1605,80	2,39	0,15		0,05	0,72	21,97	0,72	8,28
Calculated feed					0,48	8,73			
Calculated nickel feed						3,29			

Appendix 4 (1)

	Ni concentrarte mass (kg)	Pure recovered Ni (kg)	Value with Ni price US\$12,810	Value with Ni price US\$10,000
1100 rpm 8.1.2019	4837,48	215,36	2758,80	2153,63
1100 rpm 28.1.2019	6388,62	212,66	2724,15	2126,58
1400 rpm 14.12.2018	5554,20	226,32	2899,15	2263,19
1400 rpm 21.1.2019	7480,62	230,15	2948,26	2301,53
1700 rpm 10.12.2018	7064,77	218,10	2793,83	2180,98
1700 rpm 11.1.2019	7780,99	239,71	3070,74	2397,14
2000 rpm 3.12.2018	9171,65	240,04	3074,87	2400,37
2000 rpm 9.1.2019	9601,34	239,36	3066,20	2393,60
	Value with Ni price US\$15,620	Energy consumption (kW)	Cost of electricity with US\$ 0.1/kWh	Cost of electricity with US\$ 0.2/kWh
1100 rpm 8.1.2019	3363,97	80,82	56,57	113,14
1100 rpm 28.1.2019	3321,72	80,82	56,57	113,14
1400 rpm 14.12.2018	3535,10	101,24	70,87	141,74
1400 rpm 21.1.2019	3594,99	101,24	70,87	141,74
1700 rpm 10.12.2018	3406,69	131,88	92,32	184,63
1700 rpm 11.1.2019	3744,33	131,88	92,32	184,63
2000 rpm 3.12.2018	3749,37	169,40	118,58	237,17
2000 rpm 9.1.2019	3738,80	169,40	118,58	237,17

Appendix 4 (2)

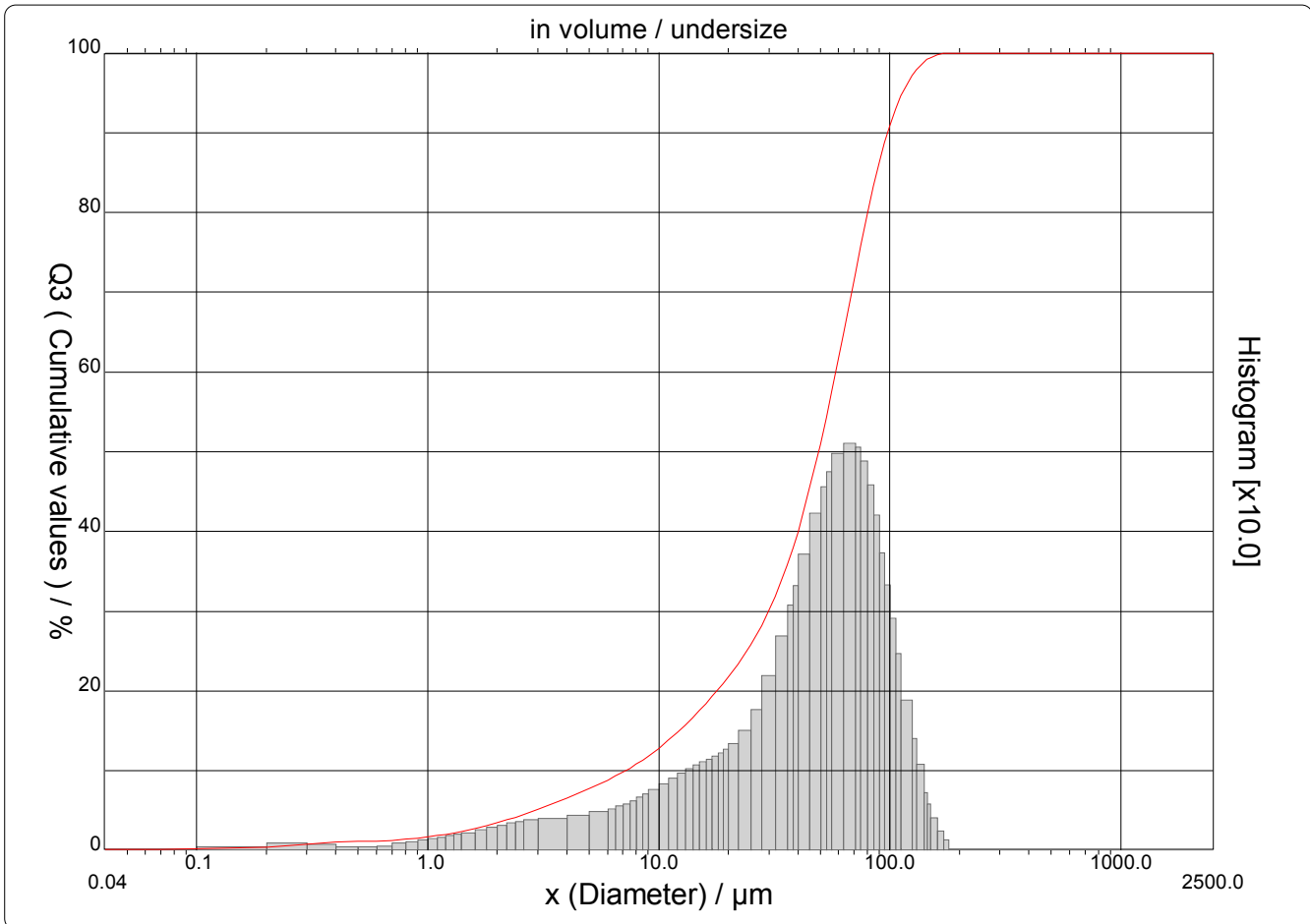
	Cost of electricity with US\$ 0.35/kWh	Cost of electricity with US\$/0.5 kWh	Profit (\$) with energy price US\$ 0.1/kWh	Profit with energy price US\$ 0.2/kWh
1100 rpm 8.1.2019	198,00	282,86	2702,23	2645,66
1100 rpm 28.1.2019	198,00	282,86	2667,58	2611,01
1400 rpm 14.12.2018	248,04	354,35	2828,28	2757,41
1400 rpm 21.1.2019	248,04	354,35	2877,39	2806,52
1700 rpm 10.12.2018	323,11	461,59	2701,51	2609,20
1700 rpm 11.1.2019	323,11	461,59	2978,42	2886,10
2000 rpm 3.12.2018	415,04	592,91	2956,29	2837,70
2000 rpm 9.1.2019	415,04	592,91	2947,61	2829,03
	Profit with energy price US\$ 0.35/kWh	Profit with energy price US\$ 0.5/kWh	Profit with Ni price US\$10,000/t and energy price US\$ 0.2/kWh	Profit with Ni price US\$15,620/t and energy price US\$ 0.2/kWh
1100 rpm 8.1.2019	2560,80	2475,95	2040,49	3250,83
1100 rpm 28.1.2019	2526,15	2441,29	2013,44	3208,58
1400 rpm 14.12.2018	2651,10	2544,80	2121,45	3393,36
1400 rpm 21.1.2019	2700,21	2593,91	2159,79	3453,25
1700 rpm 10.12.2018	2470,72	2332,24	1996,34	3222,05
1700 rpm 11.1.2019	2747,63	2609,15	2212,51	3559,70
2000 rpm 3.12.2018	2659,83	2481,96	2163,20	3512,21
2000 rpm 9.1.2019	2651,16	2473,28	2156,43	3501,63

CILAS 1190 Liquid

 Range : 0.04 μm - 2500.00 μm / 100 Classes

Sample ref.	: 8.1.2019 1100 rpm
Ore	: Ni-Cu-PGE
Sample type	: Wet
Comments	: Katariina Kauppilla
Liquid	: Water
Dispersing agent	: Water
Operator	: Kontio
Company	: OMS R&D Centre
Location	: University of Oulu
Date : 15.01.2019	Time : 07:31:34
Index meas.	: 1858
Database name	: CilasDB1

Ultrasounds	: 60	s
Obscurations	: 22 / 1.88	%
Diameter at 10%	: 7.16	μm
Diameter at 50%	: 49.11	μm
Diameter at 80%	: 80.31	μm
Fraunhofer		
Density/Factor	: -----	
Specific surface	: -----	
Automatic dilution	: No / No	
Meas./Rins.	: 60s/60s/4	
SOP name	: Katariina Kauppila	



CILAS 1190 Liquid

Range : 0.04 µm - 2500.00 µm / 100 Classes

Sample ref.	: 8.1.2019 1100 rpm
Ore	: Ni-Cu-PGE
Sample type	: Wet
Comments	: Katariina Kauppilla
Liquid	: Water
Dispersing agent	: Water
Operator	: Kontio
Company	: OMS R&D Centre
Location	: University of Oulu
Date : 15.01.2019	Time : 07:31:34
Index meas.	: 1858
Database name	: CilasDB1

Ultrasounds	: 60	s
Obscurations	: 22 / 1.88	%
Diameter at 10%	: 7.16	µm
Diameter at 50%	: 49.11	µm
Diameter at 80%	: 80.31	µm
Fraunhofer		
Density/Factor	-----	
Specific surface	-----	
Automatic dilution	: No / No	
Meas./Rins.	: 60s/60s/4	
SOP name	: Katariina Kauppilla	

Standards classes in volume / undersize

x	0.04	0.07	0.10	0.20	0.30	0.40	0.50	0.60	0.70	0.80
Q3	0.18	0.18	0.20	0.46	0.84	1.05	1.14	1.21	1.30	1.42
q3	0.01	0.00	0.00	0.03	0.07	0.06	0.03	0.03	0.04	0.08
x	0.90	1.00	1.10	1.20	1.30	1.40	1.60	1.80	2.00	2.20
Q3	1.57	1.72	1.88	2.04	2.21	2.38	2.74	3.10	3.47	3.83
q3	0.10	0.12	0.13	0.15	0.17	0.19	0.21	0.25	0.28	0.31
x	2.40	2.60	3.00	4.00	5.00	6.00	6.50	7.00	7.50	8.00
Q3	4.19	4.53	5.18	6.58	7.76	8.83	9.34	9.84	10.34	10.83
q3	0.33	0.34	0.36	0.39	0.42	0.47	0.51	0.54	0.58	0.61
x	8.50	9.00	10.00	11.00	12.00	13.00	14.00	15.00	16.00	17.00
Q3	11.33	11.83	12.81	13.79	14.76	15.72	16.65	17.56	18.44	19.30
q3	0.66	0.69	0.75	0.83	0.89	0.96	1.01	1.06	1.09	1.13
x	18.00	19.00	20.00	22.00	25.00	28.00	32.00	36.00	38.00	40.00
Q3	20.14	20.95	21.75	23.34	25.72	28.21	31.83	35.78	37.85	39.96
q3	1.17	1.21	1.25	1.33	1.50	1.76	2.17	2.68	3.07	3.31
x	45.00	50.00	53.00	56.00	63.00	71.00	75.00	80.00	85.00	90.00
Q3	45.40	50.95	54.26	57.51	64.81	72.40	75.85	79.78	83.23	86.22
q3	3.70	4.22	4.54	4.74	4.96	5.09	5.05	4.87	4.57	4.19
x	95.00	100.0	106.0	112.0	125.0	130.0	140.0	145.0	150.0	160.0
Q3	88.73	90.85	92.95	94.64	97.20	97.88	98.87	99.18	99.42	99.74
q3	3.72	3.31	2.89	2.46	1.87	1.39	1.07	0.71	0.57	0.40
x	170.0	180.0	190.0	200.0	212.0	242.0	250.0	300.0	400.0	500.0
Q3	99.91	100.00	100.00	100.00	100.00	100.00	100.00	100.00	100.00	100.00
q3	0.23	0.12	0.00	0.00	0.00	0.00	0.00	0.00	0.00	0.00
x	600.0	700.0	800.0	900.0	1000.0	1100.0	1200.0	1300.0	1400.0	1500.0
Q3	100.00	100.00	100.00	100.00	100.00	100.00	100.00	100.00	100.00	100.00
q3	0.00	0.00	0.00	0.00	0.00	0.00	0.00	0.00	0.00	0.00
x	1600.0	1700.0	1800.0	1900.0	2000.0	2100.0	2200.0	2300.0	2400.0	2500.0
Q3	100.00	100.00	100.00	100.00	100.00	100.00	100.00	100.00	100.00	100.00
q3	0.00	0.00	0.00	0.00	0.00	0.00	0.00	0.00	0.00	0.00

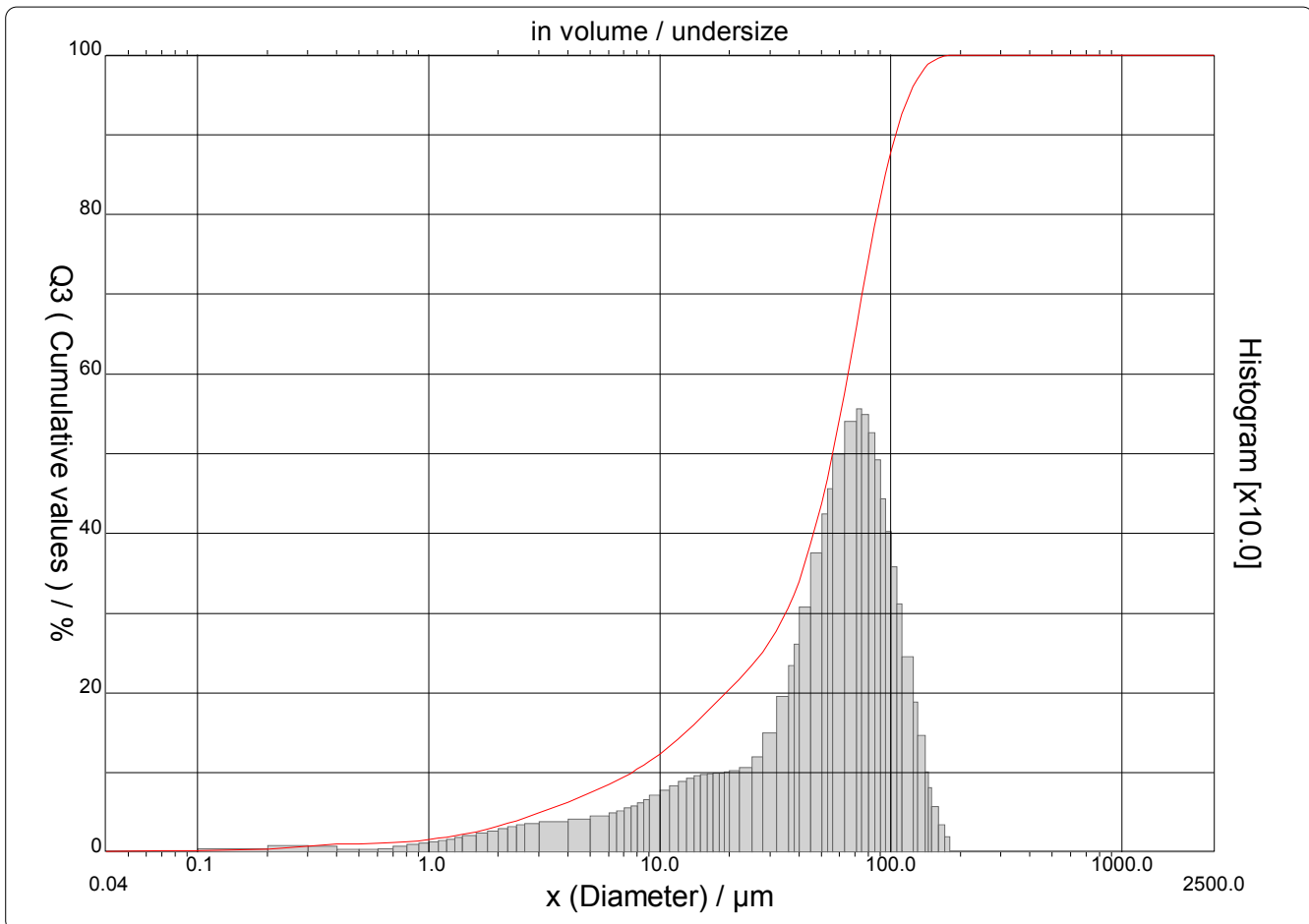
x : diameter / µm Q3 : cumulative value / % q3 : density distribution

CILAS 1190 Liquid

 Range : 0.04 μm - 2500.00 μm / 100 Classes

Sample ref.	: 28.1.2019 1100 rpm
Ore	: Ni-Cu-PGE
Sample type	: Wet
Comments	: Katariina Kauppilla
Liquid	: Water
Dispersing agent	: Water
Operator	: Kontio
Company	: OMS R&D Centre
Location	: University of Oulu
Date : 30.01.2019	Time : 07:59:01
Index meas.	: 1875
Database name	: CilasDB1

Ultrasounds	: 60	s
Obscurations	: 14 / 1.50	%
Diameter at 10%	: 7.53	μm
Diameter at 50%	: 55.95	μm
Diameter at 80%	: 87.17	μm
Fraunhofer		
Density/Factor	: -----	
Specific surface	: -----	
Automatic dilution	: No / No	
Meas./Rins.	: 60s/60s/4	
SOP name	: Katariina Kauppila	





PARTICLE SIZE DISTRIBUTION

CILAS 1190 Liquid

Range : 0.04 µm - 2500.00 µm / 100 Classes

Sample ref.	: 28.1.2019 1100 rpm
Ore	: Ni-Cu-PGE
Sample type	: Wet
Comments	: Katariina Kauppilla
Liquid	: Water
Dispersing agent	: Water
Operator	: Kontio
Company	: OMS R&D Centre
Location	: University of Oulu
Date : 30.01.2019	Time : 07:59:01
Index meas.	: 1875
Database name	: CilasDB1

Ultrasounds	: 60	s
Obscurations	: 14 / 1.50	%
Diameter at 10%	: 7.53	µm
Diameter at 50%	: 55.95	µm
Diameter at 80%	: 87.17	µm
Fraunhofer		
Density/Factor	-----	
Specific surface	-----	
Automatic dilution	: No / No	
Meas./Rins.	: 60s/60s/4	
SOP name	: Katariina Kauppilla	

Standards classes in volume / undersize

x	0.04	0.07	0.10	0.20	0.30	0.40	0.50	0.60	0.70	0.80
Q3	0.18	0.19	0.20	0.46	0.84	1.04	1.12	1.17	1.24	1.36
q3	0.01	0.00	0.00	0.03	0.07	0.06	0.03	0.02	0.04	0.07
x	0.90	1.00	1.10	1.20	1.30	1.40	1.60	1.80	2.00	2.20
Q3	1.49	1.63	1.77	1.93	2.09	2.25	2.59	2.94	3.29	3.64
q3	0.09	0.10	0.12	0.14	0.15	0.17	0.20	0.23	0.26	0.29
x	2.40	2.60	3.00	4.00	5.00	6.00	6.50	7.00	7.50	8.00
Q3	3.99	4.32	4.96	6.33	7.48	8.51	9.01	9.49	9.97	10.45
q3	0.31	0.33	0.35	0.37	0.40	0.44	0.48	0.51	0.54	0.58
x	8.50	9.00	10.00	11.00	12.00	13.00	14.00	15.00	16.00	17.00
Q3	10.92	11.40	12.35	13.29	14.22	15.13	16.00	16.84	17.64	18.40
q3	0.61	0.65	0.70	0.77	0.83	0.88	0.92	0.95	0.96	0.98
x	18.00	19.00	20.00	22.00	25.00	28.00	32.00	36.00	38.00	40.00
Q3	19.12	19.80	20.46	21.70	23.42	25.15	27.70	30.64	32.26	33.97
q3	0.98	0.99	0.99	1.01	1.05	1.18	1.49	1.94	2.33	2.59
x	45.00	50.00	53.00	56.00	63.00	71.00	75.00	80.00	85.00	90.00
Q3	38.60	43.67	46.84	50.05	57.59	65.87	69.78	74.32	78.41	82.01
q3	3.06	3.75	4.23	4.54	4.98	5.39	5.55	5.48	5.25	4.90
x	95.00	100.0	106.0	112.0	125.0	130.0	140.0	145.0	150.0	160.0
Q3	85.08	87.73	90.40	92.59	96.03	96.97	98.35	98.80	99.15	99.61
q3	4.42	4.01	3.56	3.10	2.43	1.86	1.45	0.99	0.80	0.56
x	170.0	180.0	190.0	200.0	212.0	242.0	250.0	300.0	400.0	500.0
Q3	99.87	100.00	100.00	100.00	100.00	100.00	100.00	100.00	100.00	100.00
q3	0.33	0.18	0.00	0.00	0.00	0.00	0.00	0.00	0.00	0.00
x	600.0	700.0	800.0	900.0	1000.0	1100.0	1200.0	1300.0	1400.0	1500.0
Q3	100.00	100.00	100.00	100.00	100.00	100.00	100.00	100.00	100.00	100.00
q3	0.00	0.00	0.00	0.00	0.00	0.00	0.00	0.00	0.00	0.00
x	1600.0	1700.0	1800.0	1900.0	2000.0	2100.0	2200.0	2300.0	2400.0	2500.0
Q3	100.00	100.00	100.00	100.00	100.00	100.00	100.00	100.00	100.00	100.00
q3	0.00	0.00	0.00	0.00	0.00	0.00	0.00	0.00	0.00	0.00

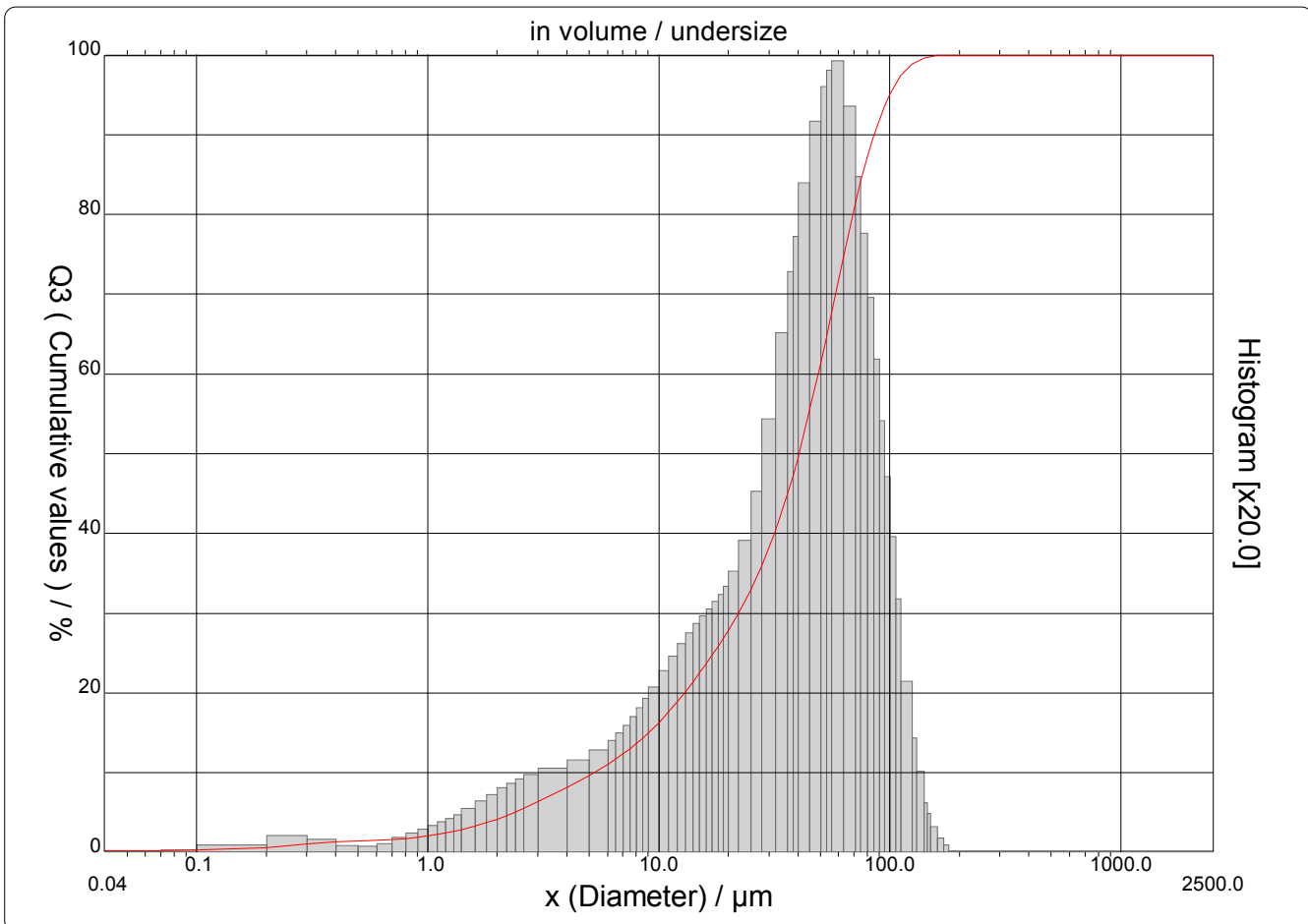
x : diameter / µm Q3 : cumulative value / % q3 : density distribution

CILAS 1190 Liquid

 Range : 0.04 μm - 2500.00 μm / 100 Classes

Sample ref.	: 14.12.2018 1400 rpm
Ore	: Ni-Cu-PGE
Sample type	: Wet
Comments	: Katariina Kauppilla 3x 50min
Liquid	: Water
Dispersing agent	: Water
Operator	: Kontio
Company	: OMS R&D Centre
Location	: University of Oulu
Date : 18.12.2018	Time : 07:35:35
Index meas.	: 1849
Database name	: CilasDB1

Ultrasounds	: 60	s
Obscurations	: 18 / 1.23	%
Diameter at 10%	: 5.24	μm
Diameter at 50%	: 40.40	μm
Diameter at 80%	: 69.24	μm
Fraunhofer		
Density/Factor	: -----	
Specific surface	: -----	
Automatic dilution	: No / No	
Meas./Rins.	: 60s/60s/4	
SOP name	: Katariina Kauppila	





PARTICLE SIZE DISTRIBUTION

CILAS 1190 Liquid

Range : 0.04 µm - 2500.00 µm / 100 Classes

Sample ref.	: 14.12.2018 1400 rpm
Ore	: Ni-Cu-PGE
Sample type	: Wet
Comments	: Katariina Kauppilla 3x 50min
Liquid	: Water
Dispersing agent	: Water
Operator	: Kontio
Company	: OMS R&D Centre
Location	: University of Oulu
Date : 18.12.2018	Time : 07:35:35
Index meas.	: 1849
Database name	: CilasDB1

Ultrasounds	: 60	s
Obscurations	: 18 / 1.23	%
Diameter at 10%	: 5.24	µm
Diameter at 50%	: 40.40	µm
Diameter at 80%	: 69.24	µm
Fraunhofer		
Density/Factor	-----	
Specific surface	-----	
Automatic dilution	: No / No	
Meas./Rins.	: 60s/60s/4	
SOP name	: Katariina Kauppila	

Standards classes in volume / undersize

x	0.04	0.07	0.10	0.20	0.30	0.40	0.50	0.60	0.70	0.80
Q3	0.24	0.26	0.28	0.62	1.10	1.36	1.45	1.52	1.60	1.74
q3	0.01	0.00	0.01	0.04	0.10	0.08	0.03	0.03	0.05	0.09
x	0.90	1.00	1.10	1.20	1.30	1.40	1.60	1.80	2.00	2.20
Q3	1.90	2.08	2.26	2.45	2.65	2.86	3.29	3.74	4.19	4.64
q3	0.11	0.14	0.16	0.19	0.21	0.23	0.27	0.32	0.36	0.40
x	2.40	2.60	3.00	4.00	5.00	6.00	6.50	7.00	7.50	8.00
Q3	5.09	5.52	6.34	8.12	9.64	11.03	11.70	12.35	13.01	13.66
q3	0.43	0.45	0.48	0.52	0.57	0.64	0.70	0.74	0.79	0.84
x	8.50	9.00	10.00	11.00	12.00	13.00	14.00	15.00	16.00	17.00
Q3	14.31	14.97	16.27	17.56	18.83	20.08	21.29	22.47	23.61	24.71
q3	0.90	0.96	1.03	1.13	1.22	1.30	1.37	1.43	1.47	1.52
x	18.00	19.00	20.00	22.00	25.00	28.00	32.00	36.00	38.00	40.00
Q3	25.78	26.82	27.84	29.84	32.82	35.88	40.21	44.79	47.14	49.50
q3	1.57	1.61	1.66	1.75	1.95	2.26	2.71	3.25	3.63	3.86
x	45.00	50.00	53.00	56.00	63.00	71.00	75.00	80.00	85.00	90.00
Q3	55.41	61.18	64.52	67.74	74.72	81.41	84.18	87.17	89.69	91.79
q3	4.19	4.58	4.79	4.89	4.96	4.67	4.23	3.87	3.47	3.08
x	95.00	100.0	106.0	112.0	125.0	130.0	140.0	145.0	150.0	160.0
Q3	93.54	94.98	96.36	97.40	98.79	99.13	99.57	99.70	99.79	99.91
q3	2.70	2.34	1.98	1.58	1.06	0.71	0.50	0.31	0.23	0.15
x	170.0	180.0	190.0	200.0	212.0	242.0	250.0	300.0	400.0	500.0
Q3	99.97	100.00	100.00	100.00	100.00	100.00	100.00	100.00	100.00	100.00
q3	0.08	0.04	0.00	0.00	0.00	0.00	0.00	0.00	0.00	0.00
x	600.0	700.0	800.0	900.0	1000.0	1100.0	1200.0	1300.0	1400.0	1500.0
Q3	100.00	100.00	100.00	100.00	100.00	100.00	100.00	100.00	100.00	100.00
q3	0.00	0.00	0.00	0.00	0.00	0.00	0.00	0.00	0.00	0.00
x	1600.0	1700.0	1800.0	1900.0	2000.0	2100.0	2200.0	2300.0	2400.0	2500.0
Q3	100.00	100.00	100.00	100.00	100.00	100.00	100.00	100.00	100.00	100.00
q3	0.00	0.00	0.00	0.00	0.00	0.00	0.00	0.00	0.00	0.00

x : diameter / µm Q3 : cumulative value / % q3 : density distribution

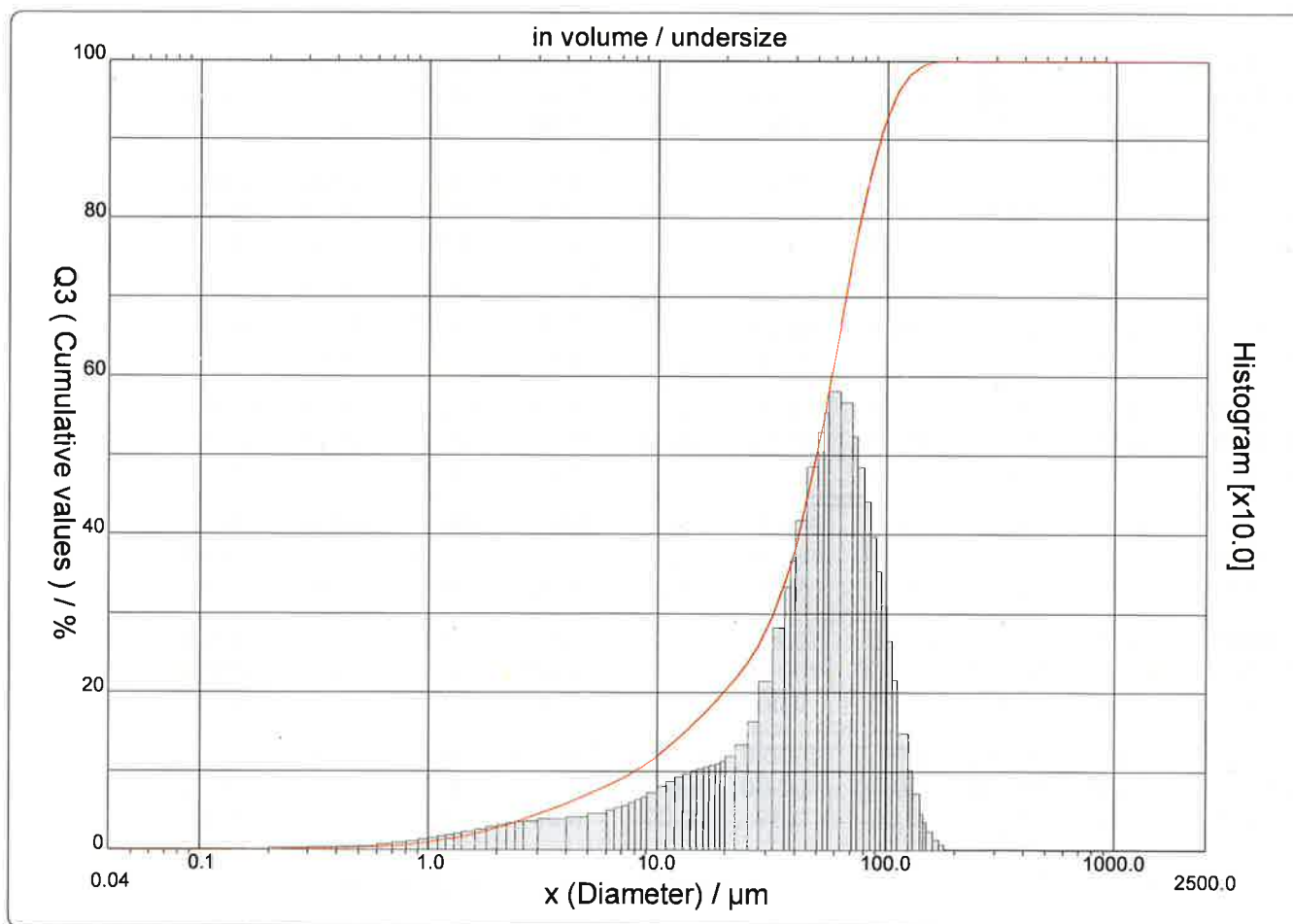
CILAS 1190 Liquid

 Range : 0.04 μm - 2500.00 μm / 100 Classes

21.1.2019 1400 rpm

Sample ref.	:	21.1.2019 1400 rpm
Ore	:	Ni-Cu-PGE
Sample type	:	Wet
Comments	:	Katariina Kauppilla
Liquid	:	Water
Dispersing agent	:	Water
Operator	:	Kontio
Company	:	OMS R&D Centre
Location	:	University of Oulu
Date : 30.01.2019	Time :	07:48:46
Index meas.	:	1874
Database name	:	CilasDB1

Ultrasounds	:	60	s
Obscurations	:	15 / 1.29	%
Diameter at 10%	:	7.93	μm
Diameter at 50%	:	49.50	μm
Diameter at 80%	:	76.84	μm
Fraunhofer	:		
Density/Factor	:	-----	
Specific surface	:	-----	
Automatic dilution	:	No / No	
Meas./Rins.	:	60s/60s/4	
SOP name	:	Katariina Kauppilla	





PARTICLE SIZE DISTRIBUTION

CILAS 1190 Liquid

Range : 0.04 µm - 2500.00 µm / 100 Classes

21.1.2019 1400 rpm

Sample ref. :
 Ore : Ni-Cu-PGE
 Sample type : Wet
 Comments : Katariina Kauppilla
 Liquid : Water
 Dispersing agent : Water
 Operator : Kontio
 Company : OMS R&D Centre
 Location : University of Oulu
 Date : 30.01.2019 Time : 07:48:46
 Index meas. : 1874
 Database name : CilasDB1

Ultrasounds : 60 s
 Obscurations : 15 / 1.29 %
 Diameter at 10% : 7.93 µm
 Diameter at 50% : 49.50 µm
 Diameter at 80% : 76.84 µm
 Fraunhofer
 Density/Factor : -----
 Specific surface : -----
 Automatic dilution : No / No
 Meas./Rins. : 60s/60s/4
 SOP name : Katariina Kauppilla

Standards classes

in volume / undersize

x	0.04	0.07	0.10	0.20	0.30	0.40	0.50	0.60	0.70	0.80
Q3	0.03	0.05	0.06	0.14	0.23	0.32	0.39	0.49	0.60	0.74
q3	0.00	0.00	0.00	0.01	0.02	0.02	0.03	0.04	0.06	0.08
x	0.90	1.00	1.10	1.20	1.30	1.40	1.60	1.80	2.00	2.20
Q3	0.89	1.06	1.22	1.40	1.58	1.76	2.12	2.50	2.87	3.23
q3	0.10	0.12	0.14	0.16	0.18	0.20	0.22	0.25	0.28	0.31
x	2.40	2.60	3.00	4.00	5.00	6.00	6.50	7.00	7.50	8.00
Q3	3.59	3.93	4.57	5.95	7.10	8.14	8.63	9.11	9.59	10.07
q3	0.33	0.35	0.36	0.39	0.42	0.46	0.50	0.53	0.56	0.59
x	8.50	9.00	10.00	11.00	12.00	13.00	14.00	15.00	16.00	17.00
Q3	10.54	11.02	11.96	12.90	13.83	14.73	15.62	16.46	17.28	18.06
q3	0.63	0.67	0.72	0.79	0.86	0.91	0.96	0.99	1.02	1.04
x	18.00	19.00	20.00	22.00	25.00	28.00	32.00	36.00	38.00	40.00
Q3	18.82	19.54	20.25	21.65	23.75	26.03	29.56	33.66	35.89	38.20
q3	1.07	1.08	1.12	1.18	1.33	1.62	2.13	2.80	3.32	3.64
x	45.00	50.00	53.00	56.00	63.00	71.00	75.00	80.00	85.00	90.00
Q3	44.29	50.61	54.41	58.18	66.63	75.00	78.55	82.41	85.72	88.52
q3	4.17	4.84	5.27	5.52	5.79	5.65	5.21	4.83	4.39	3.95
x	95.00	100.0	106.0	112.0	125.0	130.0	140.0	145.0	150.0	160.0
Q3	90.87	92.83	94.73	96.19	98.19	98.68	99.33	99.53	99.68	99.86
q3	3.51	3.08	2.63	2.14	1.47	1.00	0.72	0.45	0.35	0.23
x	170.0	180.0	190.0	200.0	212.0	242.0	250.0	300.0	400.0	500.0
Q3	99.96	100.00	100.00	100.00	100.00	100.00	100.00	100.00	100.00	100.00
q3	0.13	0.06	0.00	0.00	0.00	0.00	0.00	0.00	0.00	0.00
x	600.0	700.0	800.0	900.0	1000.0	1100.0	1200.0	1300.0	1400.0	1500.0
Q3	100.00	100.00	100.00	100.00	100.00	100.00	100.00	100.00	100.00	100.00
q3	0.00	0.00	0.00	0.00	0.00	0.00	0.00	0.00	0.00	0.00
x	1600.0	1700.0	1800.0	1900.0	2000.0	2100.0	2200.0	2300.0	2400.0	2500.0
Q3	100.00	100.00	100.00	100.00	100.00	100.00	100.00	100.00	100.00	100.00
q3	0.00	0.00	0.00	0.00	0.00	0.00	0.00	0.00	0.00	0.00

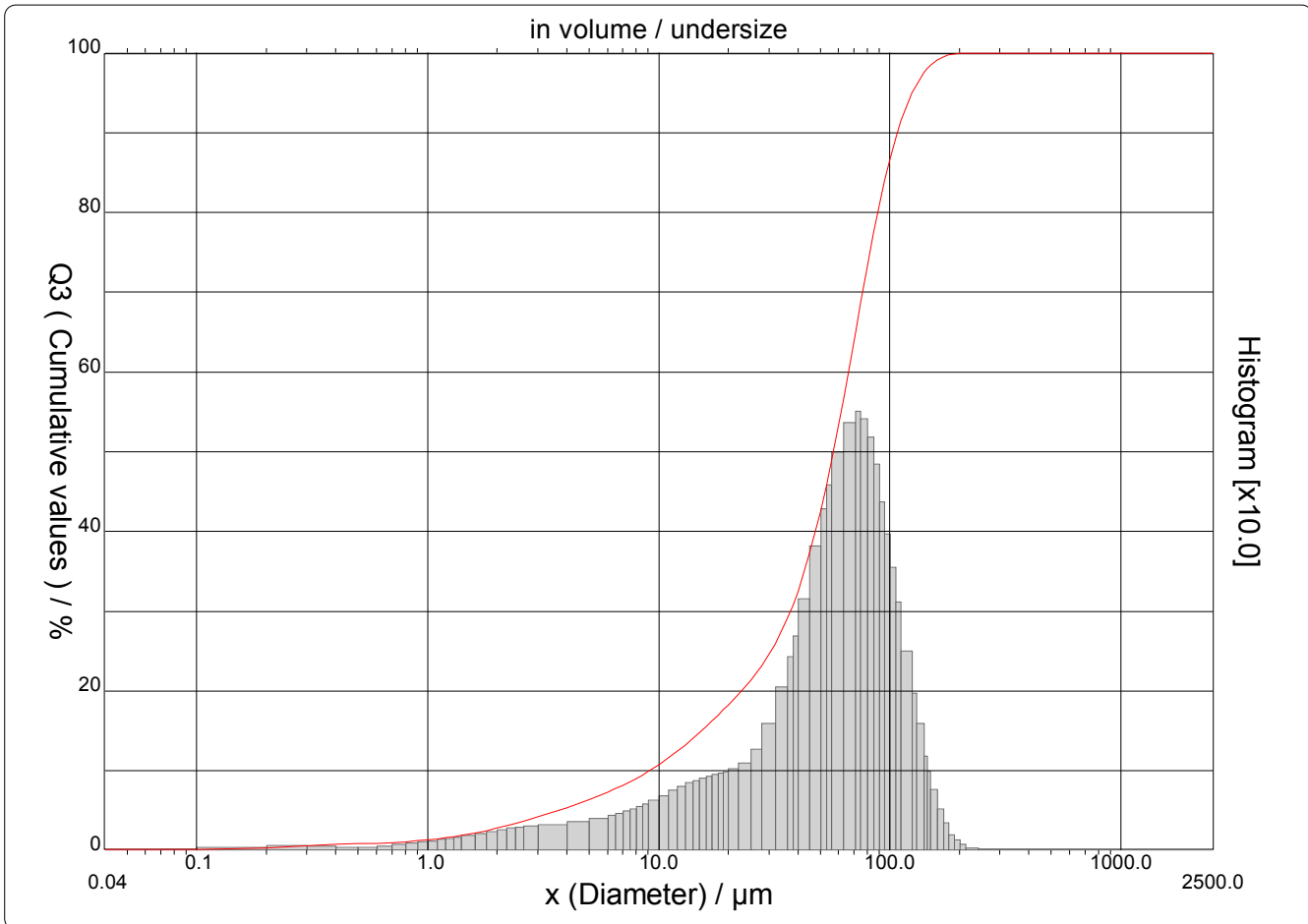
x : diameter / µm Q3 : cumulative value / % q3 : density distribution

CILAS 1190 Liquid

 Range : 0.04 μm - 2500.00 μm / 100 Classes

Sample ref.	: 10.12.2018 1700 rpm
Ore	: Ni-Cu-PGE
Sample type	: Wet
Comments	: Katariina Kauppilla
Liquid	: Water
Dispersing agent	: Water
Operator	: Kontio
Company	: OMS R&D Centre
Location	: University of Oulu
Date : 11.12.2018	Time : 07:43:57
Index meas.	: 1836
Database name	: CilasDB1

Ultrasounds	: 60	s
Obscurations	: 14 / 1.67	%
Diameter at 10%	: 9.13	μm
Diameter at 50%	: 56.93	μm
Diameter at 80%	: 88.73	μm
Fraunhofer		
Density/Factor	: -----	
Specific surface	: -----	
Automatic dilution	: No / No	
Meas./Rins.	: 60s/60s/4	
SOP name	: Katariina Kauppila	



CILAS 1190 Liquid

Range : 0.04 µm - 2500.00 µm / 100 Classes

Sample ref.	: 10.12.2018 1700 rpm
Ore	: Ni-Cu-PGE
Sample type	: Wet
Comments	: Katariina Kauppilla
Liquid	: Water
Dispersing agent	: Water
Operator	: Kontio
Company	: OMS R&D Centre
Location	: University of Oulu
Date : 11.12.2018	Time : 07:43:57
Index meas.	: 1836
Database name	: CilasDB1

Ultrasounds	: 60	s
Obscurations	: 14 / 1.67	%
Diameter at 10%	: 9.13	µm
Diameter at 50%	: 56.93	µm
Diameter at 80%	: 88.73	µm
Fraunhofer		
Density/Factor	-----	
Specific surface	-----	
Automatic dilution	: No / No	
Meas./Rins.	: 60s/60s/4	
SOP name	: Katariina Kauppilla	

Standards classes in volume / undersize

x	0.04	0.07	0.10	0.20	0.30	0.40	0.50	0.60	0.70	0.80
Q3	0.13	0.13	0.13	0.32	0.61	0.78	0.85	0.91	0.99	1.10
q3	0.01	0.00	0.00	0.02	0.05	0.05	0.02	0.03	0.04	0.06
x	0.90	1.00	1.10	1.20	1.30	1.40	1.60	1.80	2.00	2.20
Q3	1.22	1.35	1.48	1.62	1.76	1.91	2.20	2.51	2.81	3.11
q3	0.08	0.10	0.11	0.12	0.14	0.15	0.17	0.20	0.22	0.24
x	2.40	2.60	3.00	4.00	5.00	6.00	6.50	7.00	7.50	8.00
Q3	3.41	3.69	4.23	5.40	6.41	7.32	7.76	8.19	8.62	9.04
q3	0.26	0.28	0.29	0.31	0.35	0.39	0.42	0.45	0.48	0.51
x	8.50	9.00	10.00	11.00	12.00	13.00	14.00	15.00	16.00	17.00
Q3	9.46	9.89	10.73	11.57	12.40	13.22	14.02	14.79	15.54	16.26
q3	0.54	0.57	0.62	0.68	0.74	0.79	0.83	0.87	0.89	0.92
x	18.00	19.00	20.00	22.00	25.00	28.00	32.00	36.00	38.00	40.00
Q3	16.95	17.62	18.27	19.51	21.31	23.15	25.88	28.99	30.68	32.47
q3	0.94	0.95	0.97	1.01	1.09	1.25	1.58	2.04	2.42	2.68
x	45.00	50.00	53.00	56.00	63.00	71.00	75.00	80.00	85.00	90.00
Q3	37.26	42.46	45.68	48.94	56.54	64.83	68.73	73.25	77.31	80.89
q3	3.14	3.80	4.27	4.57	4.98	5.35	5.49	5.40	5.17	4.83
x	95.00	100.0	106.0	112.0	125.0	130.0	140.0	145.0	150.0	160.0
Q3	83.94	86.57	89.24	91.45	94.98	95.98	97.49	98.02	98.46	99.08
q3	4.36	3.96	3.53	3.10	2.48	1.96	1.58	1.17	0.99	0.75
x	170.0	180.0	190.0	200.0	212.0	242.0	250.0	300.0	400.0	500.0
Q3	99.48	99.73	99.86	99.93	99.98	100.00	100.00	100.00	100.00	100.00
q3	0.51	0.33	0.18	0.11	0.06	0.01	0.00	0.00	0.00	0.00
x	600.0	700.0	800.0	900.0	1000.0	1100.0	1200.0	1300.0	1400.0	1500.0
Q3	100.00	100.00	100.00	100.00	100.00	100.00	100.00	100.00	100.00	100.00
q3	0.00	0.00	0.00	0.00	0.00	0.00	0.00	0.00	0.00	0.00
x	1600.0	1700.0	1800.0	1900.0	2000.0	2100.0	2200.0	2300.0	2400.0	2500.0
Q3	100.00	100.00	100.00	100.00	100.00	100.00	100.00	100.00	100.00	100.00
q3	0.00	0.00	0.00	0.00	0.00	0.00	0.00	0.00	0.00	0.00

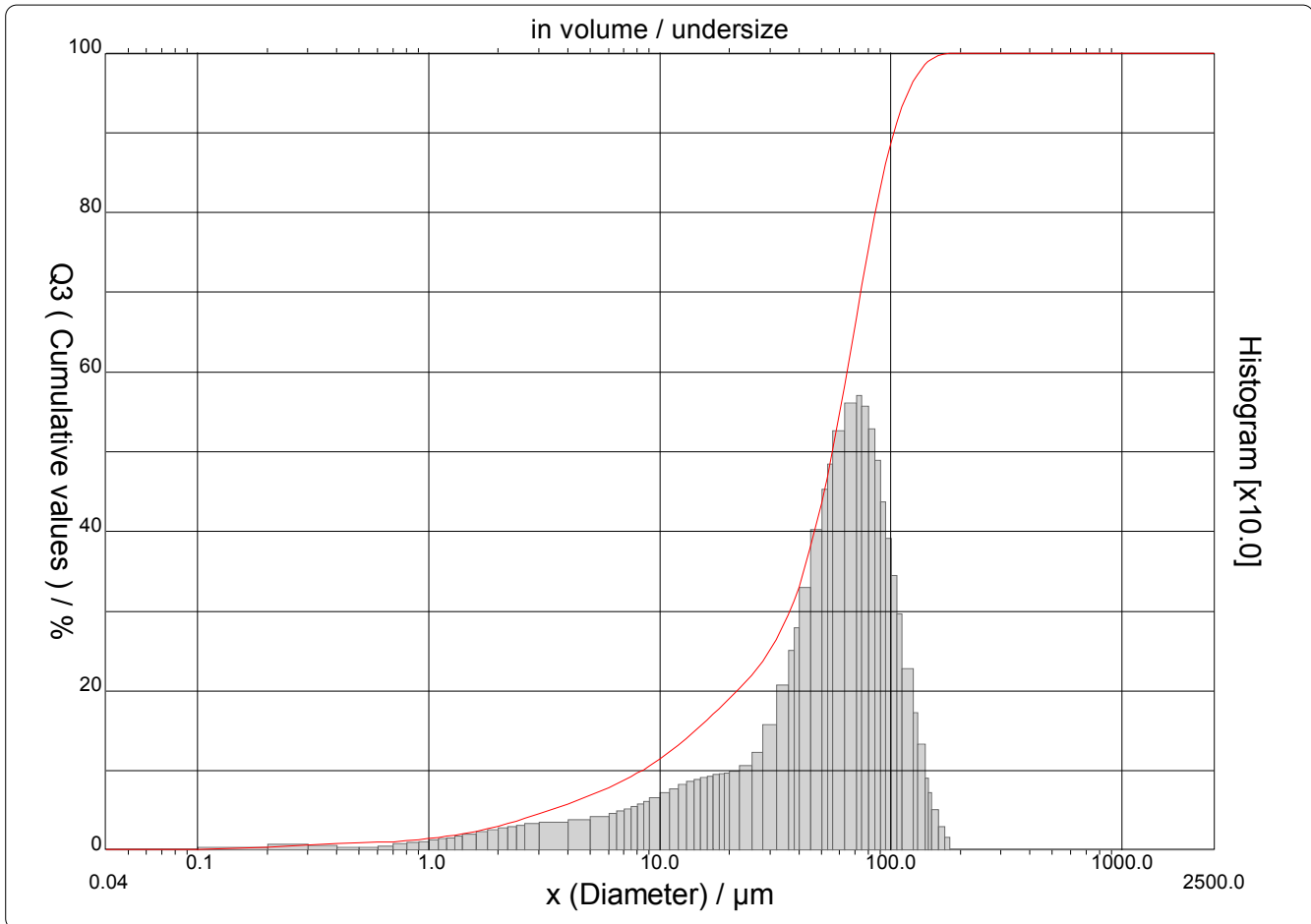
x : diameter / µm Q3 : cumulative value / % q3 : density distribution

CILAS 1190 Liquid

 Range : 0.04 μm - 2500.00 μm / 100 Classes

Sample ref.	: 11.1.2019 1700 rpm
Ore	: Ni-Cu-PGE
Sample type	: Wet
Comments	: Katariina Kauppilla
Liquid	: Water
Dispersing agent	: Water
Operator	: Kontio
Company	: OMS R&D Centre
Location	: University of Oulu
Date : 15.01.2019	Time : 07:50:55
Index meas.	: 1860
Database name	: CilasDB1

Ultrasounds	: 60	s
Obscurations	: 14 / 1.58	%
Diameter at 10%	: 8.33	μm
Diameter at 50%	: 55.78	μm
Diameter at 80%	: 85.76	μm
Fraunhofer		
Density/Factor	: -----	
Specific surface	: -----	
Automatic dilution	: No / No	
Meas./Rins.	: 60s/60s/4	
SOP name	: Katariina Kauppila	



CILAS 1190 Liquid

Range : 0.04 µm - 2500.00 µm / 100 Classes

Sample ref.	: 11.1.2019 1700 rpm
Ore	: Ni-Cu-PGE
Sample type	: Wet
Comments	: Katariina Kauppilla
Liquid	: Water
Dispersing agent	: Water
Operator	: Kontio
Company	: OMS R&D Centre
Location	: University of Oulu
Date : 15.01.2019	Time : 07:50:55
Index meas.	: 1860
Database name	: CilasDB1

Ultrasounds	: 60	s
Obscurations	: 14 / 1.58	%
Diameter at 10%	: 8.33	µm
Diameter at 50%	: 55.78	µm
Diameter at 80%	: 85.76	µm
Fraunhofer		
Density/Factor	-----	
Specific surface	-----	
Automatic dilution	: No / No	
Meas./Rins.	: 60s/60s/4	
SOP name	: Katariina Kauppilla	

Standards classes in volume / undersize

x	0.04	0.07	0.10	0.20	0.30	0.40	0.50	0.60	0.70	0.80
Q3	0.15	0.15	0.16	0.39	0.72	0.90	0.98	1.04	1.12	1.23
q3	0.01	0.00	0.00	0.02	0.06	0.05	0.03	0.03	0.04	0.07
x	0.90	1.00	1.10	1.20	1.30	1.40	1.60	1.80	2.00	2.20
Q3	1.36	1.49	1.64	1.78	1.94	2.09	2.41	2.74	3.07	3.39
q3	0.08	0.10	0.12	0.13	0.15	0.16	0.19	0.22	0.24	0.27
x	2.40	2.60	3.00	4.00	5.00	6.00	6.50	7.00	7.50	8.00
Q3	3.71	4.02	4.60	5.85	6.92	7.89	8.35	8.81	9.26	9.70
q3	0.29	0.30	0.32	0.34	0.37	0.42	0.45	0.48	0.51	0.54
x	8.50	9.00	10.00	11.00	12.00	13.00	14.00	15.00	16.00	17.00
Q3	10.15	10.59	11.46	12.33	13.18	14.02	14.82	15.60	16.35	17.07
q3	0.57	0.60	0.65	0.71	0.76	0.81	0.85	0.88	0.90	0.92
x	18.00	19.00	20.00	22.00	25.00	28.00	32.00	36.00	38.00	40.00
Q3	17.75	18.40	19.03	20.24	21.96	23.72	26.40	29.52	31.25	33.08
q3	0.94	0.94	0.96	0.99	1.05	1.21	1.56	2.07	2.49	2.78
x	45.00	50.00	53.00	56.00	63.00	71.00	75.00	80.00	85.00	90.00
Q3	38.04	43.46	46.84	50.24	58.17	66.75	70.75	75.35	79.44	83.02
q3	3.29	4.02	4.51	4.83	5.25	5.60	5.69	5.56	5.27	4.88
x	95.00	100.0	106.0	112.0	125.0	130.0	140.0	145.0	150.0	160.0
Q3	86.03	88.60	91.16	93.24	96.43	97.29	98.55	98.94	99.25	99.67
q3	4.35	3.90	3.43	2.95	2.27	1.71	1.32	0.89	0.71	0.50
x	170.0	180.0	190.0	200.0	212.0	242.0	250.0	300.0	400.0	500.0
Q3	99.89	100.00	100.00	100.00	100.00	100.00	100.00	100.00	100.00	100.00
q3	0.29	0.15	0.00	0.00	0.00	0.00	0.00	0.00	0.00	0.00
x	600.0	700.0	800.0	900.0	1000.0	1100.0	1200.0	1300.0	1400.0	1500.0
Q3	100.00	100.00	100.00	100.00	100.00	100.00	100.00	100.00	100.00	100.00
q3	0.00	0.00	0.00	0.00	0.00	0.00	0.00	0.00	0.00	0.00
x	1600.0	1700.0	1800.0	1900.0	2000.0	2100.0	2200.0	2300.0	2400.0	2500.0
Q3	100.00	100.00	100.00	100.00	100.00	100.00	100.00	100.00	100.00	100.00
q3	0.00	0.00	0.00	0.00	0.00	0.00	0.00	0.00	0.00	0.00

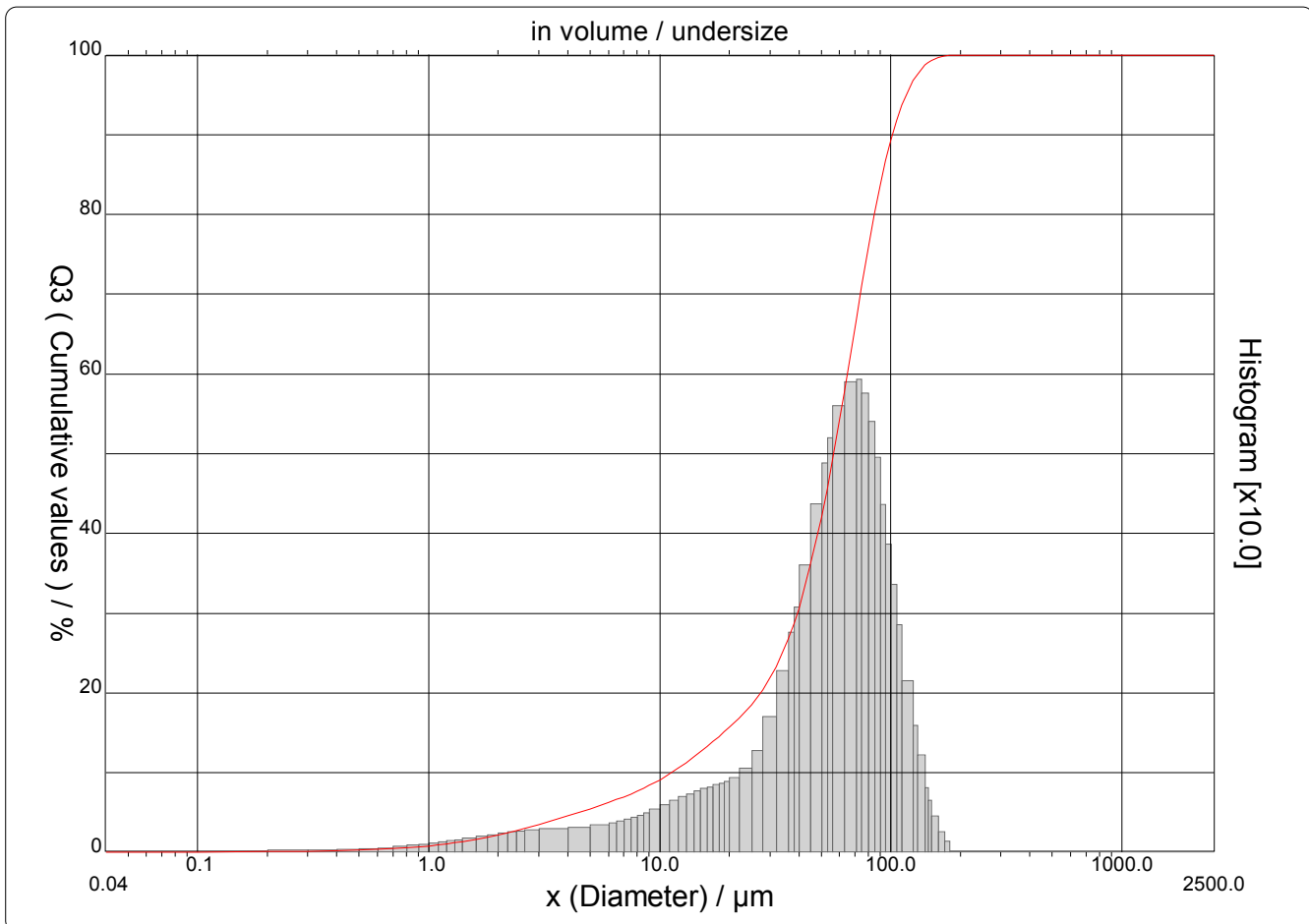
x : diameter / µm Q3 : cumulative value / % q3 : density distribution

CILAS 1190 Liquid

 Range : 0.04 μm - 2500.00 μm / 100 Classes

Sample ref.	: 3.12.2018 2000 rpm
Ore	: Ni-Cu-PGE
Sample type	: Wet
Comments	: Katariina Kauppilla
Liquid	: Water
Dispersing agent	: Water
Operator	: Kontio
Company	: OMS R&D Centre
Location	: University of Oulu
Date : 11.12.2018	Time : 07:28:01
Index meas.	: 1834
Database name	: CilasDB1

Ultrasounds	: 60	s
Obscurations	: 18 / 2.23	%
Diameter at 10%	: 11.22	μm
Diameter at 50%	: 56.52	μm
Diameter at 80%	: 84.98	μm
Fraunhofer		
Density/Factor	-----	
Specific surface	-----	
Automatic dilution	: No / No	
Meas./Rins.	: 60s/60s/4	
SOP name	: Katariina Kauppila	



CILAS 1190 Liquid

Range : 0.04 µm - 2500.00 µm / 100 Classes

Sample ref.	: 3.12.2018 2000 rpm
Ore	: Ni-Cu-PGE
Sample type	: Wet
Comments	: Katariina Kauppilla
Liquid	: Water
Dispersing agent	: Water
Operator	: Kontio
Company	: OMS R&D Centre
Location	: University of Oulu
Date : 11.12.2018	Time : 07:28:01
Index meas.	: 1834
Database name	: CilasDB1

Ultrasounds	: 60	s
Obscurations	: 18 / 2.23	%
Diameter at 10%	: 11.22	µm
Diameter at 50%	: 56.52	µm
Diameter at 80%	: 84.98	µm
Fraunhofer		
Density/Factor	-----	
Specific surface	-----	
Automatic dilution	: No / No	
Meas./Rins.	: 60s/60s/4	
SOP name	: Katariina Kauppilla	

Standards classes in volume / undersize

x	0.04	0.07	0.10	0.20	0.30	0.40	0.50	0.60	0.70	0.80
Q3	0.03	0.04	0.05	0.11	0.19	0.25	0.31	0.39	0.48	0.59
q3	0.00	0.00	0.00	0.01	0.01	0.02	0.02	0.03	0.05	0.06
x	0.90	1.00	1.10	1.20	1.30	1.40	1.60	1.80	2.00	2.20
Q3	0.71	0.83	0.96	1.09	1.23	1.37	1.65	1.94	2.22	2.50
q3	0.08	0.09	0.11	0.12	0.13	0.15	0.16	0.19	0.21	0.23
x	2.40	2.60	3.00	4.00	5.00	6.00	6.50	7.00	7.50	8.00
Q3	2.78	3.04	3.54	4.59	5.47	6.25	6.62	6.99	7.34	7.70
q3	0.25	0.26	0.27	0.28	0.31	0.33	0.36	0.38	0.40	0.43
x	8.50	9.00	10.00	11.00	12.00	13.00	14.00	15.00	16.00	17.00
Q3	8.05	8.41	9.12	9.84	10.55	11.25	11.94	12.62	13.27	13.90
q3	0.46	0.48	0.53	0.58	0.64	0.69	0.73	0.76	0.78	0.81
x	18.00	19.00	20.00	22.00	25.00	28.00	32.00	36.00	38.00	40.00
Q3	14.51	15.11	15.69	16.82	18.54	20.38	23.28	26.73	28.63	30.65
q3	0.83	0.85	0.88	0.93	1.04	1.27	1.69	2.27	2.74	3.06
x	45.00	50.00	53.00	56.00	63.00	71.00	75.00	80.00	85.00	90.00
Q3	36.10	42.01	45.66	49.33	57.80	66.86	71.04	75.80	80.01	83.65
q3	3.60	4.36	4.87	5.18	5.59	5.89	5.92	5.74	5.40	4.94
x	95.00	100.0	106.0	112.0	125.0	130.0	140.0	145.0	150.0	160.0
Q3	86.67	89.22	91.73	93.74	96.76	97.56	98.71	99.07	99.34	99.71
q3	4.35	3.86	3.35	2.84	2.14	1.58	1.21	0.80	0.64	0.44
x	170.0	180.0	190.0	200.0	212.0	242.0	250.0	300.0	400.0	500.0
Q3	99.90	100.00	100.00	100.00	100.00	100.00	100.00	100.00	100.00	100.00
q3	0.25	0.13	0.00	0.00	0.00	0.00	0.00	0.00	0.00	0.00
x	600.0	700.0	800.0	900.0	1000.0	1100.0	1200.0	1300.0	1400.0	1500.0
Q3	100.00	100.00	100.00	100.00	100.00	100.00	100.00	100.00	100.00	100.00
q3	0.00	0.00	0.00	0.00	0.00	0.00	0.00	0.00	0.00	0.00
x	1600.0	1700.0	1800.0	1900.0	2000.0	2100.0	2200.0	2300.0	2400.0	2500.0
Q3	100.00	100.00	100.00	100.00	100.00	100.00	100.00	100.00	100.00	100.00
q3	0.00	0.00	0.00	0.00	0.00	0.00	0.00	0.00	0.00	0.00

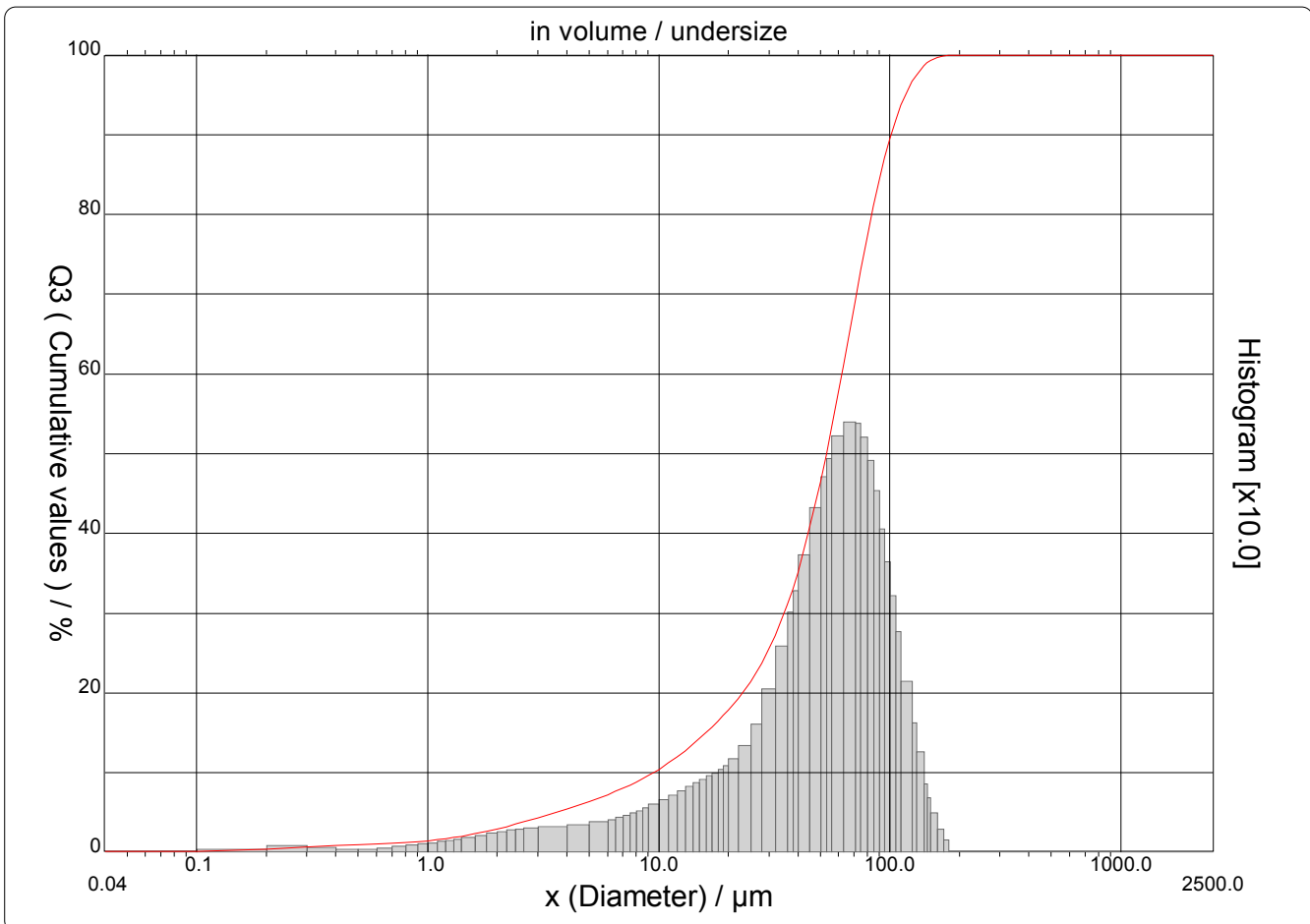
x : diameter / µm Q3 : cumulative value / % q3 : density distribution

CILAS 1190 Liquid

 Range : 0.04 μm - 2500.00 μm / 100 Classes

Sample ref.	: 9.1.2019 2000 rpm
Ore	: Ni-Cu-PGE
Sample type	: Wet
Comments	: Katariina Kauppilla
Liquid	: Water
Dispersing agent	: Water
Operator	: Kontio
Company	: OMS R&D Centre
Location	: University of Oulu
Date : 15.01.2019	Time : 07:57:38
Index meas.	: 1861
Database name	: CilasDB1

Ultrasounds	: 60	s
Obscurations	: 15 / 1.95	%
Diameter at 10%	: 9.45	μm
Diameter at 50%	: 53.07	μm
Diameter at 80%	: 83.64	μm
Fraunhofer		
Density/Factor	-----	
Specific surface	-----	
Automatic dilution	: No / No	
Meas./Rins.	: 60s/60s/4	
SOP name	: Katariina Kauppila	



CILAS 1190 Liquid

Range : 0.04 µm - 2500.00 µm / 100 Classes

Sample ref.	: 9.1.2019 2000 rpm
Ore	: Ni-Cu-PGE
Sample type	: Wet
Comments	: Katariina Kauppilla
Liquid	: Water
Dispersing agent	: Water
Operator	: Kontio
Company	: OMS R&D Centre
Location	: University of Oulu
Date : 15.01.2019	Time : 07:57:38
Index meas.	: 1861
Database name	: CilasDB1

Ultrasounds	: 60	s
Obscurations	: 15 / 1.95	%
Diameter at 10%	: 9.45	µm
Diameter at 50%	: 53.07	µm
Diameter at 80%	: 83.64	µm
Fraunhofer		
Density/Factor	-----	
Specific surface	-----	
Automatic dilution	: No / No	
Meas./Rins.	: 60s/60s/4	
SOP name	: Katariina Kauppilla	

Standards classes in volume / undersize

x	0.04	0.07	0.10	0.20	0.30	0.40	0.50	0.60	0.70	0.80
Q3	0.16	0.16	0.17	0.39	0.73	0.92	1.00	1.06	1.13	1.24
q3	0.01	0.00	0.00	0.03	0.07	0.05	0.03	0.03	0.04	0.06
x	0.90	1.00	1.10	1.20	1.30	1.40	1.60	1.80	2.00	2.20
Q3	1.36	1.49	1.62	1.76	1.90	2.05	2.34	2.65	2.95	3.25
q3	0.08	0.10	0.11	0.13	0.14	0.15	0.18	0.20	0.23	0.25
x	2.40	2.60	3.00	4.00	5.00	6.00	6.50	7.00	7.50	8.00
Q3	3.54	3.83	4.36	5.48	6.42	7.26	7.67	8.06	8.46	8.85
q3	0.27	0.28	0.29	0.31	0.33	0.37	0.40	0.42	0.45	0.48
x	8.50	9.00	10.00	11.00	12.00	13.00	14.00	15.00	16.00	17.00
Q3	9.24	9.64	10.42	11.21	11.99	12.76	13.52	14.27	15.01	15.74
q3	0.51	0.54	0.59	0.65	0.71	0.76	0.81	0.86	0.90	0.94
x	18.00	19.00	20.00	22.00	25.00	28.00	32.00	36.00	38.00	40.00
Q3	16.45	17.15	17.85	19.25	21.41	23.71	27.14	30.99	33.04	35.17
q3	0.99	1.03	1.08	1.16	1.33	1.60	2.03	2.58	3.00	3.26
x	45.00	50.00	53.00	56.00	63.00	71.00	75.00	80.00	85.00	90.00
Q3	40.70	46.46	49.92	53.35	61.12	69.27	72.99	77.24	81.00	84.28
q3	3.71	4.31	4.69	4.92	5.20	5.38	5.36	5.19	4.90	4.52
x	95.00	100.0	106.0	112.0	125.0	130.0	140.0	145.0	150.0	160.0
Q3	87.05	89.41	91.77	93.69	96.65	97.45	98.62	99.00	99.29	99.68
q3	4.04	3.63	3.20	2.75	2.13	1.61	1.24	0.84	0.68	0.48
x	170.0	180.0	190.0	200.0	212.0	242.0	250.0	300.0	400.0	500.0
Q3	99.89	100.00	100.00	100.00	100.00	100.00	100.00	100.00	100.00	100.00
q3	0.28	0.15	0.00	0.00	0.00	0.00	0.00	0.00	0.00	0.00
x	600.0	700.0	800.0	900.0	1000.0	1100.0	1200.0	1300.0	1400.0	1500.0
Q3	100.00	100.00	100.00	100.00	100.00	100.00	100.00	100.00	100.00	100.00
q3	0.00	0.00	0.00	0.00	0.00	0.00	0.00	0.00	0.00	0.00
x	1600.0	1700.0	1800.0	1900.0	2000.0	2100.0	2200.0	2300.0	2400.0	2500.0
Q3	100.00	100.00	100.00	100.00	100.00	100.00	100.00	100.00	100.00	100.00
q3	0.00	0.00	0.00	0.00	0.00	0.00	0.00	0.00	0.00	0.00

x : diameter / µm Q3 : cumulative value / % q3 : density distribution